Mapping of the cytotoxic T cell response against two human herpesviruses

Kartierung der zytotoxischen T-Zell-Antwort gegen zwei humane Herpesviren

Dissertation

der Mathematisch-Naturwissenschaftlichen Fakultät

der Eberhard Karls Universität Tübingen

zur Erlangung des Grades eines

Doktors der Naturwissenschaften

(Dr. rer. nat.)

vorgelegt von

M.Sc. Maren Lübke

aus Schwäbisch Hall

Tübingen

2020

Gedruckt mit Genehmigung der Mathematisch-Naturwissenschaftlichen Fakultät der
Eberhard Karls Universität Tübingen.

Tag der mündlichen Prüfung:	29.06.2020
Dekan:	Prof. Dr. Wolfgang Rosenstiel
1. Berichterstatter:	Prof. Dr. Stefan Stevanović
2. Berichterstatter:	Prof. Dr. Hans-Georg Rammensee

Preface

Parts of this thesis have been published. If applicable, contribution of other persons is indicated in each chapter. If not stated otherwise, experiments were performed by the author of this thesis. The following publication contains parts of this thesis:

Lübke M, Spalt S, Kowalewski DJ, Zimmermann C, Bauersfeld L, Nelde A, Bichmann L, Marcu A, Peper JK, Kohlbacher O, Walz JS, Le-Trilling VTK, Hengel H, Rammensee HG, Stevanovic S, Halenius A (2020) Identification of HCMV-derived T cell epitopes in seropositive individuals through viral deletion models. *J Exp Med* 217.

Table of contents

1 Introduction

1.1 The immune system

Organisms are confronted with a plethora of detrimental influences from their environment. Mechanical and biochemical barriers are the first line of defense against radiation, pollutants and pathogens. The elimination of pathogens that nevertheless enter the body is the task of the cellular and humoral immune defense.

The human immune system consists of the rather unspecific, broadly effective, fast innate immunity and the slower, but specific, adaptive immunity with its immunological memory. In addition to the complement system that represents the humoral component, the innate immune response is mediated by several cell types: Natural killer (NK) cells, granulocytes (neutrophils, basophils, and eosinophils), macrophages, mast cells, and dendritic cells (DCs). Those cells recognize pathogen-specific molecules, so called pathogen-associated molecular patterns, with a diverse set of pattern recognition receptors. Phagocytic cells such as DCs, macrophages, and neutrophils are able to engulf particles and pathogens while mast cells, eosinophils, and basophils release granules that contain a multitude of antimicrobial, cytotoxic, inflammatory substances. This response in turn leads to activation and recruitment of other cells and compartments of the immune system. NK cells, on the other hand, do not attack invading pathogens directly but play an important role in recognizing infected and abnormal host cells.

The adaptive immune system comes into play when antigen presenting cells (APCs) of the innate immune system present relevant antigens to B and T lymphocytes. B cells are able to produce specific antibodies targeting those antigens and are part of the humoral branch of the adaptive immune system. The cellular branch is represented by the T cells that can kill abnormal or infected cells directly or help the immune response by secreting cytokines. B and T cells can provide a long-lasting protection against pathogens by differentiating into memory cells. This immunological memory is the hallmark of adaptive immunity and is responsible for the fast and efficient immune response upon subsequent encounters with a pathogen.

1.2 T cell-mediated immune response

1.2.1 Major histocompatibility complex

The ability of T cells to distinguish between healthy host cells and infected or abnormal cells depends on the recognition of specific antigens presented by major histocompatibility complex

(MHC) molecules. MHC molecules are transmembrane glycoproteins that are not only responsible for the presentation of antigenic peptides to T cells but also play a crucial role in modulating the activity of NK cells.

The MHC, in humans known as human leukocyte antigen (HLA) complex, is a gene cluster that extends over at least 4 million base pairs on chromosome 6 and contains more than 200 genes [1, 2]. Three major groups can be distinguished: HLA class I (HLA-I), HLA class II (HLA-II), and HLA class III. HLA-I and -II mainly contain genes for classical peptide-binding molecules while class III genes encode proteins that participate in antigen processing or presentation or have other functions in the immune response. The class I region contains the classical HLA-A, -B, and -C genes and non-classical genes such as HLA-E, -F, and -G. The class II region contains three pairs of HLA-II α and β chain genes: HLA-DP, -DQ, and DR. However, many individuals possess an additional HLA-DR β chain gene. The HLA genes are among the most polymorphic genes in the genome with many different alleles throughout the population. In total, sequences for more than 25,000 HLA-I and -II alleles were listed in the international ImMunoGeneTics (IMGT) database [3] by September 2019. Due to the polygenic nature, the polymorphism, and the codominant expression of the HLA complex, up to six different HLA-I and eight different HLA-II molecules can be expressed in one individual. It is therefore highly unlikely that two individuals, apart from identical twins, express the same set of HLA molecules.

1.2.2 Structure of HLA molecules and their ligands

HLA-I and -II molecules differ in their expression pattern, structure, binding motif, peptide origin and the T cell type they can activate. While HLA-I can be expressed by almost all nucleated cells, HLA-II is only expressed by B cells, dendritic cells, macrophages, and thymic epithelial cells. However, malignant transformation of cells and the stimulation with Interferon (IFN)-γ can lead to the expression of HLA-II in other cell types [4, 5].

HLA-I molecules are heterodimers that consist of a 43 kDa α chain and a 12 kDa β_2-microglobulin (β_2m) that are non-covalently associated [2]. The β_2m gene is not located within the HLA complex but on chromosome 15 [6]. The α chain consists of three domains: the membrane-spanning α_3 domain and two polymorphic domains (α_1 and α_2) that create a cleft on the surface of the molecule. This is the peptide-binding site, also known as the peptide-binding groove [7]. The allotype of the α chain is determined by the amino acids forming the binding groove; they have a major influence on which peptides will bind [8]. HLA-II molecules consist of two non-covalently associated chains – both of which span the membrane: the 34 kDa α chain and the 29 kDa β chain.

Both chains have two domains: α_2 and β_2 are anchored in the membrane and α_1 and β_1 form the peptide-binding groove. The two domains forming the binding groove are non-covalently bonded. The fact that the binding groove is open at both ends is another difference to HLA-I molecules. The structural differences in the binding groove of the two classes cause distinctive peptide-binding specificities. The HLA-peptide binding is mediated by non-covalent interaction of amino acid residues in both the HLA binding groove and the peptide. The peptide-binding cleft of HLA-I allotypes forms six pockets (A-F), which accommodate different amino acid residues of the binding peptide [9]. Those residues are essential for the binding and are therefore called anchor residues. The position and the identity of anchor residues differ depending on the HLA molecule [10] and can be defined as an allele-specific motif [8]. This results in the fact that a peptide can normally bind well to only one HLA allotype. However, HLA allotypes with similar amino acid sequence in the binding groove tend to bind similar peptides. Such allotypes can be clustered into groups and are termed 'supertypes' [11, 12]. Several $CD8^+$ T cell epitopes have been found to show promiscuous binding to more than one HLA allotype within supertypes [13-16] but also between different supertypes [15, 16]. Peptides presented on HLA-I molecules are usually eight to ten amino acids long, 9mers on average. Longer peptides with up to 14 amino acids can either bind [17] by bulging when both terminal amino acids are accommodated within the A and F pockets [18] or in some cases by extending out of the binding groove at the C-terminus [19, 20]. Peptides bound by HLA-II are less constrained in their length due to the open ends of the binding groove; peptides with up to 25 amino acids can be presented while only a 9 amino acid long core sequence harbors the anchor residues that determine the binding specificity [10, 21]. HLA-II molecules display highly promiscuous peptide binding compared to their class I counterpart [22, 23].

Nevertheless, the specific peptide-binding motif of each HLA allotype allows the prediction of possible ligands with online tools such as SYFPEITHI (www.syfpeithi.de) [24], NetMHC (https://services.healthtech.dtu.dk/) [25], and the Immune Epitope Database (IEDB, https://www.iedb.org/) [26].

1.2.3 Antigen processing and presentation

Not only the length of peptides bound to HLA-I and -II molecules differs but also their origin and their processing pathway. HLA-I peptides originate mainly from cytosolic proteins degraded by the proteasome. The constitutive 26S proteasome is a holoenzyme with a barrel-shaped 20S core particle and two 19S regulatory cap particles. The 19S regulatory particles recognize polyubiquitinated proteins and guide them to the core particle. The proteolytic activity is mediated

by the 20S core with its four stacked hetero-heptameric rings with the stoichiometry $\alpha_7\beta_7\beta_7\alpha_7$. Three β-subunits, β1, β2, and β5, constitute the active sites, with β1 mainly cleaving on the C-terminal side of acidic residues, β2 after basic residues, and β5 after hydrophobic residues [27].

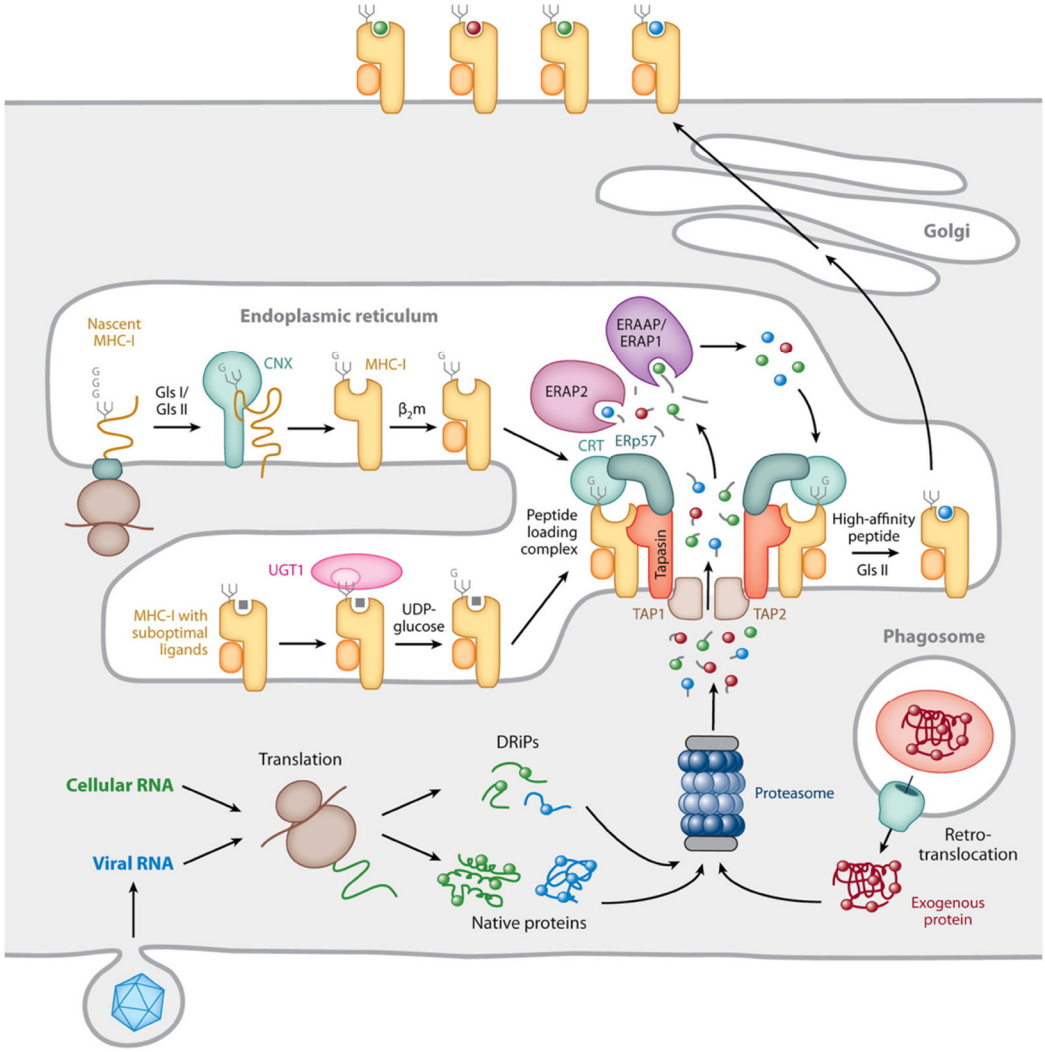

Figure 1: HLA-I antigen processing. HLA-I molecules are assembled in the endoplasmic reticulum (ER) with the help of CNX. A monoglucosylated N-linked glycan at the HLA heavy chain mediates the interaction with CNX and the peptide loading complex. Intracellular proteins are cleaved by the proteasome and the resulting peptides are transported into the ER by TAP, where they can be N-terminally trimmed by the aminopeptidases ERAP1 and ERAP2. In addition to TAP, HLA-I molecules and the chaperones tapasin, ERp57, and CRT are part of the peptide loading complex that mediates the stabilization of HLA-I molecules and the loading with their ligands. The terminal glucose of the N-linked glycan can be removed by the enzyme glucosidase II. In cases of suboptimal peptide binding, the enzyme UDP-glucose glycoprotein transferase-1 (UGT1) can re-glucosylate the glycan, enabling the HLA-I molecule to maintain or re-enter interaction with the PLC. Stable HLA-I-peptide complexes are then transported to the cell surface. An alternative processing pathway is the endosome-to-cytosol cross-presentation pathway shown in the lower right of the figure. It allows the presentation of peptides originating from extracellular proteins on HLA-I molecules. CNX, calnexin; Gls, glucosidase; CRT, calreticulin; ERAP, ER aminopeptidase; TAP, transporter associated with antigen processing; DRiPs, defective ribosomal products. Source: [28] (License No. 4793100440077).

Proteasomal products are about 1 to 26 amino acids long [29-31]. Stimulation of cells with IFN-γ induces the expression of special β-subunits (LMP2, MECL1, and LMP7) and the regulatory cap

particle PA28, leading to the formation of the immunoproteasome. It has different cleavage preferences [31, 32] and an enhanced ability to degrade short peptide substrates instead of ubiquitinated proteins [33]. Therefore, the nature of peptides generated by immunoproteasomes is altered compared to the constitutive 26S proteasome [34-36]. In general, only about 15% of the cleavage products have the appropriate size for binding to HLA-I molecules, most are too short [36, 37]. The rest needs to undergo N-terminal trimming by aminopeptidases in the cytosol [38, 39] or in the ER [40, 41]. Peptides that are not rapidly degraded in the cytosol [42] can be transported into the endoplasmic reticulum (ER) by the heterodimeric transporter associated with antigen processing (TAP). N-terminal trimming in the ER is then mediated by the IFN-γ regulated ER aminopeptidase 1 (ERAP1) [40, 43] and ERAP2 [44, 45]. TAP, consisting of the subunits TAP1 and TAP2, associates with several other proteins to form the peptide loading complex (PLC), which mediates the assembly of HLA-peptide complexes. Other parts of the PLC are the chaperones tapasin, calreticulin (CRT), and ERp57 as well as HLA-I molecules. The HLA-I-β2m dimers assemble in the ER with the help of the chaperone calnexin before they are recruited to the PLC. The chaperones of the PLC stabilize the empty HLA-I molecule and keep the binding groove in a conformation that favors the binding of high affinity peptides [46]. Stable HLA-peptide complexes are then released and transported to the cell surface where they can be recognized by $CD8^+$ T cells. In case of suboptimal peptide binding, the glycan at position 86 of the HLA-I heavy chain can be re-glucosylated by the enzyme UDP-glucose glycoprotein transferase-1 (UGT1) [47, 48]. This monoglucosylated N-linked glycan is the substrate of CRT [49] and therefore important for the interaction with the PLC. Accordingly, the re-glucosylation enables the re-entry of the HLA-I molecule in the PLC.

While most of the HLA-I bound peptides are of cytosolic origin, peptides from internalized proteins can also be loaded onto HLA-I by a process called cross-presentation [50, 51]. There are several pathways by which peptides from extracellular proteins can be loaded onto HLA-I molecules [52]. Figure 1 shows parts of the endosome-to-cytosol pathway [53].

The other major processing pathway enables the presentation of peptides derived from extracellular antigens on HLA-II molecules (Figure 2). The HLA-II dimers fold and associate in the ER with a third glycoprotein, the invariant chain (Ii) [54]. Ii can form a homotrimer that binds to three HLA-II dimers, building a nonameric complex [55]. Targeting motifs of Ii [56] direct the complex first to the Golgi compartment and then either directly [57, 58] or after recycling them from the cell surface [59, 60] to late endosomal acidic compartments called MHC-II compartments (MIIC). There, cathepsins and the acidic environment lead to the proteolysis of the invariant chain, leaving a short fragment in the binding groove of HLA-II molecules. This class II-associated invariant chain peptide

(CLIP) is a placeholder peptide and needs to be released by the enzyme HLA-DM, thereby facilitating the binding of high affinity peptides to HLA-II molecules [61]. Thus, HLA-DM acts as an exchange catalyst similar to tapasin in the HLA-I antigen processing pathway [62]. The activity of HLA-DM, in turn, is regulated by HLA-DO [63]. Stable HLA-II-peptide complexes are released from the interaction with HLA-DM and transported to the cell surface for the recognition by $CD4^+$ T cells.

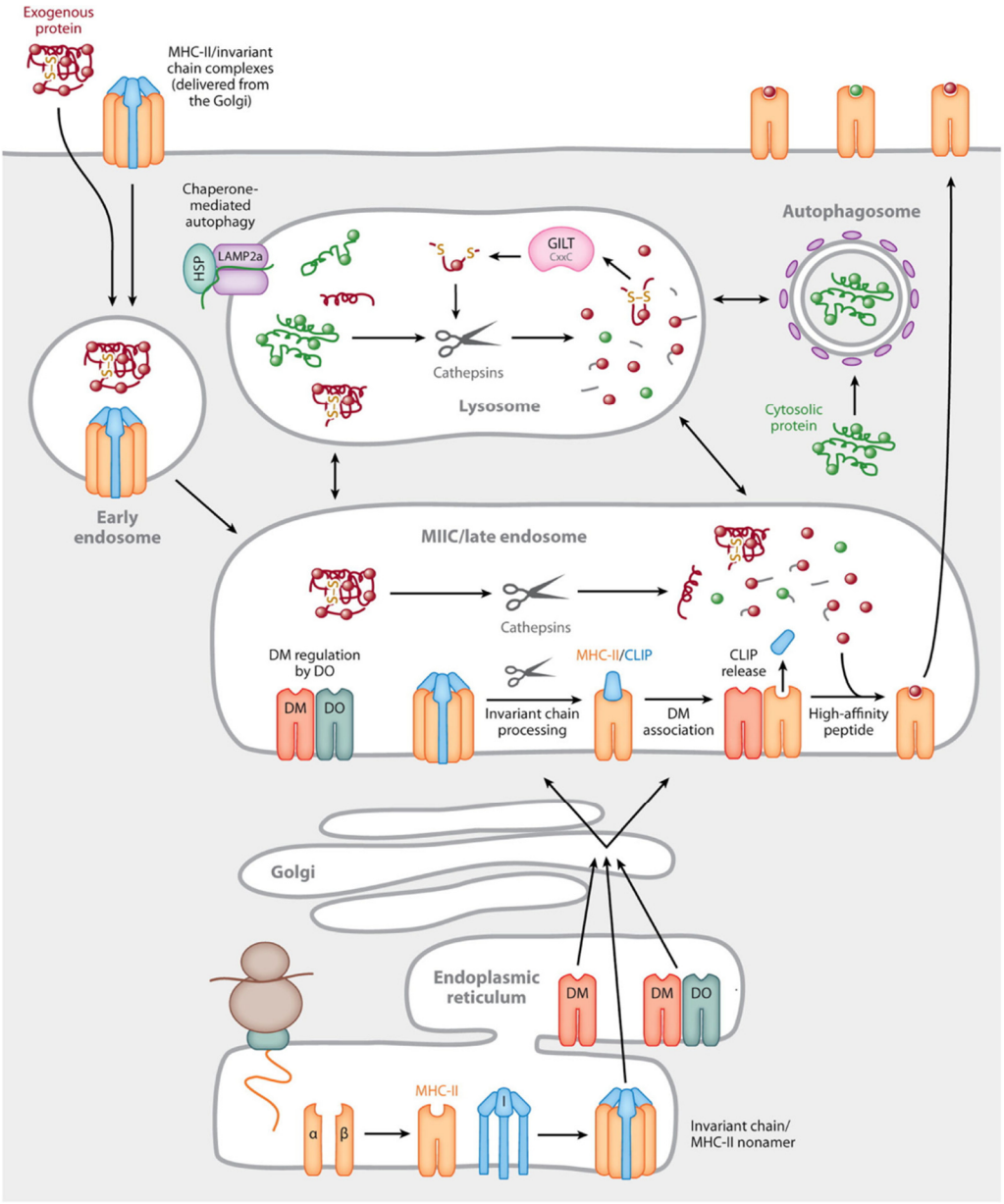

Figure 2: HLA-II antigen processing. HLA-II α and β chains assemble in the ER and form with the homotrimer Ii a nonameric complex, which is transported *via* the Golgi complex to the endocytic compartment MIIC. HLA-II-Ii complexes that were first transported to the cell surface are recycled and directed to the MIIC. There, Ii is cleaved and only the placeholder peptide CLIP (class II-associated invariant chain peptide) remains in the binding groove of HLA-II molecules. The enzymatic activity of the non-classical HLA-II protein HLA-DM is necessary for the exchange of CLIP with high affinity peptides. The activity of HLA-DM is, in turn, regulated by HLA-DO. The main source of antigenic peptides for HLA-II molecules are extracellular proteins that are internalized by endocytosis, phagocytosis, or pinocytosis. However, intracellular proteins can enter this pathway *via* autophagy. The antigenic proteins are degraded by unfoldases and proteases such as GILT (gamma-interferon-inducible lysosomal thiol reductase) and cathepsins. Source: [28] (License No. 4793100440077).

Extracellular or membrane proteins, the main source of HLA-II ligands, are internalized by endocytosis, phagocytosis, or pinocytosis and degraded by unfoldases and proteases such as GILT (gamma-interferon-inducible lysosomal thiol reductase) and cathepsins [64, 65]. Intracellular source proteins can enter the endocytic and phagocytic pathway for example *via* autophagy [66].

1.2.4 The T cell receptor

T cells are lymphocytes that are defined by the presence of the T cell receptor (TCR) on their cell surface. With this receptor T cells are able to recognize diverse antigens in the form of peptides presented by HLA molecules. The T cell receptor consists of two different transmembrane glycoprotein chains, TCRα and β, that are linked by a disulfide bond. A minority of T cells possesses a TCR that is composed of a γ and a δ chain, so called γδ T cells [67]. In this work, TCR refers always to the αβTCR. Each chain consists of a variable and a membrane-proximal constant region, which is followed by a transmembrane region and a short cytoplasmic tail. The variable region of the α and β chain is generated by VJ and VDJ recombination, respectively, and forms three hypervariable complementarity determining regions (CDRs). The immense variability of CDRs directly translates to antigen-binding diversity and is a result of somatic recombination during T cell development [68]. Insertions and deletions of nucleotides at the joining sites further increase the possible diversity [69] so that theoretically 10^{18} different receptors could be formed [70]. The actual number of unique T cell clonotypes is assumed to be around 10^{6} [71].

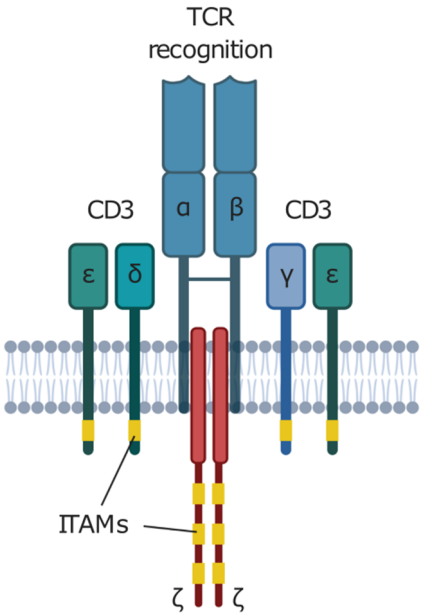

Figure 3: T cell receptor complex. The functional complex consists of the antigen-binding αβ heterodimer that is flanked by the heterodimeric signalling chains εγ and εδ (together CD3). Created with BioRender.

The TCR does not have an intracellular signaling domain and the α and β chains alone are not expressed on the cell surface [72, 73]. It is non-covalently associated in an octameric complex with CD3εγ and CD3εδ heterodimers and a TCRζζ homodimer which together mediate transduction of extracellular stimuli into intracellular signaling (Figure 3). Each CD3 subunit contains an extracellular Ig domain and a single immunoreceptor tyrosine-based activation motif (ITAM), whereas the ζ chains contain only a short extracellular domain and three intracellular ITAMs each [74]. Tyrosine phosphorylation within the ITAMs leads to T cell activation following binding of the receptor to its ligand [75].

1.2.5 T cell subsets

αβ T cells can be divided into two major groups according to co-receptor expression: CD4 and CD8. Cytotoxic T cells (CTLs) express CD8 on their cell surface and can recognize a specific antigen presented by HLA-I molecules. They are able to directly kill cancerous or infected cells by releasing cytotoxic granules that contain perforin and granzymes [76].

T helper cells (T_H cells) express CD4 on their surface and recognize antigens presented on HLA-II. They mainly support or regulate other cells during an immune response but can also have direct cytotoxic functions [77, 78]. While T_H subtypes can be increasingly differentiated, three major, well-characterized types with distinctive cytokine secretion profiles and target cells can be described: T_H1, T_H2 [79], and T_H17 cells. T_H1 cells are required for the defense against intracellular bacteria, viruses, and cancer. They mainly secret the pro-inflammatory cytokines IFNγ and IL-2 and support the cell-mediated response by macrophages [80] and CTLs [81, 82]. In contrast, T_H2 cells rather support the humoral part of the immune response against extracellular pathogens by secreting IL-4, IL-5, IL-9, IL-10, IL-13, and IL-25 and induce antibody production by B cells [83, 84]. T_H17 cells produce IL-17 and play an important role in both mucosal immunity and autoimmune disorders [85].

Regulatory T cells (Treg) are another CD4-positive subtype [86] and express CD25 and the transcription factor FOXP3 (forkhead box p3) [87, 88]. Tregs have immunosuppressive functions to prevent damage by exaggerated immune responses and are responsible for the maintenance of immunological tolerance [86].

1.2.6 Development of $CD4^+$ and $CD8^+$ T cells

T cells originate from pluripotent hematopoietic stem cells in the bone marrow that differentiate into common lymphoid progenitor cells [89]. They then migrate to the thymic cortex where they lose the ability to differentiate into B and NK cells [90]. Instead, they become double-negative (DN, $CD4^-CD8^-$), committed T cell precursors that progress through four different stages (DN1-4) with distinct surface expression patterns of CD44 and CD25 [91]. DN3 cells can differentiate into both αβ and γδ T cells. Cells of the αβ pathway start to express an invariant pre-TCRα together with a rearranged TCRβ. This rearrangement is mediated by the recombination activating genes (RAG) 1 and 2 [92, 93], which are upregulated in stage DN2. Cells that pass the β selection start to rearrange the TCRα locus during DN4 to form a mature TCR [90]. Those cells also begin to express the co-receptor proteins CD4 and CD8 and are then double-positive ($CD4^+CD8^+$) immature T cells. Only cells that recognize HLA-peptide complexes presented by cortical thymic epithelial cells receive

essential survival signals, a process called positive selection, and differentiate into CD4 or CD8 single-positive T cells. The fraction of autoreactive T cells that binds strongly to self-peptides and could therefore cause autoimmune diseases is then removed by negative selection in the medulla. Only about 2-5% of the generated, immature T cells survive both positive and negative selection and leave the thymus as naïve T cells to constitute the peripheral T cell repertoire [94].

1.2.7 Activation of T cells and their response

Naïve T cells circulate through the blood to the lymphatic system until they come into contact with their specific antigen presented by an APC. This usually occurs in peripheral lymphoid organs where DCs migrate to after the uptake of foreign antigens [95]. The homing of naïve T cells to lymphoid organs is mediated by the surface molecule L-selectin (CD62L), which interacts with addressins expressed on high endothelial venules in lymph nodes and enables the T cells to roll along the surface of these cells [96]. This initiates the entry of naïve T cells into lymphoid organs. There, the binding of the TCR to its specific HLA-peptide complex is the first of three signals required for activation of naïve T cells. Binding to an HLA-peptide complex alone indicates the recognition of a self-peptide and leads to T cell anergy or apoptosis [97, 98]. The second signal is provided by costimulatory molecules on activated APCs. There is a plethora of different stimulatory and inhibitory molecules and their ligands [99], with CD28 being the most prominent stimulatory molecule. CD28 is expressed on the majority of T cells and binds CD80 and CD86 on APCs [100]. CD28 signaling promotes T cell survival and proliferation [99] and strongly upregulates IL-2, an autocrine proliferation factor of T cells [101]. Signal three is provided by DC-derived cytokines and induces T cell polarization that determines the effector functions of the T cell [102, 103]. The first activation of naïve T cells is called priming. Primed T cells undergo clonal expansion for several days and give rise to effector and memory T cells that leave the lymph node and can be activated by the first signal alone. To recognize this signal, each T cell bears about 30,000 copies of a unique T cell receptor on its surface [104, 105]. Early *in vitro* experiments proposed that, depending on the affinity of the TCR-ligand binding and the number of HLA-peptide complexes, the engagement of about 500 to almost all TCRs on one cell is necessary for T cell activation [106]. In contrast, around 100 HLA-peptide complexes for T helper cells [107, 108] and even single complexes for CTLs [109] are sufficient for T cell activation. It is assumed that one HLA-peptide complex can serially engage and trigger up to 200 TCRs [110] although this model is still disputed [111, 112].

The T cell-mediated immune response can be divided into three phases: expansion, contraction, and memory. After the first contact with the pathogen, the priming of specific T cells and their

clonal expansion, effector memory T cells start to fight the pathogen. The T cell response usually has its peak at around 7-15 days after initial antigen contact. The antigen or pathogen clearance is followed by a contraction phase in which the vast majority of effector cells dies by apoptosis and only a small population of long-lived memory T cells remains. The half-life of T cell memory is about 8-15 years [113] while the half-life of single cells is 1-12 months [114, 115]. This indicates that the memory is maintained by a continuous turnover.

Memory T cells can be usually identified by their expression of CD45RO [116, 117] and the lack of the longer isoform CD45RA, which is expressed on naïve T cells. On the basis of the lymph node homing CC-chemokine receptor CCR7 expression, T cells of the peripheral blood can be divided into four populations. Naïve T cells ($CCR7^+CD45RA^+$) uniformly express CCR7, which reflects their predominant location in the lymphoid organs. Central memory T cells (T_{CM}) ($CCR7^+CD45RA^-$) also traffic to lymphoid organs while effector memory T cells (T_{EM}) ($CCR7^-CD45RA^-$) are able to migrate to peripheral tissues [118]. In contrast, terminal effector memory T cells re-express CD45RA (CCR7+CD45RA+) (reviewed in [114]). Another memory T cell subpopulation can be identified with further surface markers; T memory stem cells are $CD45RA^+CD45RO^-$ and express high levels of CD27, CD28, IL-7 receptor α chain (IL-7Rα), CD62L and CCR7. They have a high proliferative capacity and can differentiate into T_{CM} and T_{EM} cells [119].

1.3 Epstein-Barr virus

The Epstein-Barr virus (EBV), also known as *Human herpesvirus 4*, is a lymphotropic gammaherpesvirus. It was discovered by Michael Anthony Epstein, Budd Achong, and Yvonne Barr when they cultured cells from African Burkitt's lymphoma in 1964 [120]. Early studies uncovered the virus' potential to transform B cells into lymphoblastoid cell lines [121-123]. Evidence that EBV is not only a concomitant but could be the cause of cancer was published 1978 [124]. It was therefore the first oncogenic virus identified in humans.

EBV is highly prevalent and infects more than 90% of the human population worldwide. Primary infection is often asymptomatic but can cause infectious mononucleosis (IM) [125], especially when it occurs during or after the second decade of life [126]. In all cases, infection results in a lifelong persistence of the virus in the host. The virus has since been linked to a large variety of malignancies.

There are two major genotypes of EBV, type 1 and type 2 (originally A and B). These two types were distinguished by their variations in the EBNA2 genes and differ in their transforming and reactivation capabilities [127]. Most other genes differ by less than 5% in their sequence [128]. While both types are equally prevalent in sub-Saharan Africa, type 1 is the most common

throughout the world [129, 130]. Type 1 and 2 can be subdivided into different virus strains; mainly on the basis of LMP-1 variations [131]. The strains B95-8 and AG876 are prototype strains for type 1 and type 2, respectively.

In comparison to other human herpesviruses, EBV stands out for its extensive gene expression during the latent infection and its ability to induce proliferation of latently infected cells.

1.3.1 Structure and genome

EBV virions are relatively large, multi-layered particles with a diameter of 110-180 nm [120, 132]. The double-stranded, linear DNA is surrounded by a nucleocapsid with 162 capsomers, which is in turn surrounded by a protein tegument. The envelope with its embedded glycoproteins builds the outer layer.

The viral genome has a length of about 184,000 base pairs (184 kb) and about 90 open reading frames (ORFs). The 172 kb large genome of strain B95-8, derived from an IM patient, was completely sequenced in 1984 [133]. However, this extensively studied laboratory strain is missing a 12 kb segment in comparison to the majority of isolates [134]. But apart from a decreased expression of the gp220 envelope protein, the biological properties of B95-8 are indistinguishable from those of other strains [135]. The viral genome has 0.5 kb long terminal repeats at both ends and several internal repeats. They divide the genome in short and long unique sequence domains. The viral DNA builds circular episomes in host cells [136].

The nomenclature of the EBV ORFs was established according to the BamHI-restriction fragments in which they were found. The fragments were ordered from A to Z based on their sizes [137, 138]. BARF1 would therefore be the first rightward reading frame in the BamHI A restriction fragment. Many characterized genes are also known by more common names describing their functions.

The EBV ORFs can be divided in latent and lytic genes. Different sets of latent genes are expressed depending on the latency program. All latent gene products such as EBV nuclear antigens (EBNA1, -2, -3, -3A, -3B, -3C, and -LP), latent membrane proteins (LMP1, -2A, and -2B), and Epstein-Barr virus-encoded small RNAs (EBERs) are expressed in Latency III. In Latency II, only EBNA1, the EBERs, and LMP1 and -2A are expressed. Latency I is characterized by the exclusive expression of EBNA1 and the postulated Latency 0 by the complete arrest of viral gene expression [131]. Epstein-Barr virus BamHI A fragment transcripts (BARTs) are detectable in all three forms of virus latency [139]. Lytic genes are expressed in three consecutive stages: immediate-early, early, and late.

Table 1: Different EBV transcription programs. Adapted from [140].

Transcription program	Expressed proteins	Description or function
Pre-latency	BZLF1, BRFL1, BMRF1, BCRF1, EBNA2, BHRF1, EBNA-LP	The expression of various latent and lytic proteins improves survival and immune evasion of newly infected B cells.
Latency III	EBNA1, -2, -3A, -3B, -3C and –LP, LMP1, -2A and LMP2B	Expression of the full complement of latent proteins serves to activate naïve B cells and leads to their proliferation as B cell blasts.
Latency II	EBNA1, LMP1, LMP2A	Mimics T cell help and BCR signaling so that GC B cells are rescued into the memory compartment.
Latency I	EBNA1	The expression of EBNA1 enables the viral genome to be replicated along with the host genome during memory B cell homeostasis.
Latency 0	None	The absence of EBV antigens enables immune escape and ensures survival of long-lived memory B cells
Lytic	More than 80 viral genes are expressed	The production of virions promotes the continued infection of permissive cells within the same host and enables the horizontal transfer of virions to other individuals.

1.3.2 Biology of EBV infection and life cycle

EBV can be transmitted *via* saliva, semen, and blood. The oral route is the main route of transmission but sexual intercourse as well as organ transplantation and blood transfusions can lead to virus spread [141, 142]. Although B cells are the main target and reservoir of EBV, the virus can infect epithelial cells, T cells, and NK cells [143-145]. Primary infection usually happens in the epithelium of the tonsils. There are different mechanisms of entry depending on the infected cell type (Figure 4). B cell entry is initiated by the binding of the viral glycoprotein gp350/220 to the cellular complement receptor CR2 (CD21) [146] or CR1 (CD35) [147]. The core fusion proteins gH, gL, and gB are required for the entry and for the fusion of the viral envelope with the cellular membrane. The non-covalently linked gH/gL heterodimer, formed by membrane-bound gH and soluble gL, functions as a regulator for gB-mediated fusion. gH/gL builds a complex with gp42, which induces B cell entry after engaging cellular HLA-II. In contrast, entry into epithelial cells is thought to be mediated by a direct interaction of gH/gL with integrin receptors [148] rendering

gp350/220 and gp42 dispensable for this process. Gp42 acts as a switch of cellular tropism promoting B cell infection while inhibiting infection of epithelial cells [149].

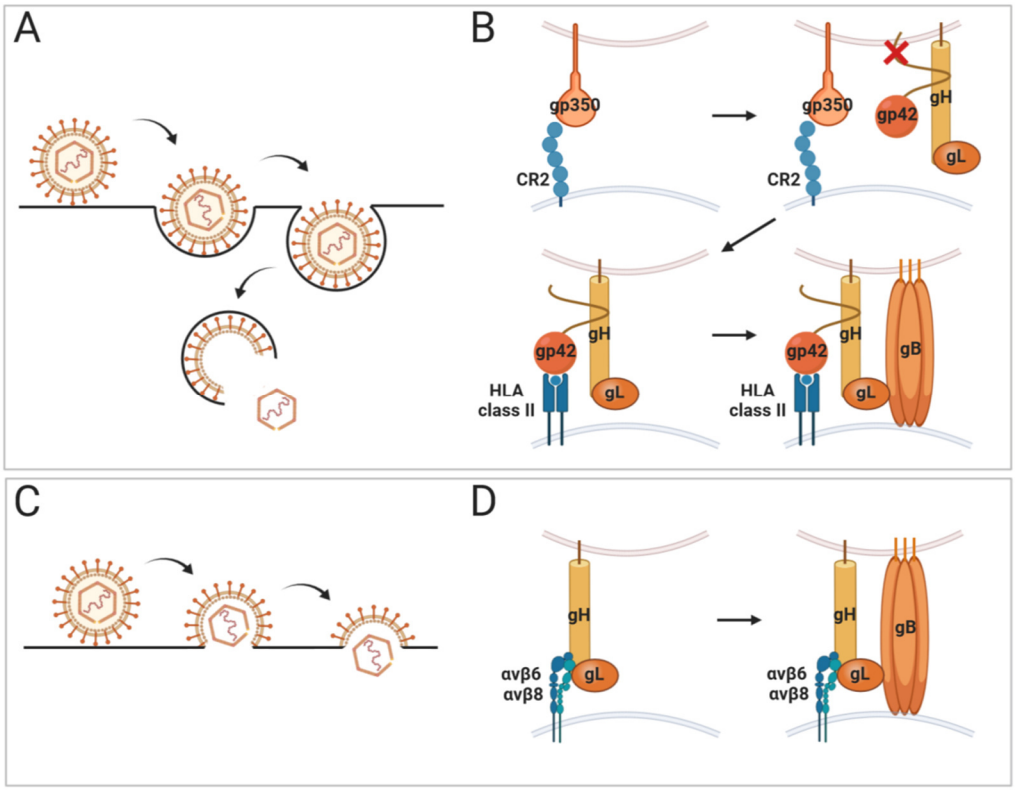

Figure 4: Entry of EBV into B cells (A, B) and epithelial cell (C, D). A) EBV entry into B cells is mediated by endocytosis. Afterwards, the viral membrane fuses with the endocytic membrane and the viral capsid is released into the cytoplasm. B) The entry into B cells is initiated by the binding of the viral glycoprotein gp350 to the cellular complement receptor CR2 or sometimes CR1. Gp42 then forms a complex with the heterodimer gH/gL. After the binding of gp42 to cellular HLA-II, the gp42/gH/gL complex activates gB, which in turn mediates the fusion of the viral envelope with the cellular, endocytic membrane. C) In contrast, the EBV entry into epithelial cells is endocytosis independent. The viral envelope fuses directly with the cellular membrane and releases the capsid into the cytoplasm. D) The entry is probably mediated by the direct interaction of gH/gL with cellular αvβ6/αvβ8 integrin receptors. This causes a conformational change of the fusion protein gB, which mediates the fusion of the viral and cellular membrane. Adapted from [150]. Created with BioRender.

Once EBV entered the cell, the viral capsid is released into the cytoplasm and disassembled. The viral genome is then transported to the cell nucleus and replicated by DNA polymerases during the lytic or productive phase of the viral life cycle. Lytic genes are then expressed in three phases: immediate-early (IE), early, and late. IE proteins such as BZLF-1 and BRLF-1 act as further transactivators of the lytic program [151]. Early gene products have a variety of functions including replication, metabolism, and inhibition of antigen processing while late gene products are mainly structural proteins or proteins responsible for immune evasion. The infection of epithelial cells is believed to be mainly lytic in nature while EBV establishes latency in memory B cells. How the virus gains access to the memory compartment is still controversial. The germinal center model

postulates that, after a short pre-latent phase with both lytic and latent gene expression, EBV initiates a growth and proliferation program in naïve B cells (Latency III). These infected B cells become activated lymphoblasts and migrate to the follicle of a lymph node where they expand to form a germinal center. Survival of such B cells usually depends on signals from antigen-presenting DCs and antigen-specific T_H cells. Those signals are assumed to be mimicked by EBV using the Latency II program [152, 153]. Virus-carrying, quiescent memory B cells (Latency 0) subsequently exit the lymph node to circulate in the peripheral blood. Those memory B cells are able to evade immune recognition since no viral antigens are expressed in this phase. During cell division, only EBNA1 is expressed to ensure the replication of the viral genome (Latency I) [154]. The number of infected B cells in the peripheral blood can vary considerably between individuals but is quite stable during latency with 1-50 per million B cells [155].

Spontaneous reactivation into the lytic cycle in infected B cells can occasionally happen and leads to the infection of other cells and virus shedding in the saliva. Since contact with foreign antigens and the subsequent terminal differentiation into plasma B cells can trigger reactivation, any new infection can lead to lytic replication [156]. Reactivation in immunocompetent carriers usually causes no symptoms because cytotoxic T cells efficiently control the infection. However, reactivation due to immunodeficiency or immunosuppression can lead to various lymphoproliferative diseases [157].

1.3.3 EBV-associated diseases and their treatment

While EBV infection is usually asymptomatic, it can be associated with a vast number of non-malignant, pre-malignant, and malignant diseases. EBV is best known as the main cause of infectious mononucleosis [158], a non-malignant clinical manifestation of primary EBV infections. The disease owes its name from the atypical, large lymphocytes that were observed and that are now known as Downey cells. They are activated, mostly EBV-specific $CD8^+$ T cells. The substantial expansion of this highly activated $CD8^+$ compartment correlates with the severity of IM symptoms, which supports the view that IM is an immunopathologic disease [159, 160]. Symptoms can vary considerably but fatigue, fever, a sore throat, and swollen posterior cervical lymph nodes are typical. The disease is generally self-limiting, and the acute symptoms resolve in two to four weeks. The fatigue, however, can last for months [161]. Rare complications include airway obstruction, meningoencephalitis, hemolytic anemia, thrombocytopenia, splenic rupture, and many more [151].

In cases of insufficient viral replication control, chronic active EBV (CAEBV) infection is a rare but life-threatening lymphoproliferative disorder. It is characterized by chronic infectious

mononucleosis-like symptoms for more than 6 months, viremia, and infiltration of organs with EBV-infected lymphocytes. CAEBV is often associated with the infection of T and NK cells. Untreated patients will develop immunodeficiency and eventually suffer from opportunistic infections, hemaphagocytosis, lymphomas or multi-organ failure. Although many treatments including antiviral therapy, immunosuppressive agents, interferon, and chemotherapy have been tried, hematopoietic stem cell transplantation is currently the only curative treatment for this disease [162].

EBV is also causally associated with most post-transplant lymphoproliferative diseases (PTLD). Those diseases range from benign polyclonal B cell proliferation to malignant B cell lymphomas and are due to the immunosuppressive treatment after transplantation. The occurrence of this often fatal disorder correlates with the type and dose of the immunosuppressant medication, and reduction of this treatment is key for the successful therapy of PTLD [163, 164]. The standard therapy after reduction of immunosuppression includes the CD20 monoclonal antibody rituximab [165, 166] combined with chemotherapy (doxorubicin, cyclophosphamide, vincristine, prednisone) [167]. However, reduced immunosuppression can lead to graft rejection while the therapy with rituximab combined with chemotherapy can be associated with rare but severe side effects such as leukopenia, infection, or even death. Further treatment options are other chemotherapeutic regiments, interferon therapy, radiation, or antiviral therapy [168]. New therapies such as adoptive T cell transfer are being studied in clinical trials [169, 170] and achieve promising results.

There is a plethora of malignant lymphoproliferative disorders linked to EBV including non-Hodgkin lymphoma, diffuse large B cell lymphoma, Burkitt lymphoma, nasopharyngeal carcinoma, gastric carcinoma, T cell and NK cell lymphomas and many more [171]. In general, it is assumed that EBV is associated with around 200,000 malignancies worldwide each year [172]. Recent studies further suggested that EBV could increase the risk of developing other major diseases such as systemic lupus erythematosus, multiple sclerosis, rheumatoid arthritis, juvenile idiopathic arthritis, inflammatory bowel disease, celiac disease, type 1 diabetes, and others [173, 174]. Altogether, this led to an increasing interest in an EBV vaccine [140].

1.3.4 Immune response against EBV

Although a large part of the population is infected with EBV, symptoms occur only in some, mostly post-pubescent, individuals. The many cases of EBV-associated diseases during immunosuppression impressively demonstrate the involvement of the immune system in the EBV-specific defense. While EBV triggers a humoral as well as a cellular immune response, the cellular arm, especially cytotoxic T cells, seems to be more effective in limiting EBV infections [160, 175]. However, the

serological response to EBV is used as a diagnostic tool and can help to define the EBV disease status. Antibodies against viral capsid antigens (VCA), EBNA1, early antigens, and gp350 are detectable. The first exposure to EBV usually triggers an early VCA-IgM reaction that decreases again before convalescence. It is therefore a marker for acute primary infection. IgG antibodies against VCA arise shortly after, can persist throughout the whole life and indicate a recent or a past infection. Neutralizing EBNA-IgG only arises months after primary infection and is also detectable for life [176]. However, 5-10% of infected individuals never develop an antibody response against this protein [131]. Due to this and other variations in individual antibody responses, the interpretation of serological tests is challenging [176]. Although studies suggested that the induction of neutralizing antibodies could prevent the development of IM [177], little attention has been given to such antibodies as therapeutic option [160].

The innate cellular immune system, mainly represented by NK cells, also participates in the fight against EBV. The exact role of NK cells in EBV infection is, however, not yet fully understood. An increase in the number of blood NK cells can be detected in infectious mononucleosis patients, which is often but not always associated with a decreased viral load [178]. Furthermore, NK cells are able to affect viral lytic replication and can kill infected B cells [179, 180]. The fact that a specific EBV-reactive NK cell population (early differentiated NK cells, $CD56^{dim}$ $NKG2A^{+}$ KIR^{-}) decreases during the first decade of life, suggests that an age-dependent defect in the NK cell response may lead to a compensation by cytotoxic T cells, which in turn causes IM [181].

As previously described, IM is accompanied with an immense expansion of the $CD8^{+}$ T cell compartment that mainly contains T cells specific for lytic EBV proteins. Following a clear hierarchy, T cells specific for immediate-early proteins are the most abundant T cells while a smaller number is specific for early proteins and only few are specific for late proteins [182]. This mirrors the increasing effect of immune evasion in the progression of the lytic cycle. $CD8^{+}$ T cell responses against latent proteins have low frequencies and are mainly directed against the EBNA3 family of proteins [183, 184]. Responses of $CD8^{+}$ cells against EBNA1, however, are hardly ever detected due to an internal glycine-alanine repeat domain that diminishes the messenger RNA translation [185] and protects the mature protein from proteasomal degradation thereby inhibiting the presentation on HLA-I molecules [186, 187]. The majority of EBV-specific T cells are highly activated with expression of HLA-DR, CD38, and CD45RO and show downregulation of the lymph node homing marker CD62L [188].

During asymptomatic primary infection, the total number of $CD8^{+}$ T cells in the blood is not elevated. Nevertheless, high frequencies of activated EBV-specific $CD8^{+}$ T cells can be detected, although lower in magnitude than in IM patients [189]. While responses to individual lytic epitopes

can constitute up to 50% of the whole $CD8^+$ T cell compartment during acute infection [190], this proportion shrinks in persistent infection to up to 2% and 0.5% for lytic and latency-specific responses, respectively [160]. EBV-specific $CD8^+$ memory T cells show differences in their phenotype depending on whether they are specific for epitopes derived from lytic or latent proteins. While latent epitope-specific $CD8^+$ memory T cells are uniformly $CD45RO^+$ and $CD28^+$, lytic epitope-specific populations are heterogeneous in CD45RO/RA and CD28 expression. They are negative for the activation markers CD69 and CD38 but show peptide-specific cytotoxicity with type 1 cytokine (IFNγ and TNF) production upon stimulation [191].

The absolute $CD4^+$ T cell number expands considerably less in IM patients compared to that of $CD8^+$ T cells. However, single EBV-specific $CD4^+$ T cell populations can strongly amplify during acute infection, reaching frequencies of 1% of $CD4^+$ T cells in the blood [160], decline rapidly thereafter and are still detectable in healthy virus carriers [192, 193]. Similar to their $CD8^+$ counterparts, EBV-specific $CD4^+$ T cells express high levels of CD38 and CD45RO and lack the lymph node homing markers CCR7 and CD62L [193].

Epitope-specific $CD4^+$ memory T cell populations can constitute up to 0.1% of the whole $CD4^+$ T cell pool, 10- to 20-fold less than those of the $CD8^+$ T cell pool [160]. The $CD4^+$ response also shows differences in comparison to the $CD8^+$ response in its epitope hierarchy with a broader distribution of lytic and latent cycle proteins as targets [194]. Moreover, the response to EBNA1 is atypical with a hardly detectable response during acute infection and a delayed but significant EBNA1-specific $CD4^+$ T cell response 2-13 months after primary infection [193]. Almost all EBV-specific $CD4^+$ memory T cells are part of the central memory ($CD45RA^-$ $CD45RO^+$ $CCR7^+$) or the effector memory ($CD45RA^-$ $CD45RO^+$ $CCR7^-$) compartment with an average ratio of 1:1 and express CD28 and mostly CD27 [193].

1.4 Human cytomegalovirus (HCMV)

HCMV or *Human herpesvirus 5* (HHV-5) is a double-stranded DNA virus that belongs to the genus *Cytomegalovirus* and subfamily *Betaherpesvirinae* within the family of *Herpesviridae*. It takes its name from the characteristic morphological changes that are induced after infection; the cells round up and increase their volume. HCMV infects the majority of adults, with a seroprevalence ranging from 45% in some European countries to almost 100% in developing countries [195]. While primary infection is usually asymptomatic, HCMV can cause severe disease in immunocompromised individuals such as AIDS patients or transplant recipients. Infection or reactivation from latency in those individuals can result in hepatitis, pneumonitis, retinitis, gastroenteritis, encephalitis,

transplant rejection, or even death. Congenital infection of the fetus can also damage the central nervous system leading to motor deficits, sensorineural hearing loss, and mental retardation (reviewed in [196]).

It is further thought that subclinical infections with HCMV are involved in a variety of diseases such as inflammatory [197], hypertensive [198], and possibly pulmonary diseases [199]. Although HCMV is not yet classified as an oncogenic virus, it expresses several potential onco-proteins with transforming capacities [200-203], and HCMV gene products are present in many tumors [204-207]. The primary infection is followed by lifelong latency with recurrent reactivation.

1.4.1 Structure and genome

HCMV is a relatively large virus with 150-200 nm in diameter [196]. The virion's linear genome is densely packed in an icosahedral capsid embedded in a proteinaceous tegument, which in turn is surrounded by the lipid envelope. The capsid has a diameter of approximately 130 nm and consists of 162 capsomers (12 pentons and 150 hexons) and 320 triplexes arranged on a T = 16 lattice. Capsomers contain five (pentons) or six (hexons) major capsid proteins (MCP, UL86). In hexon capsomers, one smallest capsid protein (SCP, a short ORF between UL48 and UL49, also UL48/49) is located on top of each MCP. The triplex structures are composed of the minor capsid protein-binding proteins (mC-BP, UL46) and minor capsid proteins (mCP, UL85) in a ratio of 2:1 [208].

The tegument contains at least 39 different viral proteins with phosphoprotein 65 (pp65) being the most abundant (reviewed in [209]). Not only viral but also cellular proteins are part of the tegument [210]. Upon virus entry, those proteins are directly released into the cytoplasm of the infected cell and are able to function before the onset of viral protein production in this cell. The lipid bilayer of the envelope contains at least 17 viral glycoproteins including gB (UL55) [211, 212], gM (UL100) [213, 214], gH (UL75) [215], gL (UL115) [216], gO (UL74) [217], gN (UL73) [218], gp48 (UL4) [219], TRL10 (RL10) [220], UL33 [221], US27 [222], UL128, UL130, UL131 [223], UL1 [224], UL78 [225], UL116 [226], and UL132 [227]. Many of those envelope proteins are required for the attachment to the host cell, the virus entry, and immune evasion.

With its almost 236 kbp long double-stranded DNA genome, HCMV has the largest genome among human herpesviruses [228]. The genome consists of two unique regions, U_L and U_S, that are flanked by inverted repeats (TR_L, IR_L, TR_S, and IR_S). The complete DNA sequence of HCMV was uncovered long ago [228, 229]. After initial estimates of 165 ORFs [228], the number of identified ORFs has risen steadily ever since [230, 231]. Conservative estimates of less than 200 ORFs probably do not capture the complexity of the HCMV genome and its coding capacity. With its over 100 splicing sites, short ORFs, upstream ORFs, transcript polycistrony, and antisense transcripts, the HCMV

genome has a highly complex transcriptome [232]. Consequently, Erhard *et al.* recently postulated a staggering number of 944 ORFs using ribosome profiling [233]. Uniprot, however, currently lists solely 193 reviewed proteins for the strain AD169 (accessed 04.03.2020) [234].

The HCMV strain AD169, found 1957 in adenoid tissue cultures, was the very first to be sequenced and has since been the model laboratory strain in HCMV research [229, 235]. However, a study of Cha *et al.* in 1996 revealed that high-passage strains such as AD169 and Towne suffered substantial deletions in the UL*/b'* region in comparison with the virulent low-passage strain Toledo and clinical isolates [236]. The repeated passaging of virus strains in cultured cells leads to a rapid selection of mutations in distinct genes including RL13, UL128, UL130, UL131A, and UL140-UL145 [237]. The clinical isolate Merlin was therefore sequenced after passage 3 [228] and has since become the first World Health Organization International Standard for HCMV [238].

Cloning of HCMV genomes as bacterial artificial chromosomes (BACs) offers the possibility to work with stable, genetically defined virus strains. The basis of the BAC used in this work, strain AD169*var*L, contains most of the UL*/b'* region including ORFs UL150, UL149, UL148A/B/C/D, UL148, UL147A, UL147, UL146, UL145, UL139, UL138, UL136, UL135, UL134, and UL133 but is lacking UL140-UL144 [239].

1.4.2 HCMV life cycle

The virus is transmitted *via* body fluids such as saliva, tears, blood, urine, and breast milk or *via* transplanted organs. HCMV has a very broad cell tropism including epithelial cells, endothelial cells, connective tissue cells (e.g. fibroblasts), hepatocytes, smooth muscle cells, and some leukocyte populations (reviewed in [240]). Especially, the infection of endothelial and hematopoietic cells facilitates the fast, systemic distribution throughout the whole body.

As all human herpesviruses, HCMV requires two highly conserved envelope glycoproteins for the entry into target cells, also called core fusion proteins: gB [241] and the disulfide-linked dimer gH/gL [242]. gH/gL can either assemble with gO [243] or with the three proteins UL128, UL130, and UL131 forming a trimer and a pentamer [244], respectively. The latter is essential for the entry into epithelial, endothelial, and myeloid cells while the trimer is sufficient for the infection of fibroblasts [244]. Defects in the genes UL128, UL130, and UL131 of the laboratory strain AD169 are the reason for its inability to infect epithelial and endothelial cells [245, 246]. A recent study found another protein, UL116, to be able to form dimers with gH [226]. However, its exact function and receptor remain unclear.

Virus attachment is probably mediated *via* binding of cell-surface heparan sulfate proteoglycans by the disulfide-linked heterodimer gM/gN [247, 248]. The binding of gH/gL complexes to their receptors leads then to the initiation of virus entry and the fusion of the viral envelope with the host membrane. The platelet-derived growth factor receptor alpha (PDGFRα) was found to be the receptor of the gH/gL/gO trimer [249, 250] while neuropilin-2 is the cell entry receptor of the pentamer [251]. The role of the homotrimer gB in entry of HCMV is controversial. While it functions only as a fusogen in other herpesviruses (reviewed in [252]), several cell-surface proteins have been proposed to be gB receptors in HCMV entry: the epidermal growth factor receptor (EGFR) [253], PDGFRα [254], and integrins [255, 256]. However, another study by Wille *et al.* supports the hypothesis that gB does not need to bind receptors but is the fusion protein which is activated by gH/gL after its binding to gH/gL receptors [257]. The current view of the entry process of HCMV is shown in Figure 5. Many more molecules (i.e. CD147, CD151, CD90) were reported to be receptors in HCMV entry (reviewed in [258]). Considering the wide cell tropism of HCMV, it seems not unlikely that those molecules function as co-receptors affecting downstream events in different cell types during the entry [258].

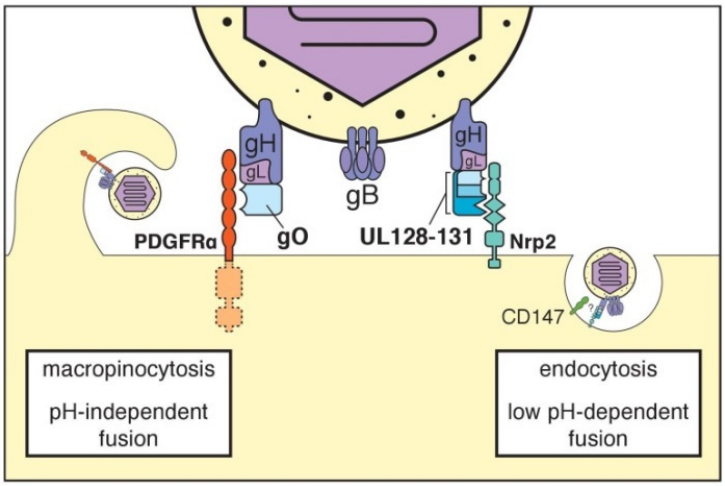

Figure 5: Receptors of HCMV gH/gL complexes. The trimer gH/gL/gO binds to PDGFRα and drives a pH-independent entry that involves macropinocytosis. The pentamer gH/gL/UL128–131 binds to Nrp2 initiating a pH-dependent entry that involves endocytosis. The entry *via* the pentamer is promoted by CD147 although the exact mechanism is unknown. Adapted from [258].

After fusion of the viral envelope with the host membrane, tegument proteins and the capsid are released into the cellular cytoplasm. Facilitated by the microtubule network and tegument proteins, the capsid with the viral genome is transported to the nucleus [259] and gene expression is initiated. HCMV gene expression during lytic or productive cycle happens in a sequentially ordered manner conventionally divided into immediate-early (IE, also called α), early (E, β), and late

phases (L, γ) [260]. IE genes are the first viral genes transcribed after infection (0-4 hours post infection (h.p.i.)) and do not rely on prior *de novo* viral protein synthesis but on the activation of the major immediate-early promoter (MIEP), which in turn is activated by tegument proteins and cellular transcription factors [261]. In contrast, early genes require the prior synthesis of viral IE proteins and cellular proteins for their transcription (4-48 h.p.i.) [262]. Late genes usually code for structural proteins and proteins required for viral egress (48-72 h.p.i.) [261]. A fourth class of genes was defined as early-late or leaky-late (E-L, γ1) that is expressed at low levels early and at greatly amplified levels after DNA replication [263]. "True late" genes (γ2), on the other hand, are completely dependent on viral DNA replication late in infection [261]. In contrast to the conventional functional classification, Weekes *et al.* found five different temporal protein profiles, Tp1, Tp2, Tp3, Tp4, and Tp5. While Tp1, Tp2, Tp3, and Tp5 resemble the functional IE, E, E-L, and L class, respectively, Tp4 peaks at 48 h and has a so far unclear functional profile [264]. The viral DNA replication for the production of new virions occurs in the nucleus within viral replication centers [265].

The viral gene expression and the infection outcome is strongly regulated by the cellular environment (reviewed in [266]). While many cell types promote lytic infection, latency is usually established in cells of the myeloid lineage including $CD14^+$ monocytes [267] and their $CD34^+$ progenitors in the bone marrow [268]. One would assume that the virus expresses no or only a limited number of genes, as seen in HHV-4, to evade the host immune system during latency. In fact, earlier studies found only few genes to be latency-associated such as UL138, an UL81-82 antisense transcript, US28, and a splice variant of UL111A, a viral IL-10 homolog [269-272]. Even fewer latency gene products could be assigned a function. However, two recent studies by Cheng *et al.* and Shnayder *et al.* revealed that the set of transcripts during latency is much broader than previously assumed [273, 274]. Moreover, they found no specific latency-associated expression program but a gene expression that largely mirrors the late lytic transcriptional program, albeit at much lower levels of expression [274].

The process of reactivation of the lytic lifecycle is not fully understood. However, the cellular differentiation of monocytes to a macrophage or a DC is known to be a key trigger in this event suggesting that the cellular environment regulates reactivation (reviewed in [275]). Moreover, the earliest events in reactivation from latency are the reactivation of IE gene expression, which is regulated by MIEP and enhancer regions.

After the reactivation, the virus replicates its genome and produces proteins required for its packaging and egress. After the genome is packed in the capsid it is translocated to the cytoplasm, a process called nuclear egress. The capsid thereby receives its primary envelope by budding at the

inner nuclear membrane and gets uncoated at the outer nuclear membrane. Virion maturation and final envelopment by budding into vesicles of the trans-Golgi network then occurs in the cytoplasm after which the vesicle membrane fuses with the cellular membrane and releases the virions from the cell (reviewed in [276]).

The replication cycle of HCMV is compared to other viruses relatively slow with 2-3 days.

1.4.3 Immune response against HCMV

Immunocompetent hosts can effectively control acute HCMV infection with a multifaceted immune response. The virus triggers the innate and the adaptive immune system including the humoral response and cellular responses by NK cells as well as by $CD4^+$ and $CD8^+$ T cells.

One of the earliest events in the immune response to HCMV is the recognition of HCMV or its particles directly after virus entry by the Toll-like receptor 2 (TLR2). TLR2 is able to recognize the envelope proteins gB and gH and activates the NF-κB pathway, which in turn mediates the induction of inflammatory cytokines and IFN-stimulated genes [277, 278].

While the important role of NK cells in murine cytomegalovirus (MCMV) infection is evident [279, 280], the extent of their involvement in controlling HCMV is less clear. In general, individuals with NK cell defects can suffer from recurrent virus infections (reviewed in [281]). The recovery of patients with HCMV disease after bone marrow transplantation was shown to correlate positively with the NK cell activity [282]. Another indicator that the NK cell-mediated response is important in fighting HCMV is the immense effort of the virus to evade NK cell activation (see 1.4.4).

Besides NK cell responses, HCMV also triggers the humoral response with antibodies directed against numerous HCMV antigens. A major target for antibody-mediated neutralization is the pentamer gH/gL/UL128-131 [283] and trimer gH/gL/gO [284], which are required for the cell entry. There are, however, antibody responses against other envelope proteins (mainly gB and gH), tegument proteins (pp65 and pp150) as well as non-structural proteins such as IE1 (reviewed in [285]).

HCMV-specific $CD8^+$ T cells seem to play the crucial part in the immune response to this virus. In mouse models, MCMV-specific $CD8^+$ T cells efficiently protected mice from lethal MCMV challenge, even in the absence of $CD4^+$ T cells [286, 287]. In humans, numerous studies with bone marrow transplantation patients showed that their protection from HCMV disease strongly correlates with the recovery of HCMV-specific $CD8^+$ T cell populations [288-290]. Successful adoptive T cell transfers of *ex vivo* proliferated HCMV-specific $CD8^+$ T cells that protect from primary infection and

reactivation additionally demonstrate the effectiveness of this arm of the immune response [291-293].

The targets of HCMV-specific $CD8^+$ T cells are manifold. The immunodominant antigens are clearly pp65, IE1, and to a lesser extent pp150 with often very strong T cell responses in almost every seropositive individual [292, 294-296]. Thus, the majority of studies screening for T cell epitopes is focused on those proteins [285, 297]. However, several studies demonstrated the broad repertoire of antigens. A bioinformatics prediction approach by Elkington *et al.* observed $CD8^+$ T cell-mediated responses against 13 out of 14 tested proteins (pp65, pp50, pp28, pp150, IE1, US2, US3, US6, US11, UL16, UL18, gB, and gH) [296]. A study, where PBMCs of healthy seropositive donors were stimulated with fibroblasts infected with a ΔUS2-US11 deletion mutant virus, identified high frequency responses against pp65, IE1, pp150, and gB. In addition to these proteins, T cell responses against undefined IE and early proteins were detected [298]. The most comprehensive study tested 13,687 predicted peptides covering 213 different ORFs for their ability to elicit a $CD4^+$ or $CD8^+$ T cell response. A remarkable number of 151 ORFs were recognized by T cells. Three of them elicited a T cell response in more than half of the tested donors: UL83 (pp65), UL123 (IE), and UL48 [299].

During primary infection, pp65-specific T cells are detectable shortly after the appearance of HCMV-specific antibodies [300], show a great expansion [301], and exhibit an activated, cytolytic phenotype with high expression of ki67, granzyme B, and perforin, as well as a $CD45RO^+$, $CD27^+$, $CCR7^-$, $CD28^-$ phenotype. After the contraction phase, many specific $CD8^+$ memory T cells re-express CD45RA and are functional as they express perforin and granzyme. Most HCMV-specific $CD8^+$ memory T cells are $CD28^-CCR7^-$ and have variable expression of CD27 (reviewed in [285]).

The total pool of HCMV-specific $CD8^+$ memory T cells can reach up to 30% of the peripheral blood T cell population and regularly reaches 5-10% although individuals vary greatly in their $CD8^+$ T cell response [299]. This is, *inter alia*, due to the phenomenon termed memory inflation. While the memory T cell population usually contracts after infections and only a small specific population is preserved, the HCMV-specific $CD8^+$ memory T cell pool is mostly maintained and undergoes prolonged expansion (reviewed in [302]). The size of this population is therefore usually extraordinarily large and increases with age [303]. Memory inflation does not focus on immunodominant epitopes since also subdominant responses can inflate at later time points [304]. There is a presumption that the selection of epitopes in memory inflation is based on their independence of the immunoproteasome in processing [305, 306].

The HCMV-specific $CD4^+$ part of the adaptive cellular immune response was shown to be essential for an effective $CD8^+$ T cell response [292, 293]. Moreover, HCMV-specific $CD4^+$ T cells do not only

have a helper function but also cytotoxic activity [307]. They arise even before the anti-HCMV antibody response and play a critical role in the protection against HCMV disease [308].

$CD4^+$ T cells have similar target ORFs as $CD8^+$ T cells with several particular ORFs (reviewed in [285]). The response is very broad with individuals responding to a median of 12 different ORFs of which five ORFs (UL55, UL83, UL86, UL99, and UL122) were recognized by more than half of the tested donors in the previously mentioned study by Elkington *et al.* [296].

HCMV-specific $CD4^+$ T cells generally constitute around 5% of the total peripheral $CD4^+$ T cell pool but can reach up to 20% [299], which is less than the $CD8^+$ population. They also hardly show memory inflation with age [309, 310]. The majority of HCMV-specific $CD4^+$ memory T cells has an effector memory phenotype with $CD45RO^+$, $CD27^-$, $CD62L^-$, $CD11a^{high}$, and $CCR7^-$ [285, 309]. There is also a significant population of $CD45RA^{high}$ cells in the HCMV-specific $CD4^+$ memory pool [309]. $CD4^+$ T cells which lack the costimulatory receptor CD28 are usually rare in peripheral blood. However, this subset is frequently detectable in HCMV-infected individuals and can execute HCMV-specific cytotoxicity *via* granzyme B and perforin [311].

The fact that a T cell-mediated immune response develops despite the extensive immune evasion strategies of HCMV (see 1.4.4) is probably also due to the fact that a large part of T cell priming takes place *via* cross presentation [312].

HCMV is also able to induce HCMV-specific Treg responses [313] and γδ T cells [314, 315]. However, their exact role in the interplay of HCMV and host immune system needs to be further investigated.

1.4.4 Immune modulation and evasion mechanisms of HCMV

Although immunocompetent individuals are usually able to control acute HCMV infection, the virus establishes a lifelong latency from which it can repeatedly reactivate. To achieve this, the virus is known to effectively evade the host immune system by employing sophisticated immune-modulation strategies. The fact that about 70% of the ORFs of AD169 are not essential for viral replication in fibroblasts mirrors the focus of HCMV on immune evasion and its broad cell tropism [316]. Most of the immune evasion proteins are encoded in the U_S region of the HCMV genome and some in the U_L region. They can be divided into four families, the UL18, US6, US12, and RL11 family (Table 2, reviewed in [317]).

One major evasion strategy is the modulation of antigen presentation on infected cells to prevent the recognition by $CD8^+$ T cells. Members of the US6 family (US2-US11) are responsible for the downregulation of HLA-I by impairing its stability and localization. The glycoproteins US2 and US11 bind HLA-I molecules and mediate their reverse transport into the cytosol for subsequent degradation by the proteasome [318-320]. The gene product of US3 directly binds to tapasin and

inhibits tapasin-dependent peptide loading, thereby blocking maturation and translocation of HLA-I molecules to the cell surface [321, 322]. US6 also prevents the assembly of HLA-I-peptide complexes by inhibiting the transport of peptides into the ER *via* TAP [323, 324]. It therefore binds TAP and inhibits the binding of ATP to TAP and the subsequent conformational changes necessary for the peptide transport [325]. Apart from inhibiting the maturation of classical HLA-I molecules, US10 seems to specifically target the non-classical HLA-G [326, 327].

The downregulation of HLA molecules on the cell surface prevents the recognition by T cells but triggers the activation of NK cell *via* a process called “missing-self recognition”. NK cells are usually kept inactive by the interaction of inhibitory NK cell receptors with self-ligands on HLA-I molecules. Thus, downregulation of HLA-I results in the loss of the inhibitory signal and subsequent target cell lysis by the NK cells [328, 329]. Therefore, HCMV developed several mechanisms to limit the activation of NK cells, mainly with the help of surrogate ligands that can be recognized by inhibitory NK cell receptors. One example is the HLA-I homologue UL18 that can associate with β2m and peptide and binds to the inhibitory receptor leukocyte immunoglobulin-like receptor subfamily B member 1 [330, 331].

NK cells also monitor HLA expression *via* the recognition of HLA-E that presents peptides derived from the leader sequence of classical HLA molecules [332, 333]. HCMV uses a peptide from the glycoprotein UL40 to mimic these cellular peptides thereby preventing NK cell activation [334, 335]. However, HCMV can not only mimic ligands of inhibitory NK cell receptors but can also downregulate the surface expression of ligands for activating receptors such as NKG2D and others (reviewed in [317]).

On the other hand, immunoevasins of the RL11 cluster are able to bind to the Fc region of CMV-specific antibodies to block the antibody-dependent cellular cytotoxicity by NK cells [317, 336].

HCMV is not only able to mimic NK cell ligands, Fc receptors, and HLA molecules but also expresses a viral IL-10 encoded by the ORF UL111A [337]. Viral IL-10 has the same anti-inflammatory effects as its human counterpart and inhibits the activation and maturation of DCs [338], upregulates the production of cellular IL-10 [338, 339], suppresses the production of pro-inflammatory cytokines [340], and hampers the expression of HLA-I and -II [341]. Another mechanism to reduce HLA-II on the cell surface is the direct degradation of HLA-II molecules by US2 and US3 [342, 343].

In total, the multifaceted and sophisticated immune evasion strategies of HCMV demonstrate its high degree of host adaption and allow the virus to establish a lifelong infection in its host.

Table 2: Immunoevasins of HCMV. Adapted from [317].

Immunoevasin	Target	Mechanism
US2[a]	MHC-I, MHC-II, HFE, CD1d	Proteasomal degradation
US3	MHC-I-tapasin	ER retention
US6	MHC-I-TAP	Prevents peptide translocation into the ER
US10	MHC-I, HLA-G	Delayed maturation of MHC-I, degradation of HLA-G
US11	MHC-I	Proteasomal degradation
pp71 (UL82)	MHC-I	May block surface expression
pp65 (UL83)[a]	MHC-II	Lysosomal degradation
miR-376a[a]	HLA-E	Blocks surface expression
miR-US4-1	ERAP1	Blocks processing of viral peptides
UL18	LIR1	Direct binding
UL40[b]	CD94-NKG2A, LIR1	Promotes surface expression of HLA-E and UL18
US2[a]	Nectin 2	Proteasomal degradation
US9	*MICA*008*	Proteasomal degradation of NKG2D ligand
US12	ULBP2	Downregulation of NKG2D ligands
US13	MICA, MICB, ULBP2	Downregulation of NKG2D ligands
US18	MICA, B7-H6	Lysosomal degradation of activating receptor ligands
US20	MICA, MICB, B7-H6, ULBP2	Lysosomal degradation of activating receptor ligands
UL16	MICB, ULBP1, ULBP2, ULBP6	Intracellular retention of NKG2D ligands
UL141[a]	Nectin 2/nectin-like protein 5	ER retention of activating receptor ligands
UL142	MICA, ULBP3	Intracellular retention of NKG2D ligands
UL148A	MICA	Lysosomal degradation of NKG2D ligand
pp65 (UL83)	NKp30	Dissociates CD3ζ adaptor module
miR-UL112	MICB	Downregulates expression of NKG2D ligand
RL11	IgG1-IgG4	Block FcγR activation and ADCC
UL119	IgG1-IgG4	Block FcγR activation and ADCC, lysosomal degradation
RL12	IgG1, IgG2	Binds to Fcγ
RL13	IgG1, IgG2	Internalizes Fcγ to endosomes
US2[a]	Integrin-α	Degradation
UL11	CD45	Direct binding
UL141[a]	TRAILR1 and TRAILR2	Retains death receptors in the ER to prevent apoptosis

Abbreviations: 7-TM, seven-transmembrane; ADCC, antibody-dependent cellular cytotoxicity; dUTPase; deoxyuridine triphosphatase; ERAP1, endoplasmic reticulum aminopeptidase 1; LIR1, leukocyte immunoglobulin-like receptor subfamily B member 1; MIC, MHC class I polypeptide-related sequence; ND, not defined; TAP, peptide transporter involved in antigen processing; TRAILR, tumor necrosis factor-related apoptosis-inducing ligand receptor; ULBP, UL16-binding protein.

[a] Immunoevasins that fit into more than one category.

[b] Inhibitory receptor surrogate ligands that are also recognized by activating receptors.

1.4.5 Treatment of HCMV

Four antiviral drugs are mainly used for systemic treatment and prophylaxis of HCMV infections: ganciclovir (and valganciclovir), cidofovir, foscarnet and the recently approved letermovir. Ganciclovir was the first therapy approved for HCMV infections and is the first line treatment against HCMV. Ganciclovir is a synthetic analogue of deoxyguanosine and becomes ganciclovir triphosphate after its phosphorylation. Its incorporation into DNA leads to the preferential inhibition of the viral DNA polymerase UL54 [344]. Valganciclovir is a prodrug with an improved bioavailability [345]. Common adverse effects are neutropenia, anaemia, thrombocytopenia, a possible long-term reproductive toxicity, and many more [346]. Drug resistance can occur *via* mutations in UL97, the kinase which is responsible for the first phosphorylation of ganciclovir, and its target UL54 [347].

Cidofovir and foscarnet are second-line drugs that both mainly inhibit the viral DNA polymerase. Cidofovir has limited benefit since it is slowly absorbed, has a poor bioavailability and causes nephrotoxicity. Foscarnet can cause renal impairment [346].

Letermovir is a relatively new antiviral drug that inhibits the viral replication *via* the viral terminase complex UL51/UL56/UL89 [348]. It has two advantages over the conventional antiviral drugs: It is only mildly toxic and targets the terminase complex instead of the DNA polymerase and can therefore not induce cross-resistance. However, resistance can still occur *via* mutations in the ORFs coding for the terminase complex proteins (reviewed in [349]). Other drugs such as maribavir, brincidofovir, and filociclovir are under investigation in advanced clinical trials [350].

Neutralizing antibodies targeting envelope proteins such as gB and gH are another treatment strategy. Therapeutic approaches using hyperimmune globulin and monoclonal antibodies showed promising results in several studies and clinical trials [351-354]. However, no antibody is so far used as a standard treatment in the clinics.

In accordance with the central role of T cell-mediated immune responses in the natural defence against the virus, adoptive transfer of HCMV-specific T cells is another attractive approach; especially in the context of hematopoietic stem cell transplantation where viral infections and reactivations cause morbidity and mortality in immunosuppressed patients. Early studies in mice demonstrated the effectiveness of transferred CMV-specific T cells in controlling the virus [355-357]. First studies by Riddell *et al.* in humans also showed that HCMV-specific $CD8^+$ T cells from autologous donors could be generated *ex vivo* and were able to prevent HCMV infections without causing graft-versus-host disease [291, 292]. This method however required extensive cell culture of 8-10 weeks. Thus, following studies focused on a faster generation of cellular therapy products. HCMV-specific T cells can be enriched by the *ex vivo* co-culture with HCMV lysate [358], proteins

[293, 359], overlapping peptide pools [360], or APCs either pulsed with peptides [361] or transfected with vectors that encode viral proteins [362]. The direct isolation of specific T cells from seropositive donors can be performed either on the basis of HLA-peptide multimer binding [363] or the induction of cytokine secretion (e.g. IFNγ catch technology) [359, 364]. The main limitation of all those approaches remains the time-consuming preparation of specific T cells. A prophylactic preparation of virus-specific T cells for each transplant patient is, however, not feasible since only a small proportion of them suffers from HCMV infection. Moreover, the generation of personalized specific T cells under "good manufacturing practice" conditions is labor- and cost-intensive. Another major drawback is the need for HCMV seropositive transplant donors, which would once more radically limit the choice of possible donors. Therefore, the establishment of biobanks with seropositive third-party donors has been a major goal in recent years [365-367]. This allows for a rapid "off-the-shelf" treatment of severe viral infections after stem cell transplantation.

Although there are several options available or in development, the search for novel therapies is still ongoing due to the limitations of current treatment options, such as side effects, ineffectiveness, drug resistance, limited availability, and high costs. Much effort is therefore invested in the development of an HCMV vaccine (reviewed in [368]). The first attempt was to attenuate HCMV strains that were isolated for laboratory work, AD169 and Towne [369, 370]. AD169 was quickly abandoned but the Towne strain underwent extensive testing. However, while the vaccine was safe [371, 372] and could protect against severe HCMV disease [373], it did not protect against primary HCMV infection [374] and was only as effective as naturally induced immunity for low-dose challenges [375]. Vaccines comprising the protein gB and different adjuvants provided also only moderate protection with quickly fading neutralizing antibody levels [376, 377]. In contrast, the proteins of the pentameric complex (gH, gL, UL128-131) caused higher levels of neutralizing antibodies than gB [244].

One exemplary peptide-based vaccine comprised an HLA-A*02:01-restricted, pp65-derived peptide ($pp65_{495–503}$, NLVPMVATV) fused to a tetanus T_H epitope ($tt_{830–843}$, QYIKANSKFIGITE) and a TLR9 agonist as adjuvant [378, 379]. Safety and immunogenicity were demonstrated in phase Ib trials [379, 380]. In another study, Schmitt et al. administered the NLVPMVATV peptide together with the adjuvant Montanide ISA 51 to HCMV seropositive patients after allogeneic hematopoietic stem cell transplantation [381]. Of the treated patients, 80% showed a clearance of HCMV after four vaccinations. Increasing frequencies of HCMV-specific $CD8^+$ and γδ T cells could be observed as well as rising titers of neutralizing antibodies. However, both peptide vaccines are limited in their applicability since they are restricted to HLA-A*02-positive individuals.

Many vaccine candidates of various approaches (vector-based, DNA, mRNA, peptide, attenuated or replication-defective strains) are in development but so far none in phase III trials (reviewed in [368]). Promising candidates should induce both antibody and T cell responses.

1.5 Aims of the thesis

Although both HCMV and EBV are usually well controlled in immunocompetent individuals, they can cause severe diseases in immunocompromised hosts such as AIDS patients or transplant recipients. EBV can also be responsible for a variety of diseases and malignancies in immunocompetent individuals. Due to the limited effectiveness and often serious side effects of current treatment options, the search for new therapies is still ongoing. Both viruses are mainly controlled by $CD4^+$ and $CD8^+$ T cells and knowledge about the T cell targets is essential for the development of a vaccine or immunotherapies such as adoptive T cell transfer.

The landscape of EBV-derived epitopes is actually well studied and characterized. While dominant epitopes for many common HLA allotypes are described, there is, however, a significant gap for HLA-A*01. Therefore, the aim of the first part of the work is to close this gap by characterizing the HLA-A*01-restricted T cell response to EBV and identifying novel EBV-derived epitopes. The basis of this part is the *in silico* prediction of potential, HLA-A*01-restricted T cell epitopes from the entire EBV proteome. Screening of memory responses in healthy blood donors *via* IFNγ ELISpot assays should then allow the identification of T cell epitopes. Functionality of peptide-specific T cells and their HLA restriction will be evaluated subsequently.

The second part of this thesis aims at the identification of HCMV-derived T cell epitopes. The considerable size of the HCMV proteome has made a comprehensive characterization of HCMV-derived T cell targets very difficult. Therefore, the majority of previous studies focused on few immunodominant antigens. However, a new approach, established by Stefanie Spalt and Anne Halenius, allows the identification of HCMV-derived HLA ligands on infected fibroblasts *via* mass spectrometry. This is an unbiased basis for the identification of naturally presented viral epitopes and should enable a comprehensive and systemic assessment of the repertoire of anti-HCMV T cell specificities in infected, seropositive individuals. The infection of different cell lines allows for the isolation of ligands of a diverse set of HLA allotypes. HCMV-derived HLA ligands will be screened for their immunogenicity *via* IFNγ ELISpot assays with healthy seropositive blood donors. Functionality and specificity of activated T cells will then be assessed by intracellular cytokine staining and tetramer staining.

The viral T cell epitopes identified in this work will contribute to our understanding of the anti-EBV and anti-HCMV T cell response and can be used in the development and improvement of therapeutic approaches.

2 Material and Methods

2.1 Material

2.1.1 Chemicals, reagents and complete solutions

“Complete Protease Inhibitor” tablet	Roche
HEPES	Gibco (Life technologies)
Acetonitrile (MS-Grade)	Thermo Scientific
Alkaline phosphatase, avidin-conjugated	Sigma-Aldrich
Ampicillin sulfate	Roth
ATP	Sigma-Aldrich
Bacto Trypton	Difco
Bacto Yeast Extract	Difco
BCIP/NBT tablet	Sigma-Aldrich
Bovine serum albumin, BSA	Sigma-Aldrich
Bradford reagent, Roti Nanoquant	Roth
Chloramphenicol	Sigma-Aldrich
Cytofix/Cytoperm	Becton Dickinson
D-Biotin	Sigma-Aldrich
Dimethyl sulfoxide (DMSO)	WAK-Chemie
DMEM (Dulbecco’s Modified Eagle Medium)	Gibco (Life technologies)
DNAse	Roche
DTT (Dithiothreitol)	Sigma-Aldrich
Ethanol	SAV LP
Ethylenediaminetetraacetic acid, EDTA	Roth
Fetal calf serum (FCS)	Capricorn Scientific
Ficoll (Biocoll)	Millipore
Formaldehyde	Fluka
Formic acid	Merck
Gentamycin	Gibco
Glycerol	Roth
Glycine	Roth
GolgiStop	Becton Dickinson
Guanidinium chloride	Roth

HSA (human serum albumin)	Biotest
Hydrochloric acid (HCl)	Roth
IL-2, human recombinant	R&D Systems
IMDM (Icove's Modified Dulbecco's Medium)	Lonza
Ionomycin	Sigma Aldrich
Isopropyl-beta-D-thiogalactopyranoside (IPTG)	Thermo Fischer Scientific
L-arginine	Sigma-Aldrich
Leupeptin	Roche
LIVE/DEAD Fixable Dead Cell Stain	Invitrogen (Life technologies)
Lysozyme	Roche
Methanol	Merck
Monosodium phosphate, NaH_2PO_4	Merck
Oxidized glutathione	Sigma-Aldrich
PBS (Phosphate buffered saline)	Gibco (Life technologies)
Penicillin (10^3 x U/ml)/Streptomycin (10 g/ml)	Sigma-Aldrich
Pepstatin	Roche
PHA (Phytohaemagglutinin)	Sigma-Aldrich
PHA-L	Roche
PMA (Phorbol myristate acetate)	Sigma-Aldrich
PMSF (Phenylmethylsulfonylfluoride)	Roche
Reduced glutathione	Sigma-Aldrich
Saponin	Sigma-Aldrich
Sodium acetate, CH_3COONa	Roth
Sodium azide, NaN_3	Merck
Sodium bicarbonate, $NaHCO_3$	Sigma-Aldrich
Sodium chloride, NaCl	VWR Chemicals
ß-Mercaptoethanol, ß-Me	Roth
Streptavidin-PE	Invitrogen (Life technologies)
Tris (Tris(hydroxymethyl)aminomethane)	Sigma-Aldrich
Tris-Base	AppliChem
Triton X-100	Sigma-Aldrich
Trypan blue	Gibco (Life technologies)
Trypsin 2.5%	Gibco (Life technologies)
Tween 20	Merck

Tween	Sigma-Aldrich
Urea	Roth
Water (MS-Grade)	Baker

2.1.2 Media and buffers

FACS buffer	0.01% NaN_3, 2 mM EDTA, 2% FCS in PBS
Freezing medium	10% DMSO in FCS
Injection buffer	10 mM Sodium acetate, 3 M Guanidinium chloride in ddH_2O; pH 4.2
LB medium	0.5% NaCl, 0.5% Bacto Yeast, 1% Bacto Trypton in ddH_2O
LB-Amp/Cam-agar plate	1.5% agar, 100 µg/ml ampicillin sulfate, 50 µg/ml chloramphenicol in LB medium
PBS-BSA	0.5% BSA in PBS
PBS-EDTA	1 mM EDTA in PBS
PBS-Tween	0.05% Tween in PBS
Permwash buffer	0.01% NaN_3, 0.1% saponin, 0.5% BSA in PBS
Refolding buffer	6.97% L-arginine in ddH_2O; pH 7.76
Resuspension buffer	0.1% NaN_3, 1 mM EDTA, 1 mM DTT, 100 mM NaCl, 50 mM Tris in ddH_2O
TBS (Tris-buffered saline)	20 mM Tris, 150 mM NaCl in ddH_2O; pH 8
TCM	50 µM β-Me, 1% Pen/Strep, 5% human plasma in IMDM
Tetramer freezing buffer	48% glycerol, 1.5% HSA, 0.06% NaN_3, 1x protease inhibitor in 20 mM Tris
Thawing medium	3 µg/ml DNAse, 50 µM β-Me, 1% Pen/Strep, 10% human plasma in IMDM
Triton buffer	0.1% NaN_3, 1 mM EDTA, 1 mM DTT, 0.5% Triton X 100, 100 mM NaCl, 50 mM Tris in ddH_2O
Trypsin solution	0.5% Trypsin in PBS
TSB	50% FCS in PBS
Urea buffer	8 M Urea, 10 mM Tris (pH 8.0), 10 mM NaH_2PO_4, 0.1 mM EDTA, 0.1 mM DTT

2.1.3 Antibodies

Anti-IFNγ primary antibody, clone 1-D-1k	MabTech
Anti-IFNγ secondary antibody, biotinylated clone 7-B6-1	MabTech

Table 3: Antibodies used for flow cytometry. Abbreviations: APC, allophycocyanin; PE, R-phycoerythrin; PerCP, peridinin chlorophyll protein.

Antigen	Fluorochrome	Source	Clone	Dilution	Manufacturer
CD8	PerCP	Mouse	RPA-T8	1:100	BioLegend
CD4	APC-Cy7	Mouse	RPA-T4	1:100	BioLegend
IFNγ	PE	Mouse	B27	1:200	BioLegend
TNFα	Pacific Blue	Mouse	Mab11	1:120	BioLegend

2.1.4 Healthy blood donors

Blood samples of healthy donors were kindly provided by the Institute for Clinical and Experimental Transfusion Medicine in Tübingen after obtaining written informed consent. Healthy blood donors were typed for HLA-A and -B if necessary. The CMV status of most of the donors was known.

2.1.5 Cell lines

Table 4: Cell lines.

Name	Origin	Source	HLA	Culture conditions
HF-99/7	Human foreskin fibroblasts	kind gift from Anne Halenius	A*01:01; A*03:01; B*08:01; B*51:01; C*01:02; C*07:01	DMEM + 10% FCS + 1% PenStrep
HF-99/5	Human foreskin fibroblasts	kind gift from Anne Halenius	A*11:01; A*24:02; B*08:01; B*52:01; C*07:01; C*12:02	DMEM + 10% FCS + 1% PenStrep
HF-γ	Human foreskin fibroblasts	kind gift from Anne Halenius	A*03:01; A*23:01; B*15:01; B*44:02; C*03:03; C*05:01	DMEM + 10% FCS + 1% PenStrep
MRC-5	Human fetal lung fibro-blasts	kind gift from Anne Halenius and Stefanie Spalt	A*02:01; A*29:02; B*07:02; B*44:02; C*05:01; C*07:02	DMEM + 10% FCS + 1% PenStrep

2.1.6 Viruses

The AD169VarL-based bacterial artificial chromosome (BAC) mutants [239] were propagated on MRC-5 cells. The recombinant HCMV mutants ΔUS2-6, ΔUS2-6/ΔUS11 and ΔUS2-11 were generated according to a previously published procedure [382] using the BAC-cloned AD169varL genome pAD169 [239] as parental BAC. Briefly, a PCR fragment was generated using the primers KL-DeltaUS11-Kana1 CAAAAAGTCTGGTGAGTCGTTTCCGAGCGACTCGAGATGCACTCCGCTTCAGTCTATAT-ACCAGTGAATTCGAGCTCGGTAC and KL-DeltaUS11-Kana2 TAAGACAGCCTTACAGCTTTTGA-GTCTAGACAGGGTAACAGCCTTCCCTTGTAAGACAGAGACCATGATTACGCCAAGCTCC and the plasmid pSLFRTKn [383] as template DNA. The PCR fragment containing a kanamycin resistance gene was inserted into the parental BAC by homologous recombination in *E. coli*. Correct mutagenesis was confirmed by Southern blot and PCR analysis. Recombinant HCMVs were reconstituted from HCMV BAC DNA by Superfect transfection into permissive MRC-5 cells. Virus titers were determined by standard plaque assay.

Table 5: HCMV virus strain used for the infection of cell lines.

Virus	Short name	Deletions
AD169VarL ΔUS2-11	ΔUS2-11	US2, US3, US4, US5, US6, US7, US8, US9, US10, US11

2.1.7 FASTAs

The proteome data used for prediction and as search database in the mass spectrometry analyses were obtained from the UniProt database and are listed in Table 6.

Table 6: FASTAs used for MS analyses and epitope predictions.

Organism	Date of access	No. of sequences
EBV (strain B95-8)	07/03/2016	109
HCMV (strain AD169, Merlin, Towne)	11/03/2014	400
HCMV (AD169 and UL133, UL135, UL136, UL138-142, UL144-148, UL150, and UL147A from Merlin)	29/09/2015	207
Homo Sapiens	11/03/2014	20,271

2.2 Methods

2.2.1 Peptide synthesis and storage

All peptides were synthesized in-house by standard 9-fluorenylmethyloxycarbonyl/tert-butyl strategy using peptide synthesizers ABI 433A (Applied Biosystems), Activo-P11 (Activotec), or Liberty Blue (CEM). Purity was assessed by reversed phase HPLC (e2695, Waters) and identity affirmed by nano-UHPLC (UltiMate 3000 RSLCnano, Dionex) coupled online to a hybrid mass spectrometer (LTQ Orbitrap XL, Thermo Fischer Scientific). Lyophilized peptides were dissolved at 10 mg/ml in DMSO and diluted 1:10 in bidestilled H_2O. Peptide dilutions were stored at -80°C. Thawed aliquots were further diluted in cell culture medium and sterile filtered if necessary.

2.2.2 Synthesis of recombinant HLA chains

First, the DNA sequence of the respective HLA heavy chain was altered by deleting the transmembrane domain and adding a BirA biotinylation sequence at the C-terminus. The sequence of the respective chain was then cloned into the expression vector pET-3a (in some cases pET-3d). Approximately 1 ng of vector was added to 100 µl of competent BL21(DE3) *E. coli* cells that carry the plasmid pLysS. The mixture was incubated on ice for 20 min and was then transferred in a 42°C water bath for 90 s. After a fast cooling down on ice for 2 min, 1 ml LB medium without antibiotics was added and incubated for 30 min at 37°C. Finally, 100 µl of this mixture were spread onto an LB-Amp/Cam agar plate (LB medium with 1.5% agar, 100 µl/ml ampicillin and 34 µg/ml chloramphenicol) and incubated overnight at 37°C. Cloning and seeding was performed by Beate Pömmerl. Colonies from the plates were picked and transferred into 5 ml of LB-Amp/Cam. Bacteria suspensions were incubated in a shaker (250 rpm) for about 6 h at 37°C, transferred into 300 ml LB-Amp/Cam, and incubated overnight at 37°C and 180 rpm.

The next day, ten baffled 2 l Erlenmeyer flasks were filled with 1l LB medium containing 100 mg ampicillin and 34 mg chloramphenicol and adjusted to at least room temperature. To each flask, 25 ml of the overnight culture was added and incubated in a shaker at 37°C and 180 rpm. Optical density $(OD)_{600}$ was measured regularly with the spectrometer Ultraspec 3000 (Pharmacia) until an OD_{600} between 0.5 and 0.6 was reached. To induce recombinant protein expression, 0.5 ml of a 1 M IPTG solution was added to each flask and incubated additional 4-5 h. The bacterial suspension was centrifuged in a SLA 3000 rotor at 5,000 rpm for 15 min. The pellets were resuspended in 180 ml PBS in total, distributed into six 50 ml tubes and stored in -80°C.

All following steps were performed at 4°C or on ice, unless described otherwise. After thawing the samples in a water bath (RT), 300 µl of 1 M MgCl, 150 µl of 10 mg/ml DNAse, and 30 µl of fresh

100mg/ml lysozyme were added to each sample. The aliquots were then treated four times with ultrasound (Sonifier 250, Branson Ultrasonic) for 30 s each (output 5, duty cycle 50%). The lysates was centrifuged in a SS-34 rotor at 15,000 rpm for 15 min. The supernatant was discarded and the slimy, brown, upper layer of the pellet (cell wall and membrane debris) was carefully removed with a spatula. The more dense and whitish layer beneath was resuspended and homogenized in triton wash buffer. This washing step was repeated four to six times until only one white layer was still visible after centrifugation. The inclusion bodies were then washed twice with resuspension buffer and finally dissolved in 15-30 ml urea buffer - depending on the size of the pellet. The solution was incubated rotating overnight. The following day, insoluble components were separated by centrifugation for 15 min at 15,000 rpm. The approximate concentration and the purity were determined with a nanodrop spectrophotometer (Thermo Fisher Scientific). The purity was considered acceptable if the ratio of absorbance at 260 nm and 280 nm was around 0.6. The concentration was determined with a Bradford assay (see 2.2.4). Concentration of heavy chains was adjusted to 20 mg/ml in urea buffer and divided into 8 mg aliquots. The original concentration of the light chain (β_2m) was maintained and aliquots of 7 mg were made. Both were stored in -80°C.

2.2.3 Refolding of HLA-I-peptide complexes

For the production of HLA-peptide complexes (monomers), the peptide of interest was refolded with β_2m and the respective heavy chain. 385 mg of reduced glutathione, 77.5 mg of oxidized glutathione and 250 µl PMSF (200 mM stock in methanol) were added to 250 ml refolding buffer. 5-7 mg of peptide was dissolved in DMSO to a final concentration of 10 mg/ml and pipetted into the mixture. Heavy chain and β_2m were thawed at room temperature. The heavy chain was diluted with 700 µl injection buffer; β_2m with 780 µl. Both were added with a syringe and a 26G needle while the injection buffer was stirred vigorously in order to avoid direct aggregation of the chains. The mixture was then incubated gently shaking for approximately 12 h at 10°C. The next day, heavy chain was added in the morning and in the evening (ideally 12 h interval) as described above. On the third day, the mixture was filtered through a 0.22 µm vacuum filter to remove aggregates of misfolded molecules. To separate correctly folded monomers from single chains and free peptide, the mixture was then filtered and concentrated in a stirred Amicon pressure cell (30-kDa NMWL filter, 4 bar, Millipore) to a volume of about 25 ml. The retentate was stored at 4°C and the permeate was used to start a second refolding reaction. Therefore, all steps described above were repeated. Since glutathione and peptide were supplied in excess before, they were not added again. Afterwards, the retentates of both reactions were pooled, centrifuged for 10 min at 4,000

rpm and 4°C to remove aggregates, and concentrated with a 10-kDa NMWL filtration tube to a final volume of 5 ml. A size exclusion chromatography was performed with an ÄKTA prime (Amersham Biosciences) using a Superdex 75 column with TBS as running buffer and a flow rate of 3 ml/min. The UV absorption at 280 nm was determined and 4 ml fractions collected. The fractions containing the monomer were collected and pooled in a 50 ml tube. Protease inhibitors PMSF (f.c. 0.2 mM), leupeptin (f.c. 1 µg/ml), and pepstatin (f.c. 0.7 µg/ml) were added immediately to avoid protein degradation. The solution was concentrated again to 5 ml using a 10-kDa NMWL filtration tube at 4,000 rpm. To enable binding and tetramerization *via* streptavidin, the monomers were enzymatically biotinylated with BirA. Therefore, 400 µl 1 M Tris (pH 8), 25 µl 1 M $MgCl_2$, and 250 µl 100 mM ATP were added and the solution was carefully mixed. Afterwards, 10-20 µg BirA enzyme and 28.5 µl 100 mM biotin were added, mixed and incubated for 12-16 h at 27°C. A second size exclusion chromatography was performed as described above to separate biotinylated monomers from, unbound biotin, enzyme, and aggregates. Fractions containing the monomer were collected and PMSF, leupeptin, and peptstatin were added as depicted before. The monomer solution was concentrated again with a 10-kDa NMWL filtration tube to 250-400 µl. The concentration was determined with a Bradford assay (see 2.2.4) and adjusted to 2 mg/ml with TBS. Aliquots of 50 µg were stored at -80°C. The presence of the correct peptide was tested by Claudia Falkenburger or Michael Ghosh with ESI-QTOF mass spectrometry.

2.2.4 Bradford assay

The protein concentration of heavy chains, light chain, and refolded monomers was determined by Bradford assay [384]. The Roti® Nanoquant (Roth) used is a Coomassie Brilliant Blue G-250 dye and has its absorption maximum in its unbound cationic form at 450 nm. Upon protein binding, the anionic form of the dye is stabilized and the absorption maximum shifts to 590 nm. The protein concentration is determined by measuring the OD at 450 nm and 590 nm and comparing the quotient $OD_{590/450}$ with a standard curve of a protein with known concentration. BSA was used as reference. For the measurement of monomer concentration it was diluted to 0, 10, 20, 40, 60, 80, and 100 µg/ml in TBS while it was diluted to 0, 10, 25, 50, 75, and 100 µg/ml in 8 M Urea for HLA heavy chains. 50 µl sample or reference protein was mixed with 200 µl Roti® Nanoquant and incubated for approximately three minutes before ODs were measured with the ELISA reader Spectramax 340 and the software Softmax Pro 2.1 (Molecular Devices). Samples were measured in triplicates while standard protein was measured in duplicates.

2.2.5 UV-induced peptide exchange of monomers

Monomers loaded with UV-sensitive peptide allow for the UV-induced degradation of the loaded peptide and the fast substitution with the peptide of interest. UV-sensitive peptides contain the UV-labile amino acid J (3-Amino-3-(2-nitrophenyl)propanoic acid) and can be cleaved with UV irradiation (366 nm). Monomers with UV-sensitive peptides were produced as described above (see 2.2.3) with the small difference that they need to be protected from light at every step of the procedure. After thawing the UV-sensitive monomer of the desired HLA, it was diluted 1:10 with 2 mM PBS-EDTA (PBS-E). The peptide of interest was dissolved to 10 mg/ml in DMSO and diluted 1:25 to a final concentration of around 400 µM in 2 mM PBS-E. 65 µl of the peptide and 65 µl of monomer were added to one well of a 96 well polypropylene microplate with V-bottom and mixed well. The plate without a lid was exposed to 366 nm UV light for 1 h with 2-5 cm distance to the UV lamp. Afterwards, the plate was centrifuged for 5 min at 4000 rpm at room temperature. 100 µl of supernatant were transferred to a 1.5 ml tube and stored at 4°C for maximum one week and otherwise at -80°C. The exchange efficiency depends on the binding affinity of the exchanged peptides. For further use, an exchange rate of 50% and a concentration of 50 µg/ml monomer were assumed.

2.2.6 Tetramerization of HLA-peptide complexes

The protein streptavidin is produced by the bacterium *Streptomyces avidinii* and possesses four binding sites for biotin. Therefore, it can mediate the tetramerization of biotinylated monomers. The streptavidin is coupled to a fluorescent dye allowing the later detection of bound tetramers *via* flow cytometry. R-phycoerythrin (Pe)-coupled streptavidin was added to monomers in a stoichiometric ratio of 1:4. Ten percent of 78.5 µl streptavidin-PE were added in ten steps to 50 µg of monomer. The solution was incubated in between for at least 20 min on a spinning wheel at 4°C in the dark. For long-term storage, tetramers were diluted 3:1 with tetramer freezing buffer and stored at -80°C. Tetramers of UV-exchanged monomers were diluted 1:6 with tetramer freezing buffer for UV-exchanged monomers.

2.2.7 Freezing and thawing of cells

Frozen cells were stored at -80°C. Cells were therefore harvested by centrifugation, resuspended in cold freezing medium (4°C) and 1-2 ml was distributed in cryotubes. Cryotubes were immediately transferred to a freezing container (4°C), which was then stored in -80°C. Isopropanol in the freezing container allowed a slow cooling down of 1°C/min.

For thawing, frozen cells were warmed up until almost thawed and then transferred into 10 ml of cold thawing medium. After centrifugation (7 min, 1,400 rpm), the cells were resuspended in 10 ml

warm thawing medium and centrifuged again. The cell pellet was resuspended in the appropriate culture medium.

2.2.8 Cell counting

Prior to cell counting, cells were pre-diluted in PBS to a reasonable concentration and then mixed with 0.05% trypan blue (in PBS). Approximately 10 µl of the cell suspension was pipetted under the cover glass of a Neubauer counting chamber. Trypan blue accumulates in dead cells and allows the differentiation of dead and living cells. Viable cells were counted in two to four big squares and the cell number calculated as shown below.

$$\frac{cell\ number}{ml} = \left(\frac{number\ of\ viable\ cells}{number\ of\ counted\ suqares}\right) \times 10^4 \times DF$$

(DF, dilution factor; 10^4, chamber factor)

2.2.9 Cell culture of cell lines and PBMCs

All cells used were cultured in humidified incubators at 37°C and 7.5% CO_2. Human foreskin fibroblasts were cultured in DMEM supplemented with 10% FCS, 100 U/ml penicillin, and 100 µg/ml streptomycin in cell culture flasks up to a confluence of 90%. Cell splitting was done two to three times a week in a ratio of 1:2 to 1:5 depending on the proliferation of the cells. For harvesting, culture medium was removed, the cells washed with PBS to remove residual medium and then detached with 0.5% Trypsin in PBS for 2 min at 37°C. The reaction was stopped with medium containing FCS that inhibits trypsin. The cells were either used directly or were split into fresh cell culture flasks for further expansion. Prior to mass spectrometric analysis, the cells were collected by scraping, washed three times with PBS and frozen as cell pellet in -80°C.

PBMCs were cultured in IMDM supplemented with 5% heat-inactivated pooled human plasma, isolated from healthy blood donors (see 2.2.10), 100 U/ml penicillin, 100 µg/ml streptomycin, 25 µg/ml gentamicin (Life technologies), and 50 µM ß-mercaptoethanol.

2.2.10 Isolation of PBMCs from buffy coats

Peripheral blood mononuclear cells (PBMCs) were isolated from buffy coats, whole blood or leukapheresis products by Ficoll-Hypaque density gradient centrifugation. Buffy coats are leukocyte-enriched blood products of heparinized whole blood where most of the plasma and erythrocytes were removed. When PBMCs were isolated from whole blood, plasma was first separated by centrifugation. The blood was centrifuged in 50 ml tubes for 20 min (2,000 rpm, RT, without brake), allowing the plasma to separate from the buffy coat and the erythrocytes. The plasma, as top layer, was removed first and heat-inactivated for 30 min at 56°C followed by two

centrifugation steps (15 min, 2,500 rpm, RT) where the supernatant was always transferred in fresh 50 ml tubes. It was then either used directly for the preparation of donor-specific T cell medium or frozen in -20°C for later use. The buffy coat was extracted and diluted 1:2 with PBS. In contrast to this, buffy coats and leukapheresis products received from the blood bank were diluted 1:4 and 1:10, respectively. 30 ml of the cell suspension were then carefully layered on top of 15 ml Ficoll in 50 ml tubes and centrifuged (20 min, 2,000 rpm, RT, without brake). After removing the PBS-diluted plasma, the lymphocyte layers were collected and pooled into fresh 50 ml tubes. The cells were then washed three times with 50 ml PBS at declining centrifugation speed (1,500 rpm, 1,300 rpm, 1,100 rpm, each 10 min, RT). The cell number was determined as described in 2.2.8. The PBMCs were then either frozen as described in 2.2.7 or resuspended in the respective culture medium.

2.2.11 Expansion of memory T cells (12-day pre-stimulation)

Specific memory T cells appear in very low frequencies in the blood of healthy individuals without an acute infection. Those frequencies are usually below the detection limits (about 0.1% of specific T cells in the T cell population) of the T cell assays used in this work and epitope-specific T cells need to proliferate to allow for detection. The cells were therefore stimulated with the peptides of interest and IL-2 for a period of 12 days.

Frozen PBMCs of healthy blood donors were thawed on day 1 as described in 2.2.7. 2-3 x 10^7 cells were resuspended in 2 ml TCM and plated in wells of a 6-well plate. On the second day, cells were stimulated with peptides in a final concentration of 1 µg/ml. Peptides were added in 500 µl TCM per well. On day 3, 6, and 8, IL-2 was added in 0.5-1 ml TCM in a final concentration of 20 U/ml. Cells were provided with fresh TCM on day 10 if necessary and incubated for two more days prior to T cell assays.

2.2.12 Enzyme-linked immunospot assay (ELISpot)

Enzyme-linked immunospot (ELISpot) assays enable the detection of cytokine-secreting cells at the single-cell level. In this work, IFNγ ELISpots were performed to identify activated antigen-specific memory T cells among the PBMCs of blood donors. Therefore, 96-well ELISpot plates containing nitrocellulose membranes (MSHAN4B, Millipore) were coated with the first antibody directed against IFNγ. IFNγ, produced by activated T cells after peptide stimulation, binds to the first antibody and is recognized by a biotinylated secondary antibody. The streptavidin-coupled enzyme alkaline phosphatase can then bind to the biotin of the secondary antibody and catalyzes a reaction with the substrates BCIP (5-bromo-4-chloro-3-indolyl phosphate) and NBT (nitro-blue tetrazolium chloride) yielding an insoluble black/purple dye. Each spot represents one activated IFNγ-secreting cell.

For coating the nitrocellulose membrane, the first antibody 1D1-K was diluted 1:500 in PBS. 100 µl of this solution was added to each well and incubated 12-72 h at 4°C. The wells were washed twice with 200 µl IMDM to remove unbound antibody. For all washing steps, the appropriate buffer was added to each well and removed by emptying the plate into a sink and tapping it dry on tissue towels. After washing with IMDM, 50 µl TCM containing human serum was added to each well and incubated for at least 1 h at 37°C to block free binding sites on the membrane. In the meantime, cells were harvested, counted and resuspended in TCM with a density of 10^7 cells per ml. Peptides of interest and negative control peptide (1 mg/ml stock) were diluted with TCM to a concentration of 3 µg/ml (final conc. in wells 1 µg/ml). One well without any stimulus (cells with medium) and two wells containing either DMSO or an HLA-matched non-immunogenic peptide (human or HIV) served as negative controls in each donor. Phytohaemagglutinin (PHA, final conc. 5 µg/ml) was used as unspecific positive control since it activates T cells by crosslinking their T cell receptors on the cell surface. 50 µl of peptide solution and 50 µl of cell suspension were added to the 50 µl TCM already contained in each well. Finally, the ELISpot plate was incubated for 22-26 h at 37°C. Any vibration had to be absolutely avoided during this incubation, since moving cells lead to “snail trails” instead of well-defined spots. The next day, plates were washed twice with PBS-Tween, twice with ddH2O and three times with PBS-Tween. Afterwards, 100 µl of secondary antibody, diluted 1:3,000 in PBS-BSA, were added to each well and incubated for 2 h at RT. The plates were then washed six times with PBS-Tween and 100 µl of alkaline phosphatase (1:1,000 in PBS-BSA) were added. After 45-60 min incubation at RT, the plates were washed three times with PBS-Tween and three times with ddH_2O before the substrate was added. One tablet of BCIP/NBT was dissolved in 10 ml ddH_2O and filtered through a 0.2 micron filter. 50 µl of the substrate was added to each well and incubated for 7-10 min. The reaction was stopped by washing the plates several times with deionized water. After drying the plates overnight, the spots were automatically counted using an ImmunoSpot S5 analyzer and ImmunoSpot 5.1.29 software (Cellular Technologies Ltd). T cell responses were considered to be positive when the mean spot count per well was > 10 spots and at least 3-fold higher than the mean number of spots in negative control wells. Background staining due to excess cytokine and overlapping spots hamper the detection of reliable counts in wells of highly responsive donors. Therefore, spot counts of > 1,000 or “too numerous to count” were set to 1,000.

2.2.13 Tetramer staining of specific T cells

Tetramer staining was performed to identify and quantify peptide-specific T cell populations with flow cytometry. Due to the low binding affinity and high dissociation rate of HLA-peptide

monomers, they are not able to establish a stable binding to T cell receptors [385]. The tetramerization of monomers by streptavidin allows the binding of multiple receptors by one tetramer and leads to a higher avidity and more stable binding. The whole protocol was carried out at 4°C or on ice if not mentioned otherwise. Washing steps were performed by vigorously adding 150 µl of appropriate washing buffer and centrifuging the plate for 2 min at 1800 rpm. Supernatant was removed by flicking the plate upside down over a sink.

For the tetramer staining, cells were harvested either 1-2 days after thawing or after a 12-day pre-stimulation. Cells were counted and 0.5-1 x 10^6 cells per well in medium or PBS were plated into a 96-well plate. After washing twice with PBS-E, cells were resuspended in 50 µl Aqua live/dead diluted in PBS-E to stain dead cells. Depending on the storage period of Aqua live/dead, it was diluted either 1:200 (if storage period was longer than 2 weeks) or 1:400. After 20 min incubation in the dark, the cells were washed once with PBS-E and tetramer staining performed. Therefore, tetramers were diluted in TBS to a concentration of 5 µg/ml. To prevent the appearance of tetramer aggregates, the dilution was prepared in excess and centrifuged for at least 10 min at maximum speed. 50 µl of tetramer solution were added to each well and incubated 30 min at RT in the dark. After a washing step with FACS buffer, the surface molecules CD4 and CD8 were stained. Therefore, CD8-PerCP and CD4-APC-Cy7 were diluted 1:100 in FACS buffer and 50 µl were added to each well. After 20 min incubation in the dark, the cells were washed twice with FACS buffer. Finally, the cells were resuspended in 200 µl FACS buffer per well. If the measurement was not carried out the same day, the cells were fixed with 100 µl of 1% formaldehyde in FACS buffer for 10 min. After two washing steps with FACS buffer, the cells were resuspended in 200 µl FACS buffer and stored at 4°C in the dark until the measurement with the flow cytometer FACS Canto II and the software BD FACSDiva (Becton Dickinson).

2.2.14 Intracellular cytokine staining (ICS)

Upon peptide stimulation, activated T cells react with the secretion of several cytokines. It is possible to block this secretion by inhibiting the intracellular protein transport with brefeldin A and monensin (GolgiStop). This leads to the accumulation of cytokines in the Golgi complex. These cytokines can be bound by intracellular fluorescent antibodies enabling the identification of the T cell subset that is activated by a specific stimulus.

For the ICS, cells were harvested either 1-2 days after thawing or after a 12-day pre-stimulation. Cells were counted and 1-2 x 10^7 cells per ml resuspended in 1 medium. 50 µl cell suspension per well were plated into a 96-well plate. Three wells per donor were prepared in order to test a peptide of interest and to have a positive and a negative control. Human or HIV peptides of the

same HLA restriction as the peptide of interest were used as negative control and ionomycin and PMA (Phorbol 12-myristate 13-acetate) as positive control. Ionomycin is a calcium ionophore derived from *Streptomyces conglobatus* and is able to rapidly raise the intracellular calcium level [386] while PMA is an activator of the protein kinase C [387]. Together they serve as unspecific activators of T cells and stimulate the cytokine production. To the 50 µl of cell suspension, 50 µl of either peptide of interest, negative peptide (both 10 µg/ml final concentration) or ionomycin (f.c. 1 µM) and PMA (f.c. 50 ng/ml) were added to each well. Afterwards, 50 µl of brefeldin A (f.c 10 µg/ml) and GolgiStop (1 µl/well) were added to each well and plates were incubated at 37°C for 6-14 h. After the incubation, the staining was performed. All following steps were carried out at 4°C or on ice if not mentioned otherwise. Washing steps were performed by vigorously adding 150 µl of appropriate washing buffer and centrifuging the plate for 2 min at 1,800 rpm. Supernatant was removed by flicking the plate upside down over a sink.

Cells were washed twice with PBS-E and were resuspended in 50 µl Aqua live/dead diluted in PBS-E to stain dead cells. Depending on the storage period of Aqua live/dead, it was diluted either 1:200 (if storage period was longer than 2 weeks) or 1:400. After 20 min incubation in the dark, the cells were washed once with PBS-E. Surface molecules CD4 and CD8 were stained by adding 50 µl of CD8-PerCP and CD4-APC-Cy7, both diluted 1:100 in FACS buffer, to each well. After 20 min incubation in the dark, the cells were washed once with FACS buffer and 100 µl of Cytoperm/Cytofix were added. After permeabilization of the cells in the dark for 20 min, they were washed once with 100 ml of permwash buffer. Antibodies IFNγ-PE and TNF-PacificBlue for intracellular cytokines were diluted 1:200 and 1:120, respectively, in permwash buffer and 50 µl were added to each well. After 20 min incubation in the dark, cells were washed twice with permwash buffer and resuspended in FACS buffer for analysis by flow cytometry. All measurements were performed with the flow cytometer FACS Canto II and the software BD FACSDiva (Becton Dickinson). Data were subsequently analyzed with the software FlowJo v10 (Tree Star Inc).

2.2.15 Infection of human foreskin fibroblasts

Infection of human foreskin fibroblast cells HF-99/7, HF-99/5, and HF-γ prior to mass spectrometry analyses was performed by Liane Bauersfeld from the group of Anne Halenius (Institute of Virology, Freiburg).

Approximately 2-3 x 10^8 HF-99/7 cells were infected with an MOI of 5. In contrast, HF-99/5 and HF-γ cells were infected with an MOI of 1. At 48 h.p.i. (HF-99/7) or 4 d.p.i. (HF-99/5 and HF-γ), the cells were collected by scraping and washed three times with PBS. Cell pellets were stored at -80° C.

2.2.16 Flow cytometry analysis of infected cells

Cells were detached with accutase (Sigma) and stained with antibodies diluted in 3% FCS/PBS. Cells were washed in 3% FCS/PBS supplemented with DAPI and fixed in 3% paraformaldehyde. For intracellular staining of viral Fc-receptors, cells were fixed and permeabilized using the BD Cytofix/Cytoperm™ Kit and stained with Fc-FITC (Rockland Immunochemicals Inc). Cells were measured with a BD FACSCanto™ II system (BD Biosciences) and acquired data was analyzed by FlowJo (v10.1, Tree Star Inc.).

2.2.17 Preparation of cells for HLA immunoprecipitation

The preparation of cells was performed at 4°C or on ice. The cell pellet was thawed by adding one volume of 2x solubilisation buffer and vortexing it until it was completely resuspended. The cell suspension was transferred to a beaker. The original vial was washed twice with 1x solubilisation buffer and the suspension was transferred to the beaker. It was stirred at 4°C for 1 h and homogenized afterwards by sonication with an output level of 5 for 20 s. Sonication was repeated three times with 20 s breaks in between. The lysate was then incubated on a shaker for 1 h and centrifuged subsequently at maximum speed for 45 min to remove cell debris.

2.2.18 HLA immunoprecipitation

HLA-I ligands were isolated as described before [388, 389] using standard immunoaffinity purification employing the pan-HLA-I-specific monoclonal antibody W6/32. Therefore, the in-house produced antibody W6/32 was coupled to cyanogen bromide-activated (CNBr) sepharose beads in a ratio of 1:40 (w/w). The appropriate amount of sepharose was covered with approximately 45 ml 1 mM HCl and rotated for 30 min at RT to activate the reactive group. The sepharose beads were then centrifuged 4 min at 300 rpm without brake and the supernatant was discarded. After resuspending the beads in about 20 ml coupling buffer, the antibody was added and the mixture filled up to 45 ml with coupling buffer. For coupling the antibody to the beads, the mixture was rotated for 2 h at RT. Afterwards, the sepharose-antibody mixture was centrifuged as described above and the supernatant was discarded. The beads were resuspended in 45 ml 0.2 M glycine and rotated for 1 h to block free binding sites. After centrifugation as described above, the beads were washed twice with PBS and then filled up with PBS to an antibody concentration of 1mg/ml (40 mg sepharose per ml). Coupled antibody was stored at 4°C.

Econo columns were rinsed with 70% EtOH and PBS and assembled at 4°C. 2 ml of coupled antibody were added to each column. With PBS, the pump rate of the peristaltic pumps was set to 10 rpm and the flow rate of pumps was fine-tuned and adjusted to each other. Columns were set up that HLA I molecules were isolated first followed by HLA II. After washing the system, PBS was

exchanged by solubilisation buffer. The cell lysate (see 2.2.17) was then linearly aspirated until it reached the outlet and was run over columns cyclically overnight at 10 rpm. After the affinity chromatography, the system was washed linearly with PBS for 30 min and H_2O for 1 h at 10 rpm. Elution was carried out by incubating the columns four times for 15 min with 100-300 µl 0.2% TFA on a shaker. 10 µl of 10% TFA was added only at the first elution step to quickly decrease the pH. After each incubation, eluates were pushed into LoBind Eppendorf tubes with a syringe.

During the elution, 3 kDa and 10 kDa Amicon filter units (Millipore) were prepared and washed. HLA-I and HLA-II ligands were separated from remaining HLA chains, antibody fragments and unspecifically bound proteins by 3 kDa and 10 kDa filters, respectively. Each washing step was performed by adding 500 µl of the respective solution and centrifugation for 15 min at 13,000 rpm. Flow through and retentate were discarded by tapping on tissue towels. One washing step with Baker H_2O was followed by 0.1 N NaOH, Baker H_2O and two times 0.2% TFA.

Eluate of the affinity chromatography was centrifuged for 5 min at 13,000 rpm to sediment aggregates. The supernatant was transferred to the prepared Amicon filter units and also centrifuged at 13,000 rpm until the eluate was completely run through the filter. Flow through was transferred to LoBind Eppendorf tubes and the filter unit was washed once with 450 µl AB_E to elute remaining peptides. The peptide solution was then concentrated to a volume of 30-50 µl by lyophilisation.

To desalt and purify the peptide solution, ZipTip$_{C18}$® Pipette Tips were employed. 10 µl of different solutions were therefore aspirated and dispensed repeatedly without introducing air into the tip. First, AB_E was aspirated and dispensed ten times to wash the pipette tip, followed by equilibrating with A* ten times. The sample, which was centrifuged before for 5 min at 13,000 rpm and 4°C, was loaded by slowly pipetting ten times in the peptide solution. To desalt the sample, A* was slowly aspirated and dispensed three times. Afterwards, peptides were eluted by quickly pipetting ten times in 35 µl AB_E. The steps from equilibration to elution were repeated five times in total. The AB_E-peptide solution was reduced to 1-5 µl in a vacuum concentrator, filled up with 25 µl A_{Load}, and stored in -80°C until mass spectrometric analyses were performed.

2.2.19 Analysis of HLA ligands by LC-MS/MS

HLA ligand extracts (see 2.2.18) were separated by reversed-phase liquid chromatography (nanoUHPLC, UltiMate 3000RSLCnano, Dionex) using a 75 µm x 25 cm PepMap C18 column (Thermo Fisher Scientific). Linear gradients were applied ranging from 2.4% to 32% AcN over the course of 90 min. Cell extracts were analyzed in an online coupled LTQ Orbitrap Fusion Lumos mass

spectrometer (Thermo Fisher Scientific) using a top speed CID method leading to Orbitrap MS/MS spectra.

2.2.20 Database search and filtering

The SEQUEST HT search engine [390] were used to search the human and HCMV proteome. Fragment spectra were searched against a concatenated FASTA consisting of the reviewed Swiss-Prot human (March 2014; 20,271) and HCMV proteomes (March 2014; 400 sequences). The search combined data of technical replicates and was not restricted by enzymatic specificity. Precursor mass tolerance was set to 5 ppm and fragment mass tolerance to 0.02 Da. Oxidized methionine was allowed as the only dynamic modification. FDR was estimated using the Percolator algorithm [391]. Identifications were filtered to an FDR of 5% assessed on peptide spectrum match (PSM) level, search engine rank = 1 and peptide lengths of 8–12 amino acids. Peptide identifications were annotated to their respective HLA motifs using both SYFPEITHI [24] with a normalized score of ≥ 50% and NetMHCpan (version 3.0) [392] with a percentile rank < 2% as cutoffs. Peptides fulfilling the cutoff in either or both prediction tools were designated predicted HLA ligands. In case of multiple possible annotations, the HLA allotype yielding the best rank/score was selected, if matching with the HLA typing of the respective cell line. Peptides were tested in donor samples of different HLA restrictions if the two algorithms resulted in inconsistent allotype annotations.

2.2.21 Whole proteome prediction

Whole proteome predictions were performed by Leon Bichmann. SYFPEITHI and NetMHCpan3.0 were employed for the *in silico* epitope prediction [393] of the whole HCMV proteome using a concatenated FASTA consisting of the reviewed Swiss-Prot HCMV AD169 proteome (March 2014; 193 sequences) and the reviewed sequences of UL133, UL135, UL136, UL138-UL142, UL144-UL148, UL150,and UL147A of strain Merlin [239]. The additional proteins are part of the ULb' region that is included in the used BAC construct.

3 Results

3.1 Novel EBV-derived, HLA-A*01-restricted T cell epitopes

3.1.1 Prediction of HLA-A*01-restricted epitope candidates

The first step for the identification of HLA-A*01 restricted T cell epitopes from EBV antigens was the prediction of candidate epitopes. Therefore, the complete proteome of the prototype strain B95-8 was cut in 9mers, 10mers, 11mers, 12mers, and 13mers and prediction was performed with SYFPEITHI and NetMHC 3.4. Peptides with a SYFPEITHI score of ≥ 60 were selected (Supplemental Table 1 to Supplemental Table 5). From this list of 598 peptides, the highest scoring peptides were tested for their immunogenicity. The peptides were ranked according to their SYFPEITHI score and all peptides above a defined threshold (Table 7) were synthesized and tested. For 12mers and 13mers, the additional criteria of a NetMHC score of < 50 nM had to be fulfilled. Selection criteria are listed in Table 7.

Table 7: Selection criteria for immunogenicity testing.

Length	Tested peptides
9mers	SYFPEITHI score ≥ 67.5
10mers	SYFPEITHI score ≥ 69.23
11mers	SYFPEITHI score ≥ 69.23
12mers	SYFPEITHI score ≥ 73.17 AND NetMHC 3.4 < 50 nM
13mers	SYFPEITHI score ≥ 73.17 AND NetMHC 3.4 < 50 nM

Additional peptides with lower scores were tested if they were already synthesized for other projects and were ready to use.

3.1.2 Identification of T cell epitopes *via* IFNγ ELISpot screening

The immunogenicity of all selected peptides was evaluated with IFNγ ELISpot assays. In order to increase the number of peptide-specific memory T cells above the detection limit, PBMCs of healthy donors were pre-stimulated with peptide and three times with IL-2 over twelve days. In total, 171 peptides were tested (Table 9). The peptide ETDQMDTIYQCY from the protein gB could not be produced and was abandoned after three attempts. On the basis of our experience with epitope prediction studies, we expected the majority of the peptides to be non-immunogenic. Hence, 134 peptides were tested in pools first to reduce the amount of necessary ELISpot assays. For this purpose, 15 peptide pools, containing nine peptides each, were generated and each pool was tested with six different HLA-A*01-positive donors. If the pool was able to elicit an IFNγ

response in two or more donors, the peptides of this pool were individually tested in subsequent ELISpot assays. Peptides of all other pools were not further evaluated. Figure 6 shows the number of IFNγ spot forming cells (SFC) of each donor stimulated with different peptide pools. Positive results are depicted by black rhombs, negative results by grey rhombs. Spot counts exceeding the threshold of 1,000 were reduced to 1,000, as all counts above this value are not reliable. Table 8 lists the numbers of positive donors of each peptide pool.

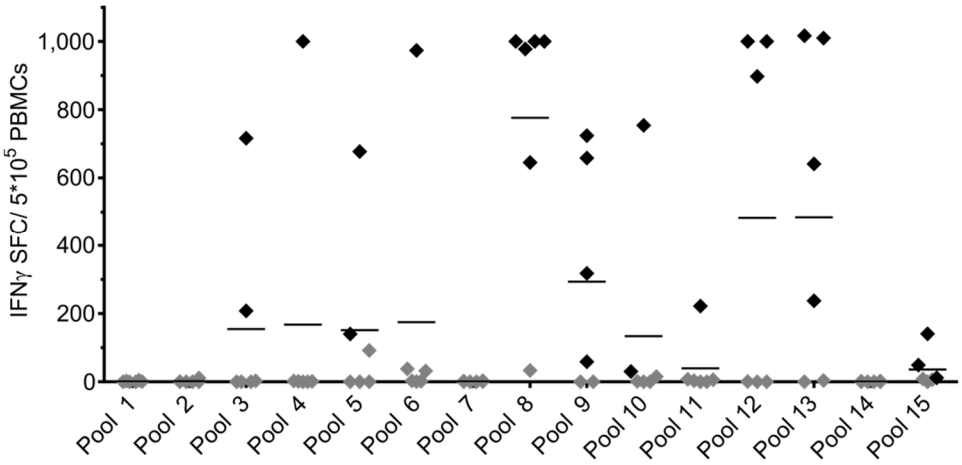

Figure 6: ELISpot results of peptide pools containing EBV-derived, HLA-A*01-restricted peptides. Depicted are numbers of IFNγ SFC for each tested PBMC culture minus the spot numbers of the negative control of the PBMCs. Positive evaluated PBMC cultures are depicted in black, negative tested PBMC cultures in grey. Peptide pools were tested once in technical duplicates in six different HLA-matched PBMC cultures. Bars represent the mean IFNγ SFC. Abbreviations: SFC, spot forming cells.

Table 8: ELISpot results of peptide pools. Six PBMC samples per pool were stimulated for 12 days prior to the ELISpot assay. Peptides of positive pools (green background) were further tested individually.

Pool	Positive/tested	Pool	Positive/tested	Pool	Positive/tested
Pool 1	0/6	Pool 6	1/6	Pool 11	1/6
Pool 2	0/6	Pool 7	0/6	Pool 12	3/6
Pool 3	2/6	Pool 8	5/6	Pool 13	4/6
Pool 4	1/6	Pool 9	4/6	Pool 14	0/6
Pool 5	2/6	Pool 10	2/6	Pool 15	3/6

Seven of the tested peptide pools stimulated peptide-specific memory T cells only in one or in none of the PBMC samples and were therefore excluded from further testing. Peptides of pools 3, 5, 8, 9, 10, 12, 13, and 15, however, were then individually screened for immunogenicity in at least six different HLA-matched donors. The results of the ELISpot screening are listed in Table 9. Of 109 individually tested peptides, 29 elicited an IFNγ response in at least one of the tested PBMC samples. All peptide lengths that were predicted are present in this set of epitopes (Figure 7). With

nine unique epitopes, 9mers were most common followed by 10mers; but also 11mers, 12mers, and 13mers were not as rarely represented as observed in other HLA types.

The novel epitopes represented 20 different proteins expressed in various expression stages. Twenty-two epitopes originated from genes expressed during the lytic phase of the viral life cycle; six from the early expression stage (e.g. RIR1, BBLF2, DUT) and 16 from the late expression stage (e.g. BILF1, BDLF2, PORTL, CEP2, LTP). However, no peptide from the immediate-early genes BZLF1 and BRLF1 (Rta) were immunogenic. A small fraction of four epitopes represented proteins produced during latency (LMP1, LMP2, EBNA2, EBNA6).

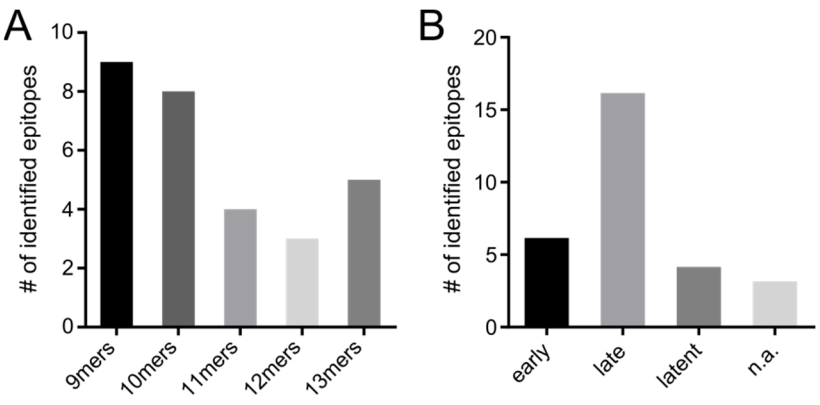

Figure 7: Length distribution (A) and expression program of source antigens (B) of the 29 identified epitopes. Abbreviation: n.a., not assigned.

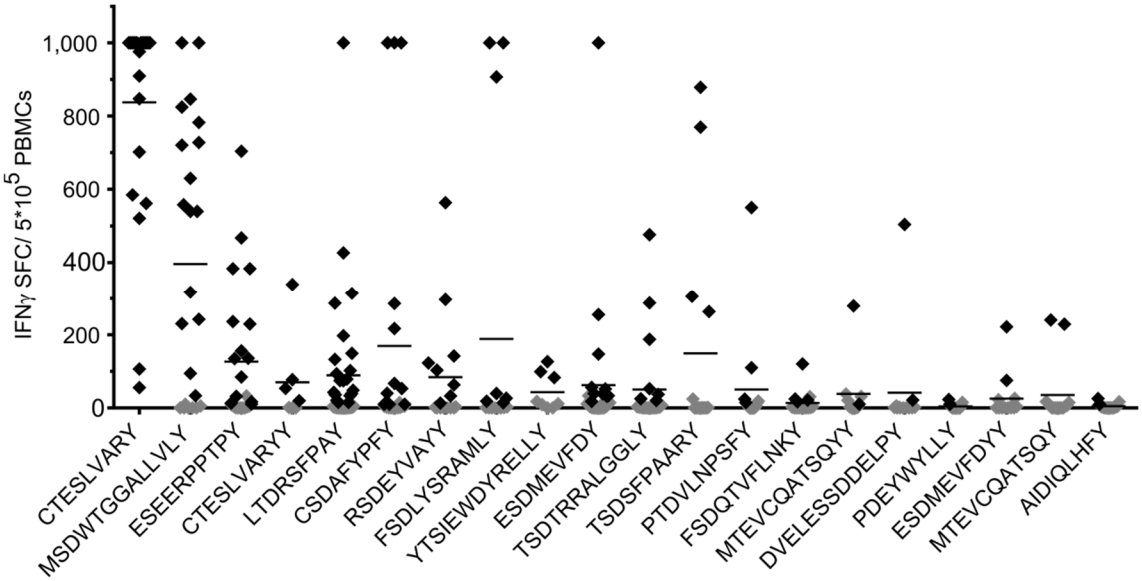

Figure 8: ELISpot screening results of EBV-derived epitopes that elicited an IFNγ response in at least two PBMC samples. Depicted are numbers of IFNγ SFC for each tested PBMC culture minus the spot numbers of the negative control of the PBMCs. Positive evaluated PBMC cultures are depicted in black, negative tested PBMC cultures in grey. Epitopes were tested once in technical duplicates in at least seven different HLA-A*01-positive PBMC cultures. Bars represent the mean IFNγ SFC. Abbreviations: SFC, spot forming cells.

Figure 8 shows the IFNγ ELISpot results of the 20 epitopes that were able to stimulate memory T cells in two or more PBMC samples, ordered from the epitope with the highest recognition rate to the lowest from left to right.

The response rate for each peptide was determined as the percentage of responding PBMC cultures of all tested cultures. According to their response rate, peptides were assigned to three categories: dominant epitopes (≥ 50% response rate), subdominant epitopes (< 50% response rate), and non-immunogenic. Seven of the 29 epitopes were dominant epitopes with a response rate of ≥ 50%, with CETSLVARY (BILF1) being the epitope with the highest response rate. CTESLVARY was able to elicit an IFNγ immune response in all tested PBMC samples after a 12-day stimulation and thus reached a response rate of 100%. The mean number of IFNγ SFC was 837, which was the highest of all epitopes. The second-best epitope achieving a recognition rate of 69.5% was an unusually long peptide: the 13mer MSDWTGGALLVLY originating from the latent protein LMP1. Four other peptides were also found to be dominant epitopes with response rates ranging from 50% to 58%. One of them, CTESLVARYY, was a length variant of the epitope with the highest response rate and was therefore not further analyzed. A general trend can be observed in Figure 8: peptides with a high recognition rate also elicited higher mean spot counts in ELISpots after 12-day stimulation. Since the number of spots after stimulation does not allow any conclusions about the original number of peptide-specific memory T cells in the blood, the peptides were also examined in *ex vivo* ELISpot assays (without previous stimulation).

Table 9: IFNγ ELISpot results of all tested EBV-derived, HLA-A*01-restricted peptides.

Antigen	Position	Sequence	SYFPEITHI [% max. score]	NetMHC [nM]	Peptide pool No.	ELISpot RR (12 d stim.)
BILF1	258-266	CTESLVARY	80.0	8	8	23/23 (100%)
LMP1	44-56	MSDWTGGALLVLY	75.6	6	12	16/23 (70%)
LMP2	484-493	ESEERPPTPY	69.2	55	13	14/24 (58%)
BILF1	258-267	CTESLVARYY	74.4	18	8	4/7 (57%)
BDLF2	402-410	LTDRSFPAY	85.0	7		18/31 (56%)
RIR1	604-612	CSDAFYPFY	72.5	6	5	11/22 (50%)
PORTL	220-228	RSDEYVAYY	75.0	7	9	8/16 (50%)
CEP2	313-323	FSDLYSRAMLY	79.5	5	13	7/16 (44%)
LTP	1058-1070	YTSIEWDYRELLY	75.6	7		3/8 (38%)
RIR1	149-157	ESDMEVFDY	75.0	8	5	10/29 (35%)
BBLF2	468-479	TSDTRRALGGLY	75.6	7	15	7/22 (32%)
LTP	314-323	TSDSFPAARY	76.9	14	3	4/15 (27%)
LTP	2540-2549	PTDVLNPSFY	82.1	15		4/15 (27%)
DUT	198-208	FSDQTVFLNKY	82.1	6		4/17 (24%)

Table 9 continued (1/4)

Antigen	Position	Sequence	SYFPEITHI [% max. score]	NetMHC [nM]	Peptide pool No.	ELISpot RR (12 d stim.)
gB	584-595	MTEVCQATSQYY	75.6	9	3	2/10 (20%)
EBNA6	380-392	DVELESSDDELPY	75.6	376	8	2/13 (15%)
n.c.	79-87	PDEYWYLLY	67.5	1730		2/13 (15%)
RIR1	149-158	ESDMEVFDYY	74.4	13	5	2/14 (14%)
gB	584-594	MTEVCQATSQY	79.5	16		2/15 (13%)
UL32	167-175	AIDIQLHFY	67.5	17		2/15 (13%)
gH	61-72	VTEDLASMLNRY	78.1	9		1/10 (10%)
ITP	908-920	LNERVEHALELGY	75.6	4999	5	1/13 (8%)
BILF1	23-32	ATEDACTKSY	79.5	161	8	1/14 (7%)
gM	71-80	YLEPPEMFVY	69.2	95	9	1/15 (7%)
HELI	648-658	LLDYASTTENY	69.2	66	9	1/15 (7%)
UL92	167-179	SSEKVVDVVLSLY	80.5	25	13	1/15 (7%)
EBNA2	112-120	PLDRDPLGY	72.5	25	13	1/15 (7%)
gB	131-139	ETDQMDTIY	80.0	7		1/15 (7%)
UL32	115-124	FEDYALLCYY	69.2	607		1/18 (6%)
DPOL	388-396	ILDRARHIY	67.5	114		0/18
TRM1	373-384	PPEVAELSELLY	80.5	11878		0/10
TRX1	259-270	PADARLYVALTY	75.6	40		0/10
CEP2	24-35	LSDASTPQMKVY	73.2	16		0/10
TRM1	622-634	SSEHLHALTHSLY	80.5	11		0/10
UL32	185-197	SSDMIRNANLGYY	75.6	6		0/10
LTP	241-253	ETEDPRIFMLEHY	75.6	38		0/8
LTP	2020-2032	ETESPCDPLNPAY	75.6	44		0/8
MTP	1237-1247	GTDAWRFAMNY	79.5	8		0/8
DPOL	903-913	STELSRKLSAY	84.6	39		0/8
BRRF1	143-153	GSDYTAVSLQY	82.1	11		0/8
BRRF1	278-290	VTDAITLPDCAEY	78.1	7		0/8
HELI	654-663	TTENYTLLGY	87.2	9		0/8
TRM1	755-764	DSDRPLILLY	84.6	58		0/8
UL17	83-92	YCDEGLPELY	69.2	51		0/8
LTP	714-722	TLDTARSQY	67.5	384	3	0/8
LTP	2034-2043	SADTQEPLNY	74.4	162	3	0/8
LTP	1060-1070	SIEWDYRELLY	71.8	329	3	0/8
LTP	3138-3148	IADLERLKFLY	71.8	33	3	0/8
gB	148-156	TKDGLTRVY	67.5	14816	3	0/8
gB	656-664	DLEGIFREY	67.5	9058	3	0/8
gB	635-644	NIDFASLELY	71.8	40	3	0/8
UL95	10-19	PDDPMLARRY	69.2	10639	10	0/8
BDLF3	170-180	VPDERQPSLSY	71.8	5013	10	0/8
BDLF2	228-237	GRDFGVPLSY	71.8	10212	10	0/8
MCP	985-993	RPEQLFAEY	70.0	15890	10	0/8
MCP	706-714	VGDESVGQY	67.5	1940	10	0/8

Table 9 continued (2/4)

Antigen	Position	Sequence	SYFPEITHI [% max. score]	NetMHC [nM]	Peptide pool No.	ELISpot RR (12 d stim.)
MCP	804-813	HADVLEKIFY	69.2	280	10	0/8
UL25	375-383	ALEALMLVY	75.0	32	10	0/8
LF2	304-313	ITELEYNNTY	76.9	91	10	0/8
ICP27	416-425	HDEVEFLGHY	66.7	4562	10	0/8
TRM1	443-453	ATERLFCGGVY	76.9	16	15	0/8
TRM1	527-537	LSDALKRKEQY	76.9	36	15	0/8
BKRF4	47-55	VSDTDESDY	75.0	12	15	0/8
BKRF4	86-94	PSDSDESDY	72.5	17	15	0/8
BBLF2	490-499	AADLGLTWAY	71.8	328	15	0/8
BBLF2	186-196	HSESPGQLDVY	76.9	46	15	0/8
n.c.	674-684 152-162	ATEHGLSPTAY	74.4	15	15	0/8
BTRF1	250-260	NPDLLPLQHLY	69.2	1055	15	0/8
DNBI	206-218	NSDLSRCMHEALY	75.6	7		0/8
AN	94-105	ATDEQRTVLCSY	78.1	7		0/7
TRM3	357-366	SADQATSFLY	69.2	111		0/7
LF2	264-273	LDDVIIAFRY	69.2	2974		0/7
n.c.	28-36	STRACVLLY	67.5	542		0/7
GP350	804-814	GGDSTTPRPRY	69.2	3857		0/7
PORTL	118-127	VRDLLTTNIY	69.2	5440	9	0/7
HELI	314-324	GLELSPDILAY	71.8	215	9	0/7
HELI	639-651	TSDEPLLHGLLDY	85.4	8	9	0/7
HELI	653-663	STTENYTLLGY	69.2	45	9	0/7
AN	236-246	KSEFDPIYPSY	71.8	213	9	0/7
AN	78-88	SKDGPSLKSIY	69.2	13423	9	0/7
DNBI	767-776	FPDTKLSSLY	66.7	1897	12	0/7
DNBI	691-701	DLDAALQGRVY	69.2	1424	12	0/7
BARF1	204-214	KNDKEEAHGVY	69.2	9374	12	0/7
gH	523-532	DRDAWHLPAY	69.2	6147	12	0/7
gH	62-72	TEDLASMLNRY	74.4	3550	12	0/7
gH	469-479	GTESGLFSPCY	74.4	39	12	0/7
gH	555-566	SSDREVRGSALY	80.5	14	12	0/7
UL25	548-556	ASDDYDRLY	77.5	10	12	0/7
ICP27	381-389	VVETLSSSY	62.5	285	13	0/7
EBNA2	464-474	TTESPSSDEDY	74.4	33	13	0/7
UL92	171-179	VVDVVLSLY	67.5	18	13	0/7
UL92	15-27	GTDEPNPRHLCSY	75.6	11	13	0/7
TEG2	48-57	CGETNEGLEY	69.2	917	13	0/7
LTP	2024-2032	PCDPLNPAY	67.5	394		0/6
LF2	263-273	LLDDVIIAFRY	69.2	14		0/6
ICP27	415-425	RHDEVEFLGHY	69.2	7226		0/6
LF1	421-429	NLDAGRIFY	70.0	21		0/6
LF1	418-429	RSDNLDAGRIFY	80.5	8		0/6

Table 9 continued (3/4)

Antigen	Position	Sequence	SYFPEITHI [% max. score]	NetMHC [nM]	Peptide pool No.	ELISpot RR (12 d stim.)
n.c.	78-87	VPDEYWYLLY	76.9	534		0/6
ITP	521-533	SSELLRSLLWVRY	75.6	19	5	0/6
RIR1	654-662	LPEALRQRY	67.5	14986	5	0/6
RIR1	52-61	YLEVFSDKFY	66.7	87	5	0/6
RIR1	195-205	SSEWDVTQALY	74.4	26	5	0/6
RIR1	715-725	SYELGLKTIMY	66.7	10831	5	0/6
GP42	176-185	SLDGGTFKVY	71.8	474	8	0/6
BZLF1	25-33	AFDQATRVY	70.0	11562	8	0/6
BZLF1	172-180	DSELEIKRY	70.0	3423	8	0/6
BZLF1	8-18	SEDVKFTPDPY	69.2	5048	8	0/6
BZLF1	170-180	ECDSELEIKRY	66.7	3253	8	0/6
KITH	465-473	VNDAYHAVY	67.5	1135	1	Pool
KITH	156-166	GADSTSRSFMY	64.1	**82**	1	Pool
MTP	382-390	ALDTVRYDY	70.0	77	1	Pool
MTP	175-183	LFDNALRKY	67.5	12537	1	Pool
MTP	426-434	ALELFSALY	65.0	69	1	Pool
MTP	650-658	PLDLPLADY	65.0	528	1	Pool
MTP	1073-1082	VRDNTFLDKY	71.8	2244	1	Pool
MTP	531-540	ACDMAGCQHY	66.7	459	1	Pool
MTP	105-117	ALEASGNNYVYAY	65.9	268	1	Pool
IL10H	151-160	MSEFDIFINY	69.2	43	2	Pool
UL32	115-123	FEDYALLCY	70.0	622	2	Pool
UL32	243-251	PGDVGRGLY	70.0	3311	2	Pool
UL32	472-481	VCDSLITLVY	76.9	83	2	Pool
UL32	114-123	FFEDYALLCY	71.8	104	2	Pool
UL32	139-149	GMDFLHILIKY	71.8	32	2	Pool
LTP	2723-2731	ASEQGPIVY	77.5	23	2	Pool
LTP	1062-1070	EWDYRELLY	72.5	3647	2	Pool
MTP	101-113	GTESALEASGNNY	75.6	63	2/4	Pool
EAR	42-50	PEDTVVLRY	75.0	1755	4	Pool
EAR	41-50	SPEDTVVLRY	71.8	10525	4	Pool
UL32	185-196	SSDMIRNANLGY	90.2	7	4	Pool
UL34	236-247	FSEAETEDEASY	73.2	11	4	Pool
LTP	1603-1613	NTDLEAPYAEY	87.2	9	4	Pool
TRX1	329-340	ATDGWRRSAFNY	78.1	14	4	Pool
gB	654-664	VFDLEGIFREY	69.2	5421	4	Pool
ITP	318-327	LLEPSGALFY	71.8	40	4	Pool
EAD	192-200	NPDLYVTTY	65.0	9316	6	Pool
EAD	202-211	SGEACLTLDY	71.8	4275	6	Pool
EAD	105-114	AVEQASLQFY	66.7	132	6	Pool
BMRF2	238-248	HAEVFFGLSRY	69.2	146	6	Pool
PRIM	261-269	SADLVRYVY	70.0	87	6	Pool

Table 9 continued (4/4)

Antigen	Position	Sequence	SYFPEITHI [% max. score]	NetMHC [nM]	Peptide pool No.	ELISpot RR (12 d stim.)
gN	43-51	LTEAQDQFY	77.5	8	6	Pool
DPOL	96-104	VYDILETVY	70.0	6003	6	Pool
DPOL	879-887	VIDILNQAY	67.5	23	6	Pool
DPOL	262-271	HRDSYAELEY	74.4	1300	6	Pool
DPOL	957-966	KTEMAEDPAY	74.4	195	7	Pool
DPOL	445-454	CRDKLSLSDY	71.8	3568	7	Pool
GP350	143-151	HAEMQNPVY	62.5	159	7	Pool
GP350	312-324	SQDMPTNTTDITY	75.6	396	7	Pool
GP350	319-331	TTDITYVGDNATY	75.6	9	7	Pool
EBNA4	328-336	TNEEIDLAY	65.0	1282	7	Pool
EBNA4	809-820	TSDKIVQAPIFY	80.5	7	7	Pool
EBNA6	41-51	ASERLVPEESY	69.2	111	7	Pool
EBNA6	382-392	ELESSDDELPY	69.2	99	7	Pool
MCP	1216-1225	NQEVAEGLIY	69.2	4530	11	Pool
MCP	525-535	PTEDFLHPSNY	74.4	21	11	Pool
MCP	789-799	DHDFRLHLGPY	69.2	7887	11	Pool
MCP	829-841	GVDFQHVAQTLAY	75.6	16	11	Pool
DNBI	519-527	PDDEPRYTY	65.0	11636	11	Pool
DNBI	588-596	YKDLVKSCY	65.0	8712	11	Pool
DNBI	153-162	ITEAFKERLY	76.9	65	11	Pool
DNBI	292-301	SHETPASLNY	69.2	12336	11	Pool
DNBI	518-527	RPDDEPRYTY	66.7	13837	11	Pool
LMP2	410-420	LTEWGSGNRTY	74.4	40	14	Pool
KR2	295-303	RLDLQSLGY	75.0	18	14	Pool
KR2	103-111	LYDSVTELY	67.5	266	14	Pool
KR2	72-82	RCDHLPITCEY	69.2	250	14	Pool
KR2	295-307	RLDLQSLGYSLLY	82.9	10	14	Pool
BFRF2	44-56	LLDLGLACLDLSY	78.1	16	14	Pool
TRM1	746-754	PPDGLYLTY	72.5	6421	14	Pool
TRM1	771-779	FKDLYALLY	72.5	32	14	Pool
TRM1	376-384	VAELSELLY	70.0	25	14	Pool

n.c., not characterized; RR, response rate; Pool, peptides were only tested in pools.

Ex vivo ELISpot was performed with 16 randomly selected HLA-matched PBMC samples stimulated overnight with the most immunogenic epitopes. Only the two epitopes with the highest recognition rate, CTESLVARY and MSDWTGGALLVLY, stimulated detectable numbers of peptide-specific memory T cells in several donors with a recognition rate of 37.5% and 18.8%, respectively (Table 10). Thus, the initial number of peptide-specific T cells appears to be in fact higher for epitopes with high recognition rates in some cases. All other specificities have such low cell numbers in peripheral blood that they are not detectable by this assay. However, the significant increase in the response

rate in 12-day ELISpots compared to *ex vivo* ELISpots and the high spot counts after stimulation demonstrate the immense proliferation capability of EBV-specific memory T cells.

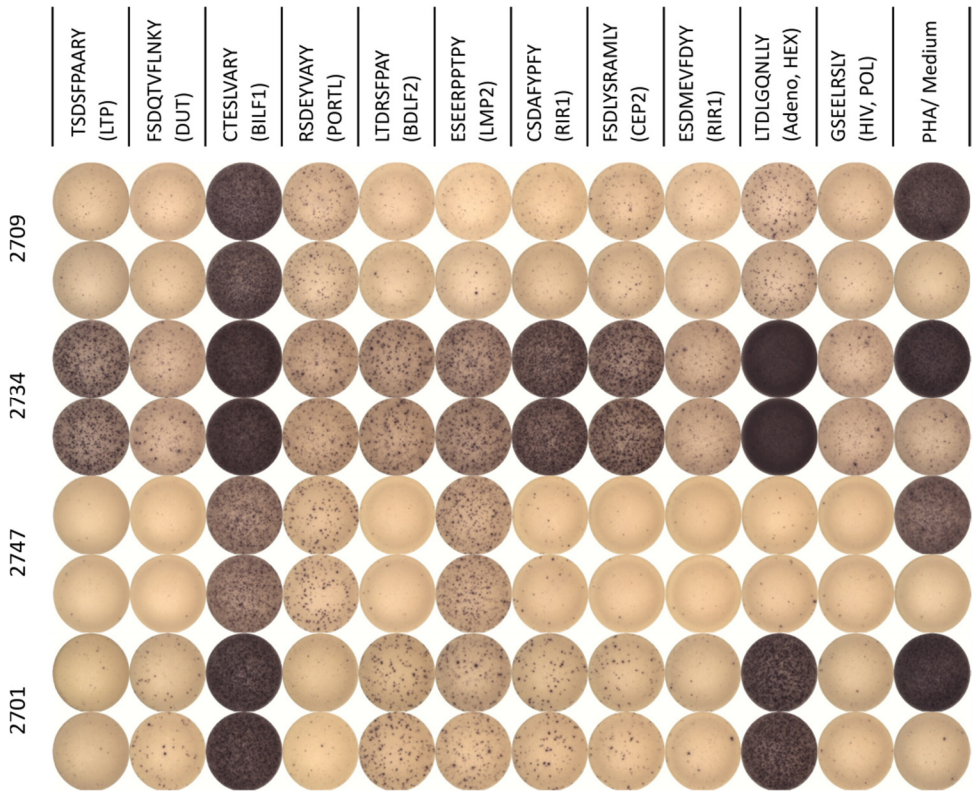

Figure 9: Parallel recognition of several epitopes by PBMC cultures. Shown is an ELISpot plate with four PBMC samples (2709, 2734, 2747, and 2701) after 12-day stimulation with nine test peptides, the positive and the negative control. The adenovirus epitope LTDLGQNLY and PHA served as positive control and the HIV epitope GSEELRSLY and medium served as negative control.

Parallel testing of several epitopes in 12-day ELISpot assays revealed multiple memory responses in each PBMC sample (Figure 9). PBMC cultures recognized different sets and different numbers of epitopes. A maximum of seven epitopes was recognized in parallel by PBMCs from donor 2734 while other PBMC cultures recognized only three epitopes (2709, 2747). In all tested PBMC samples, CTESLVARY elicited the strongest response among the EBV-specific epitopes. Apart from that, no clear hierarchy could be observed.

3.1.3 Evaluation of functionality and HLA specificity of EBV-specific memory T cells

While IFNγ ELISpot assays are highly sensitive and efficient in detecting activated memory T cells, almost no conclusions can be drawn regarding the type of the activated cells and their HLA restriction. 'Mismatch' ELISpots in which PBMCs are tested that are not HLA-matched can provide a first indication of the HLA restriction of the reactive cells. Therefore, 16 PBMC samples, which were

HLA-A*01-negative, were stimulated with the ten epitopes with the highest immunogenicity for 12 days. Only one epitope was able to stimulate memory T cells in HLA-A*01-negative samples in the following ELISpot: two PBMC cultures pulsed with MSDWTGGALLVLY showed IFNγ SFCs. Both donors are HLA-A*03- and HLA-B*44-positive, but none of the binding motifs match the epitope. This may suggest a binding of HLA-II molecules.

In order to validate the functionality and the HLA restriction of the stimulated T cells, ICS and tetramer staining was performed. The cells underwent 12-day stimulation prior to both of the assays and the same initial gating strategy was applied for all analyses; first, the lymphocytes were gated using the forward scatter (FSC) and side scatter. FSC-area (FSC-A) versus FSC-height was then used to exclude doublets from the analyses. Lastly, FSC-A was plotted against Aqua live/dead to allow for the gating of living, Aqua live/dead-negative cells.

ICS was performed to determine the functionality of the stimulated T cells and whether the respective response to dominant epitopes was mediated by $CD4^+$ or $CD8^+$ T cells. For this purpose, CD8-PerCP was plotted against CD4-APC-Cy7 to enable gating of the $CD8^+$ and the $CD4^+$ population. Both populations were then separately analyzed for their TNF (PacificBlue) and IFNγ (PE) production (Figure 10B). The TNF^+, $IFN\gamma^+$, and double-positive populations of the cells stimulated with the test peptide had to be at least twice as large as those of the negative control to be considered positive. All dominant epitopes caused an IFNγ and TNF secretion by $CD8^+$ T cells in at least two tested donors with LTDRSFPAY being the exception with no TNF production.

HLA tetramer staining was then performed to validate the HLA restriction of the stimulated memory T cells. $CD8^+$ T cells were therefore gated from the living cell population and plotting of CD8-PerCP against tetramer-PE enabled the identification of $CD8^+tetramer^+$ cells (Figure 10C). The $tetramer^+$ population of the tetramer of interest had to be at least twice as large as that of the negative control to be considered positive. Specific, $tetramer^+$ T cell populations could be detected for all dominant epitopes in at least one donor sample (Table 10). This indicates that T cells activated by the tested epitopes can recognize this peptide in complex with HLA-A*01:01 and are therefore restricted to HLA-A*01.

The activation of $CD8^+$ T cells in the ICS and the positive tetramer staining with donor PBMCs stimulated with MSDWTGGALLVLY confirmed the HLA-A*01 restriction of this epitope. The positive PBMC cultures in the mismatch ELISpot, however, indicated a binding of this peptide by other HLA allotypes. Either the same epitope can be bound by different HLA allotypes or the relatively long peptide harbors different epitopes.

In total, the HLA restriction to HLA-A*01 and the functionality of the peptide-specific cells could be confirmed for all dominant epitopes.

Table 10: Summary of ELISpot, tetramer staining and ICS results for the epitopes with the highest recognition rates in ELISpot assays.

Antigen	Position	Sequence	ELISpot response rate (12 d stim.)	ELISpot response rate (*ex vivo*)	ICS	Tetramer staining
BILF1	258-266	CTESLVARY	23/23 (100.0%)	6/16 (37.5%)	$CD8^+$, $IFN\gamma^+$, TNF^+	positive
LMP1	44-56	MSDWTGGALLVLY	16/23 (69.5%)	3/16 (18.8%)	$CD8^+$, $IFN\gamma^+$, TNF^+	positive
LMP2	484-493	ESEERPPTPY	14/24 (58.3%)	0/16	$CD8^+$, $IFN\gamma^+$, TNF^+	positive
BILF1	258-267	CTESLVARYY	4/7 (57.1%)	-	-	-
BDLF2	402-410	LTDRSFPAY	18/31 (55.6%)	0/16	$CD8^+$, $IFN\gamma^+$, TNF^-	positive
RIR1	604-612	CSDAFYPFY	11/22 (50.0%)	0/16	$CD8^+$, $IFN\gamma^+$, TNF^+	positive
PORTL	220-228	RSDEYVAYY	8/16 (50.0%)	0/16	$CD8^+$, $IFN\gamma^+$, TNF^+	positive
CEP2	313-323	FSDLYSRAMLY	7/16 (43.8%)	0/16	$CD8^+$, $IFN\gamma^+$, TNF^+	-

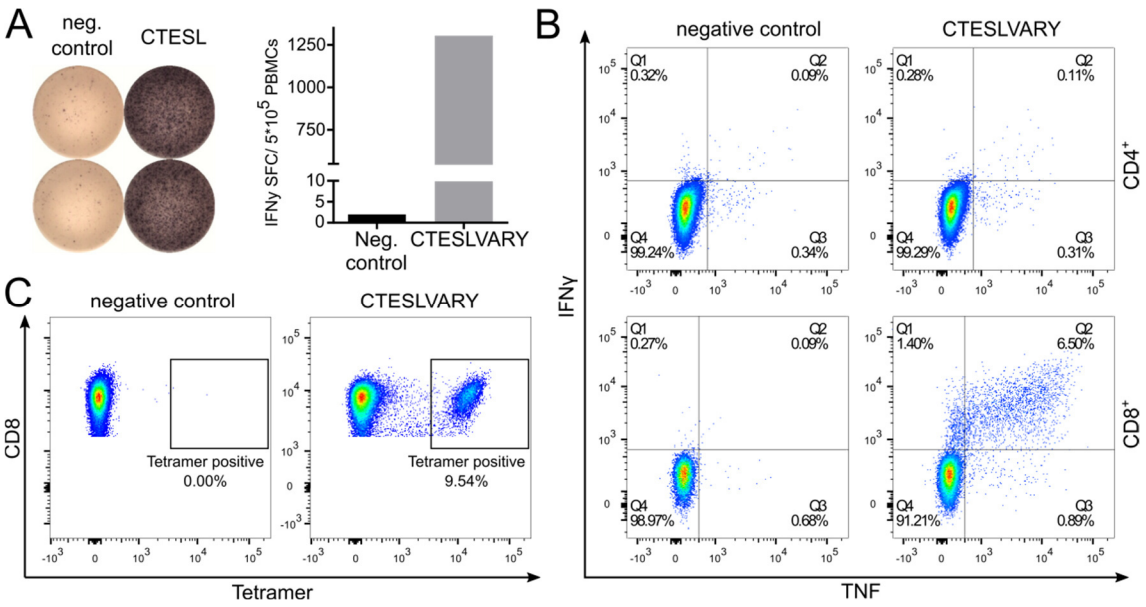

Figure 10: Characterization of CTESLVARY and its specific memory T cells. Shown are exemplary results of an ELISpot assay (A), an ICS (B), and a tetramer staining (C) with PBMCs of donor 2544 pulsed with CTESLVARY or negative control. The cells were stimulated for 12 days prior to each assay. The HIV-derived peptide GSEELRSLY served as negative control for the ELISpot and the ICS. The negative control of the tetramer staining was a HLA-A*01-tetramer with GSEELRSLY.

3.2 Naturally presented HCMV-derived T cell epitopes

3.2.1 Identification of naturally presented HCMV-derived ligands

The infection of human foreskin fibroblast cell lines with mutant HCMV lacking immunoevasins US2-US11 (ΔUS2-11) enabled the isolation of HCMV-derived HLA ligands from the cell surface and the identification by LC-MS/MS. As shown in Figure 11, the infection of fibroblasts with WT AD169VarL usually leads to a drastic decrease of the HLA-I surface expression. However, infection with ΔUS2-11 led to a clear increase in HLA-I expression, almost reaching the levels of uninfected cells (mock). Infection and HLA-I expression analysis were performed by Liane Bauersfeld from the group of Dr. Anne Halenius in Freiburg.

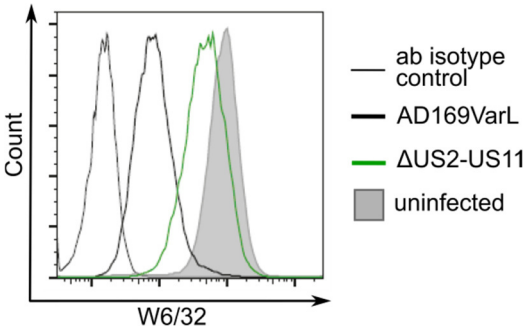

Figure 11: Cell surface expression of HLA-I. HF-99/7 fibroblasts were mock-treated or infected with AD169VarL wild-type virus or deletion mutants with an MOI of 5. Cell surface expression of HLA-I (W6/32) was analysed by flow cytometry at 48 h.p.i. Shown are representative results of two experiments. Adapted from Dr. Anne Halenius, Freiburg.

For the identification of HCMV-derived HLA ligands, HF-99/7 cells were infected with ΔUS2-11 (n = 1) or mock treated (n = 1) and ligands were isolated with immunoaffinity purification. The sequences were then identified *via* liquid chromatography-coupled tandem-mass spectrometry (LC-MS/MS) in three technical replicates. MS analyses identified 3052 peptides in the mock treated sample and 5793 peptides in the infected sample. SYFPEITHI and NetMHCpan 3.0 predicted 2839 (mock) and 5511 (ΔUS2-11) to be binders, which represents a purity of 93% and 95%, respectively.

Table 11: Summary of mass spectrometry analyses of HF-99/7 cells either infected with ΔUS2-11 or mock treated.

Sample	Peptides	Binders	Purity	HCMV-derived binders	HCMV source proteins
HF-99/7 mock	3052	2839	93%	0	0
HF-99/7 ΔUS2-11	5793	5511	95%	181	80

Of these binders, 37, 44, 21, 43, 17, and 4 viral peptides (altogether 181) were restricted to HLA-A*01:01, -A*03:01, -B*08:01, -B*51:01, -C*01:02, and -C*07:01, respectively (Figure 12). The HLA annotation of 15 peptides was ambiguous.

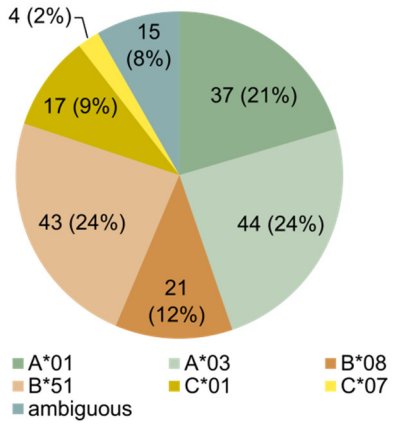

Figure 12: Distribution of HLA restrictions among the 181 HF-99/7 ligands. Ligands were predicted with SYFPEITHI and NetMHCpan 3.0. Ligands are designated ambiguous when the prediction tools were inconsistent in their restriction assignment.

The infection time of 48 h was chosen to enable the detection of peptides originating from proteins with various expression kinetics. Indeed, the source proteins of the identified ligands represent all classes or profiles of gene expression as described by Weekes *et al.* [264] (Figure 13). The distribution of ligands mirrors well the proportions of proteins assigned to each profile by Weekes *et al.*

All identified HCMV-derived ligands are listed in Supplemental Table 6.

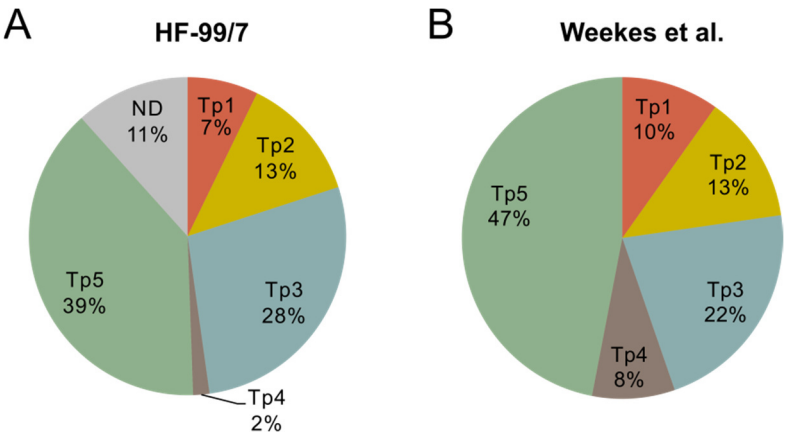

Figure 13: Distribution of temporal profiles among identified ligands of the HF-99/7 cell line (A) and proteins as assigned by Weekes *et al.* (B). ND, not determined; Tp, temporal profile.

3.2.2 IFNγ ELISpot screening for HCMV-derived T cell epitopes

All ligands with a SYFPEITHI score of ≥ 70% or a NetMHC IC_{50} of ≤ 50 nM or a percentile rank of < 0.5% were further evaluated for their immunogenicity. Therefore, peptides were tested for memory T cell responses in at least seven different HCMV-seropositive, HLA-matched individuals by IFNγ ELISpot assay with prior 12-day stimulation. Of the HLA-A*01:01, -A*03:01, -B*08:01, and -B*51:01-restricted ligands, 32, 39, 20, and 30, respectively, were tested in ELISpot (Figure 14). Some HLA-C-restricted peptides were tested randomly. However, they were not further evaluated and included in the analyses since the healthy blood donors were not typed for HLA-C. It was therefore impossible to draw conclusions from those immunogenicity assays, especially for rare HLA types such as C*01:02. Of the 32 tested, HLA-A*01-restricted peptides, 16 were able to elicit an IFNγ response in PBMCs of at least one healthy blood donor. For HLA-A*03-restricted peptides, 13 out of 39 peptides were recognized by memory T cells. For HLA-B*08 and -B*51-restricted peptides, 10 out of 20 and 12 out of 30, respectively, were immunogenic in at least one PBMC sample. Overall, the proportion of epitopes among the identified peptides was 31%. The response rate for each peptide was determined as the percentage of positively tested donor samples out of tested samples. Based on the response rate peptides were grouped into three categories: negative (no memory response in any individual), subdominant (recognized by < 50% of individuals), and dominant (recognized by ≥ 50% of individuals). Two to five peptides of each HLA restriction were shown to be dominant epitopes with a response rate of ≥ 50%. The numbers of identified, tested, and immunogenic peptides for each HLA type are summarized in Figure 14.

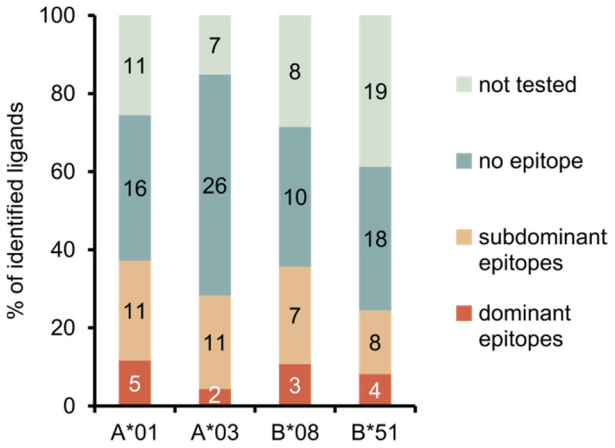

Figure 14: Distribution of tested, subdominant, and dominant HCMV ligands restricted to HLA-A and -B allotypes.

Figure 15 to Figure 18 depict the IFNγ ELISpot screening results of all epitopes in the form of numbers of spot forming cells (SFC) for each PBMC culture. PBMC samples with a positively evaluated spot count are depicted in black, PBMCs evaluated as negative in grey.

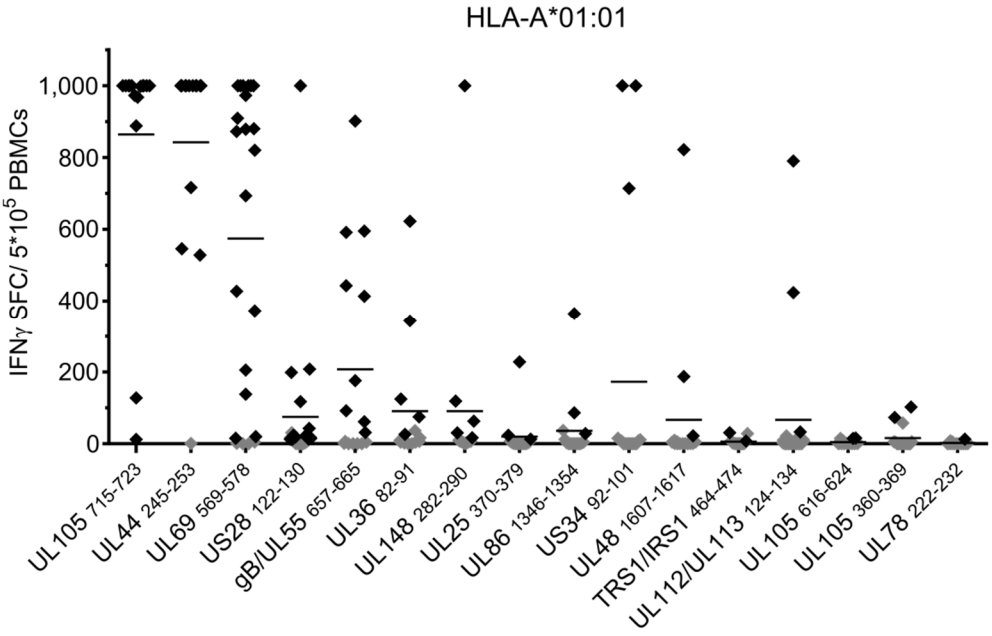

Figure 15: ELISpot screening results of HLA-A*01:01-restricted epitopes. Depicted are numbers of IFNγ SFC for each tested PBMC culture minus the spot numbers of the negative control of the PBMCs. Positive evaluated PBMC cultures are depicted in black, negative tested PBMC cultures in grey. Epitopes were tested once in technical duplicates in at least seven different HLA-matched PBMC cultures. Bars represent the mean IFNγ SFC. Abbreviations: SFC, spot forming cells.

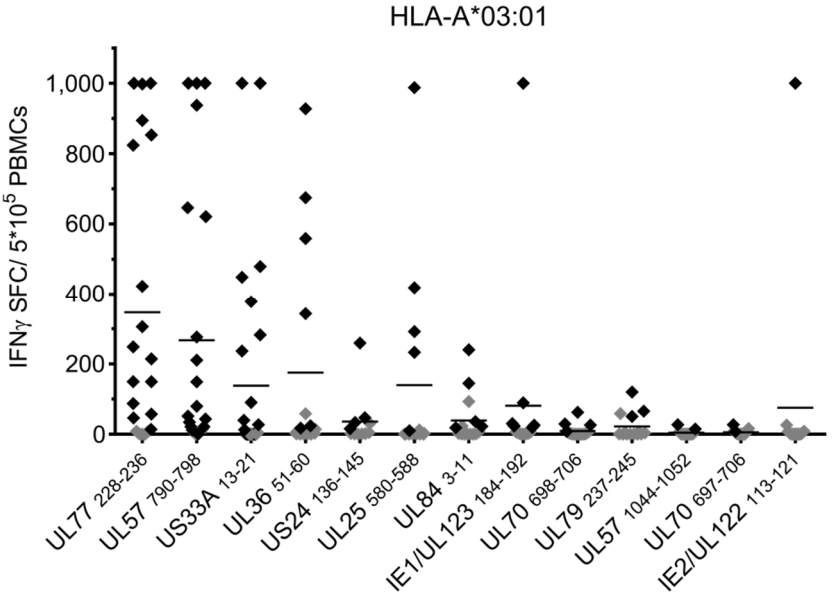

Figure 16: ELISpot screening results of HLA-A*03:01-restricted epitopes. Depicted are numbers of IFNγ SFC for each tested PBMC culture minus the spot numbers of the negative control of the PBMCs. Positive evaluated PBMC cultures are depicted in black, negative tested PBMC cultures in grey. Epitopes were tested once in technical duplicates in at least seven different HLA-matched PBMC cultures. Bars represent the mean IFNγ SFC. Abbreviations: SFC, spot forming cells.

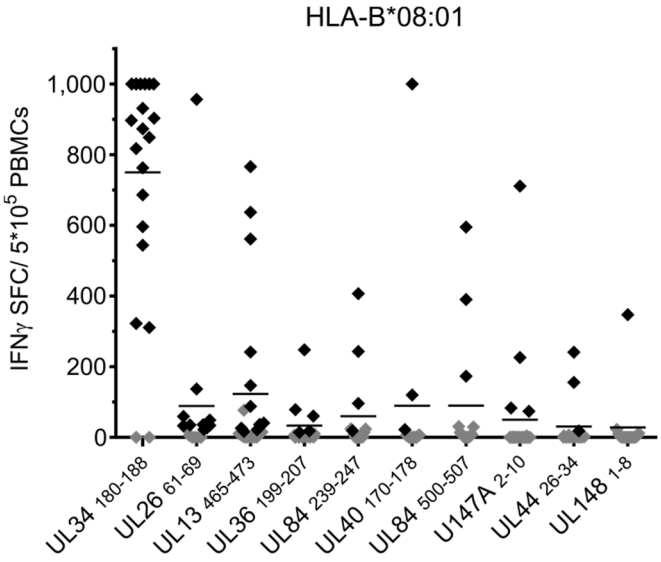

Figure 17: ELISpot screening results of HLA-B*08:01-restricted epitopes. Depicted are numbers of IFNγ SFC for each tested PBMC culture minus the spot numbers of the negative control of the PBMCs. Positive evaluated PBMC cultures are depicted in black, negative tested PBMC cultures in grey. Epitopes were tested once in technical duplicates in at least seven different HLA-matched PBMC cultures. Bars represent the mean IFNγ SFC. Abbreviations: SFC, spot forming cells.

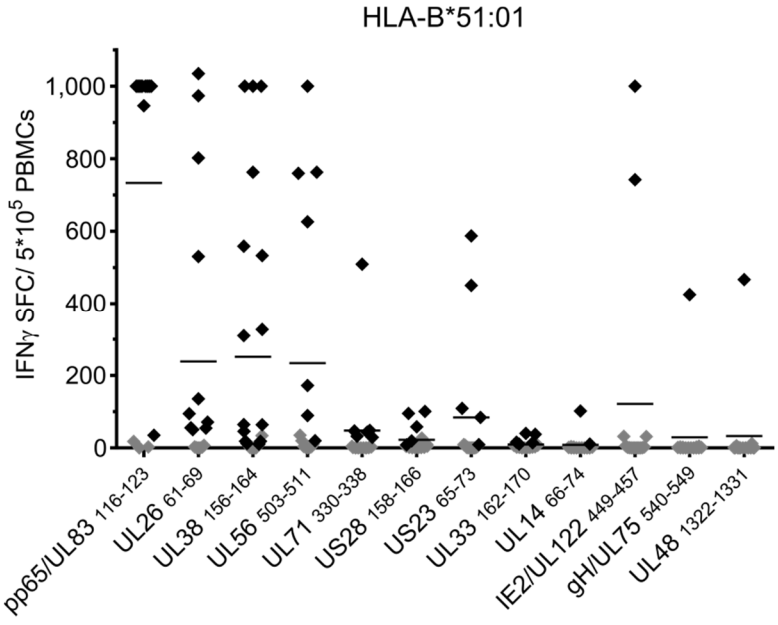

Figure 18: ELISpot screening results of HLA-B*51:01-restricted epitopes. Depicted are numbers of IFNγ SFC for each tested PBMC culture minus the spot numbers of the negative control of the PBMCs. Positive evaluated PBMC cultures are depicted in black, negative tested PBMC cultures in grey. Epitopes were tested once in technical duplicates in at least seven different HLA-matched PBMC cultures. Bars represent the mean IFNγ SFC. Abbreviations: SFC, spot forming cells.

Normalized spot counts in IFNγ ELISpot assays after 12-day stimulation were donor dependent and in part highly variable. While some PBMC cultures stimulated with one peptide showed very high numbers of SFCs, sometimes out of the countable range ("too numerous to count"), other PBMC cultures reached numbers barely above the threshold for being evaluated as positive. The epitopes in Figure 15 to Figure 18 are ordered according to their response rate beginning with the epitopes with the highest recognition rate on the left. It can be seen that the average number of specific memory T cells after 12-day stimulation is usually higher for highly immunogenic epitopes compared to the average spot counts of peptides with lower recognition rates. Interestingly, some peptides with low response rates such as US34$_{92\text{-}101}$ (GSDALPAGLY, A*01:01), IE2/UL122$_{113\text{-}121}$ (SVSSAPLNK, A*03:01), and IE2/UL122$_{449\text{-}457}$ (MPVTHPPEV, B*51:01) showed very high numbers of SFCs in those few PBMC cultures that were tested positive.

In total, ELISpot screening identified 50 unique T cell epitopes with specific memory T cells in at least one of the tested donors (Table 12). Of these 50 epitopes, four epitopes were already known and published: UL105$_{715\text{-}723}$ (YADPFFLKY, HLA-A*01:01), UL44$_{245\text{-}253}$ (VTEHDTLLY, HLA-A*01:01), UL123$_{184\text{-}192}$ (KLGGALQAK, HLA-A*03:01), and UL83$_{116\text{-}123}$ (LPLKMLNI, HLA-B*51:01). Thirteen of the epitopes identified in this work were dominant epitopes, ten of them novel epitopes discovered in this work and first published in "Identification of HCMV-derived T cell epitopes in seropositive individuals through viral deletion models." in the Journal of Experimental Medicine [394]. The dominant epitope UL26$_{61\text{-}69}$ (LPYPRGYTL) was predicted to bind HLA-B*08 as well as HLA-B*51 and was therefore tested for both allotypes. Interestingly, it was able to elicit IFNγ responses in HLA-B*08-positive and HLA-B*51-positive donor samples as well as in "mismatch" donor samples that were typed for neither of them.

The recognition rate of all T cell epitopes in ELISpot assays after 12-day stimulation is listed in Table 12.

Table 12: HCMV-derived T cell epitopes.

ID	Sequence	Tested HLA	ELISpot response rate (12 d stim.)	ELISpot response rate (*ex vivo*) †
UL105$_{715\text{-}723}$	YADPFFLKY [395]	A*01:01	15/15 (100%)	90.9
UL44$_{245\text{-}253}$	VTEHDTLLY [296]	A*01:01	13/14 (92.9%)	100.0
UL69$_{569\text{-}578}$	RTDPATLTAY	A*01:01	19/23 (82.6%)	66.7
US28$_{122\text{-}130}$	ITEIALDRY	A*01:01	14/24 (58.3%)	14.3
UL55$_{657\text{-}665}$	NTDFRVLELY	A*01:01	9/16 (56.3%)	0.0
UL36$_{82\text{-}91}$	FVEGPGFMRY	A*01:01	5/14 (35.7%)	
UL148$_{282\text{-}290}$	SLDRFIVQY	A*01:01	5/14 (35.7%)	
UL25$_{370\text{-}379}$	YTSRGALYLY	A*01:01	3/14 (21.4%)	
UL86$_{1346\text{-}1354}$	TSETHFGNY	A*01:01	3/15 (20.0%)	
US34$_{92\text{-}101}$	GSDALPAGLY	A*01:01	3/16 (18.8%)	

Table 12 continued (1/1)

ID	Sequence	Tested HLA	ELISpot response rate (12 d stim.)	ELISpot response rate (*ex vivo*) †
UL48$_{1607-1617}$	VTDYGNVAFKY	A*01:01	3/16 (18.8%)	
IRS1/TRS1$_{464-474}$	LLDELGAVFGY	A*01:01	2/13 (15.4%)	
UL112/UL113$_{124-134}$	ISENGNLQVTY	A*01:01	3/20 (15.0%)	
UL105$_{616-624}$	VTDPEHLMM	A*01:01	2/14 (14.3%)	
UL105$_{360-369}$	DLDFGDLLKY	A*01:01	2/16 (12.5%)	
UL78$_{222-232}$	YSDRRDHVWSY	A*01:01	1/16 (6.3%)	
UL77$_{228-236}$	GLYTQPRWK	A*03:01	16/21 (76.2%)	50.0
UL57$_{790-798}$	RVKNRPIYR	A*03:01	14/23 (60.9%)	33.3
UL36$_{51-60}$	RSALGPFVGK	A*03:01	6/15 (40.0%)	
UL123$_{184-192}$	KLGGALQAK [396]	A*03:01	6/15 (40.0%)	
US33A$_{13-21}$	KLGYRPHAK	A*03:01	11/29 (37.9%)	
US24$_{136-145}$	RVYAYDTREK	A*03:01	4/11 (36.4%)	
UL25$_{580-588}$	GVSSVTLLK	A*03:01	5/14 (35.7%)	
UL84$_{3-11}$	RVDPNLRNR	A*03:01	5/15 (33.3%)	
UL70$_{698-706}$	SVRLPYMYK	A*03:01	4/16 (25.0%)	
UL79$_{237-245}$	RTFAGTLSR	A*03:01	3/14 (21.4%)	
UL57$_{1044-1052}$	RLADVLIKR	A*03:01	2/13 (15.4%)	
UL70$_{697-706}$	RSVRLPYMYK	A*03:01	2/15 (13.3%)	
UL122$_{113-121}$	SVSSAPLNK	A*03:01	1/14 (7.1%)	
UL34$_{180-188}$	LPHERHREL	B*08:01	20/22 (90.9%)	85.7
UL26$_{61-69}$	LPYPRGYTL	B*08:01	11/16 (68.8%)	16.7
UL13$_{465-473}$	YLVRRPMTI	B*08:01	11/22 (50.0%)	33.3
UL36$_{199-207}$	VMKFKETSF	B*08:01	5/13 (38.5%)	
UL84$_{239-247}$	TPLLKRLPL	B*08:01	4/14 (28.6%)	
UL40$_{170-178}$	HLKLRPATF	B*08:01	3/13 (23.1%)	
UL84$_{500-507}$	FISSKHTL	B*08:01	3/14 (21.4%)	
UL147A$_{2-10}$	SLFYRAVAL	B*08:01	4/22 (18.2%)	
UL44$_{26-34}$	QLRSVIRAL	B*08:01	2/14 (14.3%)	
UL148$_{1-8}$	MLRLLFTL	B*08:01	1/14 (7.1%)	
UL83$_{116-123}$	LPLKMLNI	B*51:01	12/15 (80.0%)	87.5
UL38$_{156-164}$	FPVEVRSHV	B*51:01	15/23 (65.2%)	0.0
UL26$_{61-69}$	LPYPRGYTL	B*51:01	10/16 (62.5%)	33.3
UL56$_{503-511}$	DARSRIHNV	B*51:01	8/15 (53.3%)	
UL71$_{330-338}$	IPPPQIPFV	B*51:01	6/15 (40.0%)	
US28$_{158-166}$	IAIPHFMVV	B*51:01	5/15 (33.3%)	
US23$_{65-73}$	IPHNWFLQV	B*51:01	5/15 (33.3%)	
UL33$_{162-170}$	VPAAVYTTV	B*51:01	5/15 (33.3%)	
UL14$_{66-74}$	FPAHDWPEV	B*51:01	2/15 (13.3%)	
UL122$_{449-457}$	MPVTHPPEV	B*51:01	2/15 (13.3%)	
UL75$_{540-549}$	FPDATVPATV	B*51:01	1/15 (6.7%)	
UL48$_{1322-1331}$	LPYLSAERTV	B*51:01	1/15 (6.7%)	

†*Ex vivo* ELISpot assays were performed using donors that were positively tested in ELISpot assays with prior 12-day stimulation.
Abbreviation: nt, not tested

The ELISpot assay with prior stimulation is a highly sensitive method to detect peptide-specific memory T cells. The prior stimulation allows the amplification of small numbers of specific memory T cells that can later be detected in the ELISpot assay. However, due to the immense proliferative capacity of memory T cell, it does not allow direct conclusions about the initial number of memory T cells in the blood. To address this and to exclude possible competitive effects among the different epitopes during the 12-day amplification, *ex vivo* IFNγ ELISpots without pre-stimulation were performed. For this purpose, dominant epitopes were retested with PBMC samples of previously tested positive donors. Only a few of the epitopes with the highest recognition rates elicited frequent, detectable responses *ex vivo* (Table 12). In most cases, memory T-cell numbers were too small to be detectable *ex vivo* but underwent, in part massive, amplification (up to 1,000-fold) upon pre-stimulation. Figure 19 shows exemplarily the ELISpot results of two HLA-B*08-restricted epitopes: $UL34_{180-188}$ (LPHERHREL) and $UL26_{61-69}$ (LPYPRGYTL). The graph shows again the high, donor- and peptide-dependent variability in peptide-specific memory T cell numbers after 12-day stimulation. The initial number of specific memory T cells in the blood and their proliferative capacity also varied considerably between donors. Many PBMC cultures (2736, 2825, 3061) showed no detectable or barely detectable spot counts *ex vivo* but had high numbers of reactive, peptide-specific cells after stimulation. In contrast, donor 3025 had already considerable amounts of $UL34_{180-188}$-specific memory T cells without any pre-stimulation. Except for one donor (2736), $UL26_{61-69}$-specific cells showed a rather low proliferative capacity overall.

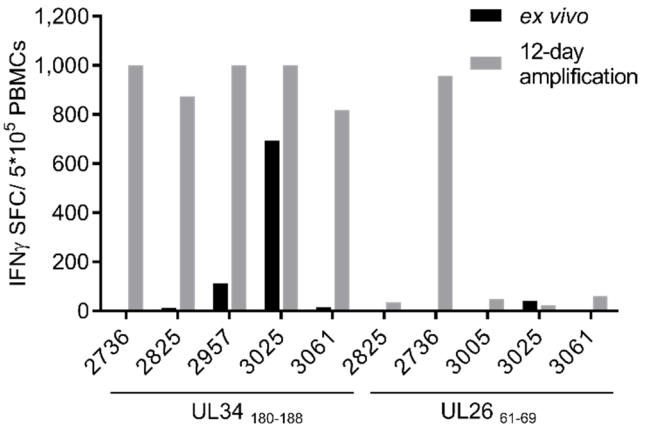

Figure 19: Comparison of IFNγ SFC in *ex vivo* ELISpots (black) and ELISpots with prior 12-day amplification (grey). Shown are exemplary results of two independent experiments with PBMCs of five donors (coded by four-digit numbers) each for two B*08 epitopes ($UL34_{180-188}$ and $UL26_{61-69}$). SFC, spot forming cells.

3.2.3 Evaluation of functionality and HLA specificity of HCMV-specific memory T cells

Functional activity of memory T cells after 12-day stimulation with HCMV peptides was tested by ICS *via* detection of IFNγ and TNF. ICS was performed with all dominant epitopes and some arbitrarily selected epitopes that were close to the threshold of dominant epitopes. The TNF^+, $IFN\gamma^+$ and double-positive populations of cells stimulated with the test peptide had to be at least twice as large as those of the negative control to be considered positive.

All dominant epitopes except YLVRRPMTI ($UL13_{465-473}$) caused $CD8^+$ memory T cell-mediated responses. This is probably due to the fact that all available PBMC samples tested for YLVRRPMTI showed relatively low spot counts and therefore low numbers of specific T cells in the ELISpot. The lower sensitivity of flow cytometric assays compared to ELISpot might be responsible for the failure to detect these cells by ICS. The subdominant epitope SLDRFIVQY elicited a $CD4^+$ T cell-mediated immune response. Exemplary results of the ICS with the immunodominant B*08 epitope LPHERHREL are depicted in Figure 21B.

Tetramer staining was then performed with all dominant and two subdominant epitopes in order to validate the HLA-A*01:01 restriction of the peptide-specific T cells. Tetramer stainings were performed after prior 12-day stimulation with the peptide of interest and negative control peptide. This negative control peptide was also refolded with the respective HLA and served as the negative control in the tetramer staining. For some donors and epitopes, freshly thawed cells of the same donor served as additional negative control for the staining. The $CD8^+tetramer^+$ population of cells stained with the tetramer of interest had to be twice the size of the negative control to be determined as positive. All dominant epitopes had specific $tetramer^+$ populations in at least two PBMC samples. Even small YLVRRPMTI-specific, $tetramer^+$ populations were observed in two PBMC cultures although the peptide was not able to elicit detectable IFNγ and TNF production in ICS with the same two PBMC samples. The possibility that not all peptide-specific cells are also functional might explain this discrepancy. In total, the size of $tetramer^+$ T cell populations was highly donor and peptide dependent, which is in accordance with observations in ELISpot assays. Specific T cell populations ranged from 0.06% to up to 53.56% of $CD8^+$ cells after 12-day amplification. The highest percentage of $tetramer^+$ cells reached a PBMC culture stimulated with the B*51-restricted epitope LPLKMLNI (Figure 20). Figure

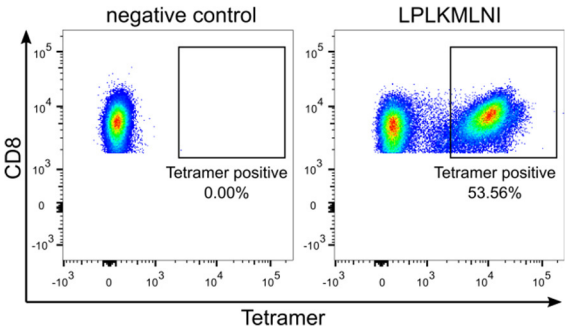

Figure 20: Tetramer staining of HLA-B*51-restricted epitopes LPLKMLNI. Prior to the staining, PBMCs were stimulated for 12 days with LPLKMLNI and negative control (DPYKATSAV, human). As negative control for the staining served a B*51-DPYKATSAV tetramer.

21 shows a representative characterization of the epitope LPHERHREL (B*08) with the ELISpot, ICS, and tetramer staining results of one PBMC sample.

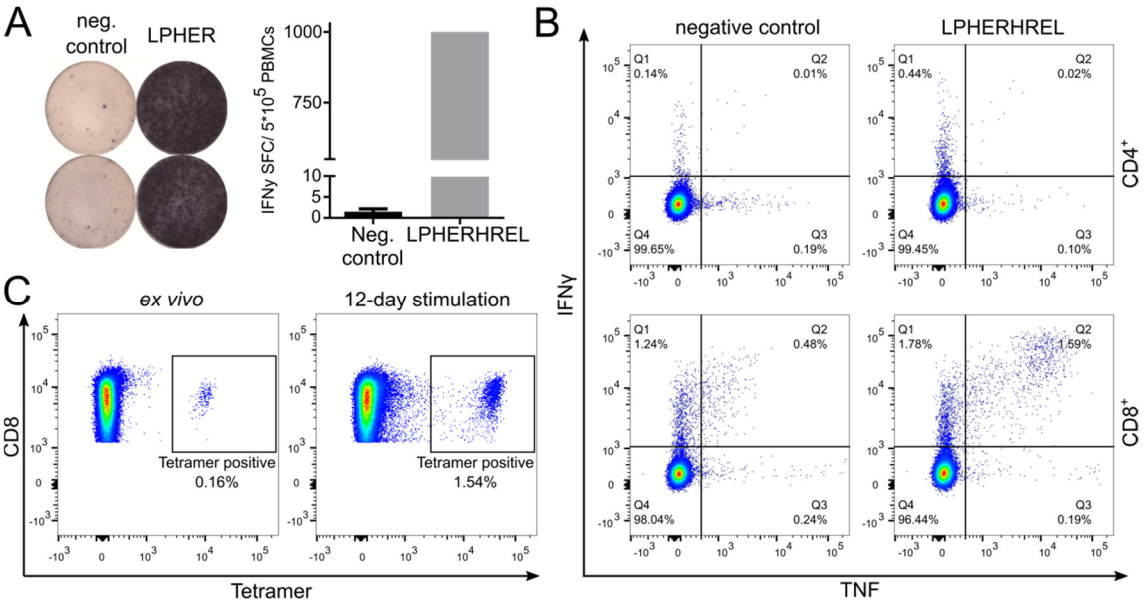

Figure 21: Characterization of LPHERHREL and its specific memory T cells. Shown are exemplary results of an ELISpot assay (A), an ICS (B), and a tetramer staining (C) with PBMCs of donor 2917 pulsed with LPHERHREL (B*08) or negative control peptide. A) The spot count of the test peptide was 'too numerous to count' and was therefore set to 1,000. The cells were stimulated for 12-days prior to each assay. The HIV-derived peptide GGKKKYKL (B*08) served as negative control for the ELISpot and the ICS. The negative control of the tetramer staining was a HLA-B*08-tetramer with GGKKKYKL.

Table 13: Summary of ELISpot, ICS and tetramer staining results for the best HCMV-derived epitopes. Nt, not tested.

ID	Sequence	Tested HLA	ELISpot RR (12-d stim.)	ELISpot RR (*ex vivo*)	ICS	Tetramer staining
UL105$_{715-723}$	YADPFFLKY	A*01:01	100.0%	90.9%	CD8$^+$, IFNγ$^+$, TNF$^+$	positive
UL44$_{245-253}$	VTEHDTLLY	A*01:01	92.9%	100.0%	CD8$^+$, IFNγ$^+$, TNF$^+$	positive
UL69$_{569-578}$	RTDPATLTAY	A*01:01	82.6%	66.7%	CD8$^+$, IFNγ$^+$, TNF$^+$	positive
US28$_{122-130}$	ITEIALDRY	A*01:01	58.3%	14.3%	CD8$^+$, IFNγ$^+$, TNF$^+$	positive
UL55$_{657-665}$	NTDFRVLELY	A*01:01	56.3%	0.0%	CD8$^+$, IFNγ$^+$, TNF$^+$	positive
UL148$_{282-290}$	SLDRFIVQY	A*01:01	35.7%	nt	CD4$^+$, IFNγ$^+$, TNF$^+$	nt
UL77$_{228-236}$	GLYTQPRWK	A*03:01	76.2%	50.0%	CD8$^+$, IFNγ$^+$, TNF$^+$	positive
UL57$_{790-798}$	RVKNRPIYR	A*03:01	60.9%	33.3%	CD8$^+$, IFNγ$^+$, TNF$^+$	positive
UL36$_{51-60}$	RSALGPFVGK	A*03:01	40.0%	nt	CD8$^+$, IFNγ$^+$, TNF$^+$	positive
US33A$_{13-21}$	KLGYRPHAK	A*03:01	37.9%	nt	CD8$^+$, IFNγ$^+$, TNF$^+$	positive
UL34$_{180-188}$	LPHERHREL	B*08:01	90.9%	85.7%	CD8$^+$, IFNγ$^+$, TNF$^+$	positive
UL26$_{61-69}$	LPYPRGYTL	B*08:01	68.8%	16.7%	CD8$^+$, IFNγ$^+$, TNF$^+$	positive
UL13$_{465-473}$	YLVRRPMTI	B*08:01	50.0%	33.3%	negative	positive
UL83$_{116-123}$	LPLKMLNI	B*51:01	80.0%	87.5%	CD8$^+$, IFNγ$^+$, TNF$^+$	positive
UL38$_{156-164}$	FPVEVRSHV	B*51:01	65.2%	0.0%	CD8$^+$, IFNγ$^+$, TNF$^+$	positive
UL26$_{61-69}$	LPYPRGYTL	B*51:01	62.5%	33.3%	CD8$^+$, IFNγ$^+$, TNF$^+$	positive
UL56$_{503-511}$	DARSRIHNV	B*51:01	53.3%	nt	CD8$^+$, IFNγ$^+$, TNF$^+$	positive

3.2.4 Promiscuous presentation of epitopes

HLA-specific binding motives usually result in the fact that a peptide can bind well to only one HLA allotype. This is supported by the predominantly negative mismatch ELISpot assays. Moreover, ligands that were ambiguously predicted such as DARSRIHNV (B*08/B*51) mostly elicited memory responses in association with only one of the two predicted HLA allotypes. Nevertheless, as mentioned above, there are epitopes that can be recognized in conjunction with multiple HLA allotypes - within HLA supertypes and in between. The ligand LPYPRGYTL ($UL26_{61-69}$) identified in this work was predicted to bind B*08 and B*51 and was able to stimulate T cells of different PBMC donors harboring either of both HLA types. Interestingly, the ELISpot response rates with B*08- and B*51-positive donors were relatively similar with 68.8% and 62.5%, respectively. Due to the unusual anchor residue at position five (Figure 22A), HLA-B*08 is prone to bind peptides that can also be bound by other HLAs although it is not part of any HLA supertype. The HLA restriction of this peptide was verified by tetramer staining for both HLA types (Figure 22B). However, in a following mismatch ELISpot with HLA-B*08$^-$/B*51$^-$ donors, two HLA-B*14$^+$ donors showed strong IFNγ responses.

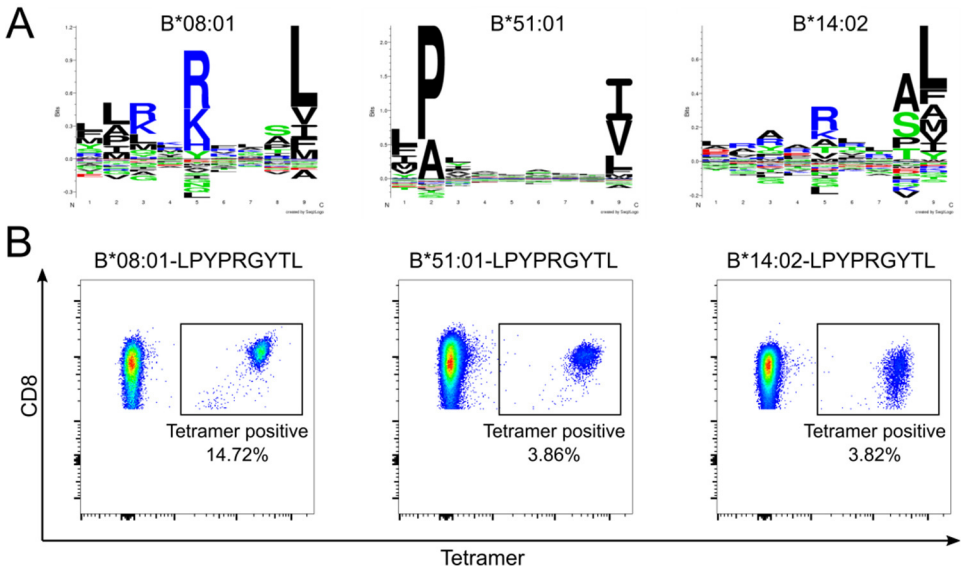

Figure 22: A) Binding motives of HLA-B*08:01, -B*51:01 and -B*14:02 obtained from NetMHC [25, 397]. B) Tetramer staining of HLA-B*08-, -B*51-, and -B*14-positive PBMC cultures with LPYPRGYTL-tetramers of the respective HLA type. Prior to the staining, PBMCs were stimulated for 12 days with LPYPRGYTL and the respective negative control peptide (B*08: GGKKKYKL (HIV), B*51: DPYKATSAV (human), B*14: DRLQTALLV (human)). HLA-matched tetramers with the respective negative control peptide served as negative controls in the staining.

Subsequent ICS with those reactive, HLA-B*14$^+$ PBMCs demonstrated a CD8$^+$ T cell-mediated response. The peptide matched the binding motif of HLA-B*14:02 quite well (Figure 22A) and was

therefore refolded with HLA-B*14:02. The following tetramer staining with PBMCs of the two PBMC donors positively tested in ELISpot validated the restriction to HLA-B*14:02. Both B*14:02$^+$ PBMC samples were also stained with B*08:01-LPYPRGYTL and B*51:01-LPYPRGYTL tetramers as controls. Surprisingly, B*08:01-LPYPRGYTL and B*51:01-LPYPRGYTL tetramers stained specific T cells in both HLA-B*08$^-$/B*51$^-$/B*14$^+$ PBMC cultures (Figure 23). This binding seemed to be specific since B*08:01-LPYPRGYTL and B*51:01-LPYPRGYTL tetramers did not stain specific population in unstimulated samples. Stimulated HLA-B*08$^+$/B*14$^-$ PBMCs that showed B*08:01-LPYPRGYTL tetramer-positive populations displayed no staining by B*51:01-LPYPRGYTL and HLA-B*51$^+$/B*14$^-$ and B*51:01-LPYPRGYTL tetramer-positive PBMCs showed no staining with the B*08:01-LPYPRGYTL tetramer. Moreover, staining of both B*14:02$^+$ PBMC samples with irrelevant viral HLA-B*08 and -B*51 tetramers was also negative which excludes unspecific binding of the HLA complex to the TCR. This observation is remarkable since T cells are usually restricted by one HLA allotype. The fact that PBMCs of one donor recognize one peptide with three different HLA allotypes, two of which he does not express, indicates that the peptide-HLA complexes must be very similar in their spatial structure. Subsequent ELISpot assays with HLA-B*14$^+$ donors revealed a recognition rate of 40.0%. Epitope LPYPRGYTL is therefore presented and recognized on three different HLA allotypes, which are all assigned to different supertypes.

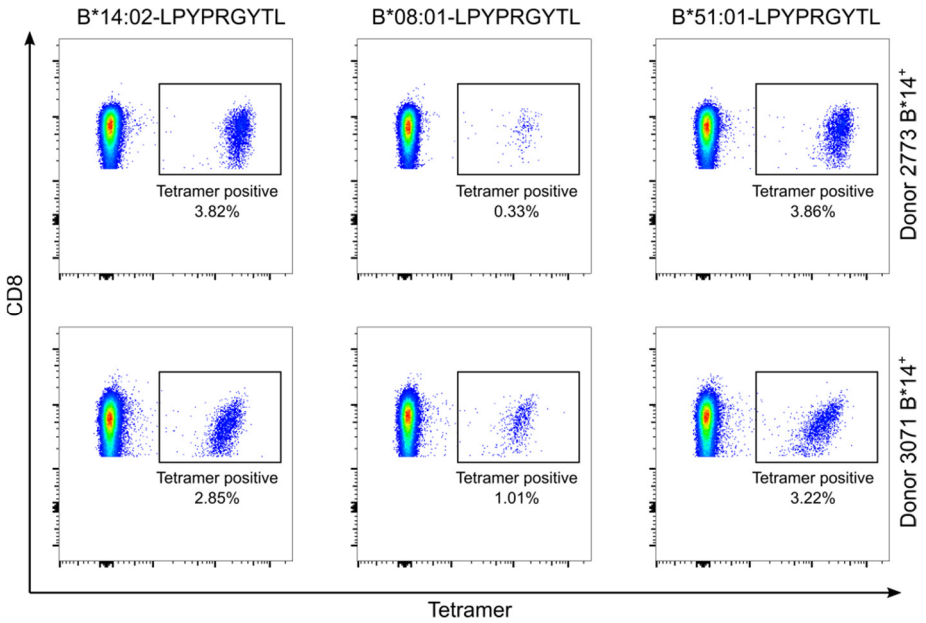

Figure 23: Tetramer staining of two B*14$^+$ PBMC cultures with LPYPRGYTL tetramers. PBMCs of donors 2773 and 3071 were stimulated for 12 days with LPYPRGYTL and negative control peptides (B*08: GGKKKYKL (HIV), B*51: DPYKATSAV (human), B*14: DRLQTALLV (human)). Tetramers with the negative control peptide and the respective HLA allotype served as negative controls for the staining. All negative controls had 0.00% or 0.01% tetramer$^+$ populations and are not shown in this figure.

3.2.5 Comparison of mass spectrometry-based identification of ligands and the *in silico* prediction of candidate epitopes

To compare the mass spectrometry-based approach of identifying naturally presented epitopes with an established *in silico* prediction method, Leon Bichmann applied the prediction tools SYFPEITHI and NetMHCpan3.0 to the proteome of HCMV. All HCMV-derived peptides were ranked according to their prediction score and the position of the dominant epitopes within this dataset was determined (Table 14). For both algorithms, SYFPEITHI and NetMHC, 25 of the 26 identified dominant epitopes are among the top-scoring 2% of all predicted peptides. This is in line with previous experience that the top 2% of predicted peptides with SYFPEITHI usually contain the natural T-cell epitopes [24]. NetMHC categorizes its predicted peptides into weak (affinity < 500 nM, %rank < 2) and strong binders (affinity < 50 nM, %rank < 0.5). Thus, it would be necessary to test approximately 1,300 (SYFPEITHI) or 2,000 (NetMHC) peptides for each HLA-I allotype and length variant in order to screen epitopes from the entire HCMV proteome within these thresholds. Therefore, evidence of presentation on HLA molecules considerably reduced the number of possible candidates to be tested, as opposed to HLA binding prediction alone.

Table 14: Position of dominant epitopes within whole proteome prediction.

			NetMHCpan3.0			SYFPEITHI		
HLA Restric-tion	**Sequence**	**Total number of peptides***	**NetMHC percentile rank [%]**	**Position within ranked peptides**	**Epitope within % top predicted peptides**	**Norma-lized score [%]**	**Position within ranked peptides**	**Epitope within % top predicted peptides**
A*01	YADPFFLKY	67116	0.01	8	0.012	82.5	3	0.004
	VTEHDTLLY	67116	0.01	7	0.010	85.0	2	0.003
	RTDPATLTAY	66919	0.01	8	0.012	87.2	2	0.003
	ITEIALDRY	67116	0.02	16	0.024	75.0	14	0.021
	NTDFRVLELY	66919	0.01	7	0.010	87.2	1	0.001
A*03	GLYTQPRWK	67116	0.15	84	0.125	59.1	269	0.401
	RVKNRPIYR	67116	0.50	305	0.454	52.3	1099	1.637
B*08	LPHERHREL	67116	0.08	176	0.262	62.8	104	0.155
	LPYPRGYTL	67116	0.06	133	0.198	55.8	361	0.538
	YLVRRPMTI	67116	0.04	105	0.156	46.5	1339	1.995
B*51	LPLKMLNI	67296	0.25	32	0.040	68.4	53	0.079
	LPYPRGYTL	67116	0.01	13	0.019	63.2	219	0.326
	FPVEVRSHV	67116	0.03	40	0.060	63.2	180	0.268
	DARSRIHNV	67116	3.50	3430	5.111	60.5	306	0.456

* numbers of 9mer and 10mer peptides spanning the whole proteome

3.2.6 Infection of further cell lines allows the expansion of HLA types and epitopes

The HLA restriction of the identified T cell epitopes is limited to the HLA types of the infected cell line HF-99/7. In order to expand the set of HLA types and T cell epitopes, fibroblast cell lines HF-99/5 and HF-γ were also infected with ΔUS2-11. Apart from the differences in the HLA type, the new infection scheme with an MOI of only 1 and the harvest after 4 days should allow the isolation of a different set of ligands. Not all fibroblasts would be infected at the beginning due to the low MOI, and the long incubation period together with the HCMV life cycle of 2-3 days should result in cells in different infection stages. The infection and cell culture of cell lines was performed by Liane Bauersfeld from the working group of Dr. Anne Halenius in Freiburg. The isolation of HLA ligands was carried out by Ana Marcu.

Table 15: Summary of mass spectrometry analyses of HF-99/5 and HF-γ cells either infected with ΔUS2-11.

Sample	Peptides	Binders	Purity	HCMV-derived binders	HCMV source proteins
HF-99/5 ΔUS2-11	7448	6768	93%	348	99
HF-γ ΔUS2-11	10555	9703	92%	538	122

The peptide sequences were identified *via* LC-MS/MS in three technical replicates. MS analyses identified 7448 peptides in the HF-99/5 sample and 10555 in the HF-γ sample. SYFPEITHI and NetMHCpan 4.0 [398] predicted 6768 (HF-99/5) and 9703 (HF-γ) to be binders, which represents a purity of 93% and 92%, respectively. From the HF-99/5 sample and the HF-γ sample, 348 and 538 unique HCMV-derived ligands, respectively, could be identified. There was an overlap of 115 ligands, which were identified in both cell lines. Although the cell lines do not share any HLA types, they harbor the supertypes HLA-A*03/A*11 and HLA-A*23/A*24, which explains this considerable overlap. The 348 HF-99/5 ligands originate from 99 different source proteins while the 538 HF-γ ligands represent 121 different proteins. In total, the infection of HF-99/5 and HF-γ cells enabled the identification of 696 novel HLA ligands; 75 ligands were already identified on HF-99/7 cells.

The distribution of the HLA restrictions among the identified ligands is shown in Figure 24. While the proportions of HLA-A and -B ligands were almost equally distributed in HF-99/7 (Figure 12), they are distributed very differently in the two newly analyzed cell lines. HF-99/5 cells presented a significantly higher proportion of HA-A ligands than of HLA-B ligands (Figure 24A). In contrast, more than half of the HF-γ ligands were predicted to be HLA-B ligands with HLA-B*15:01 owing by far the greatest share (Figure 24B). With proportions of 12% each, the HLA-C ligands of HF-99/5 and HF-γ take up a similar proportion as in the HF-99/7 cell line (11%). The in general smaller proportion of

HLA-C ligands is in line with the fact that HLA-C molecules are less abundant than HLA-A and -B molecules on the cell surface [399, 400].

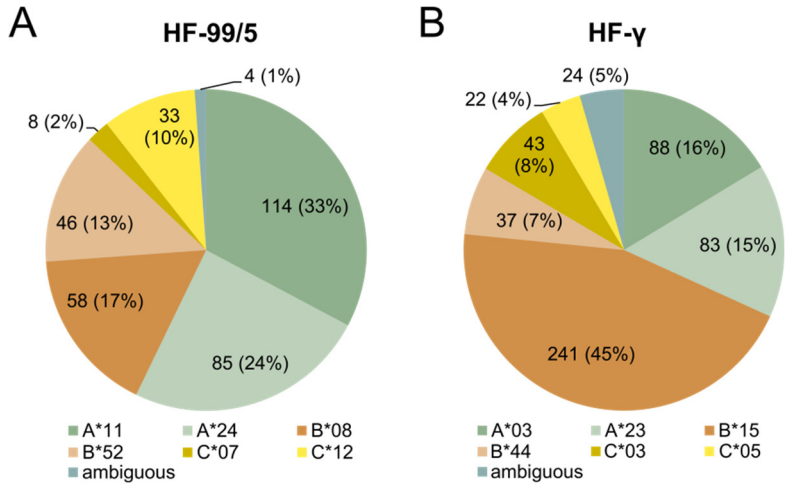

Figure 24: Distribution of HLA restrictions among the HF-99/5 (A) and HF-γ ligands (B). HLA ligands were assigned with SYFPEITHI and NetMHCpan 4.0. Ligands are designated ambiguous when the prediction tools were inconsistent in their restriction assignment.

The new infection scheme considerably changed the composition of the temporal expression profiles reflected by the HLA ligands in comparison to the HF-99/7 infection scheme (Figure 25). The proportion of Tp5 peptides increased significantly, while the proportion of all other profiles decreased, with Tp3 shrinking the most.

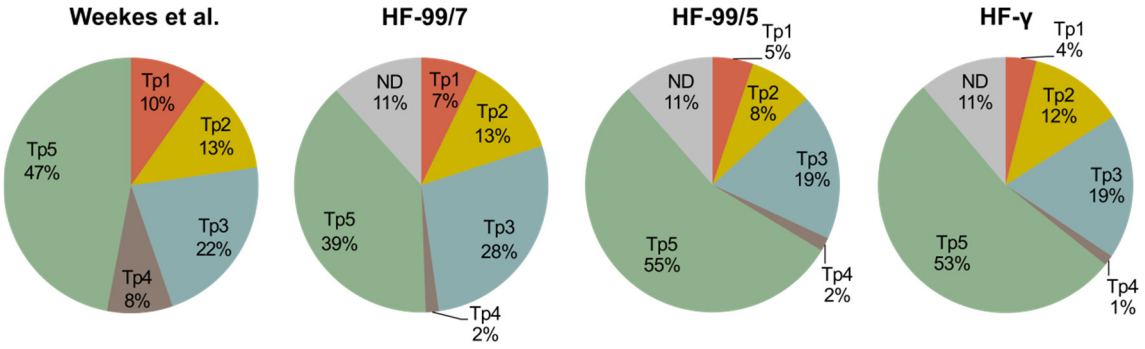

Figure 25: Distribution of temporal profiles defined by Weekes *et al.* (left) among identified ligands of the HF-99/7, HF-99/5 and HF-γ cell line. ND, not determined; Tp, temporal profile.

In total, the infection of two other cell lines enabled the identification of 696 novel ligands, which can be subjected to immunogenicity testing in the future.

4 Discussion

4.1 EBV-derived, HLA-A*01 restricted T cell epitopes

T cell responses against EBV play a crucial role in fighting the virus. In order to optimally employ this part of the immune defense for therapeutic approaches, a detailed knowledge of the T cell epitopes is indispensable. A positive example is the successful use of an EBV peptide pool in adoptive T-cell transfer. The PepTivator® EBV Select (Miltenyi Biotec) containing 43 different HLA-I and-II-restricted peptides efficiently stimulates EBV-specific T cells in almost all donors *in vitro* (personal communication with Dr. Britta Eiz-Vesper and [401]).

In principle, the T cell epitope landscape of EBV is well studied. TheIEDB [26], which catalogs experimental data on T cell epitopes, currently lists 652 EBV-derived epitopes (accessed 27.04.2020). There are well characterized, dominant epitopes for all common HLA types: GLCTLVAML (ICP27, A*02) [402], RLRAEAQVK (EBNA3, A*03) [403], AVFDRKSDAK (EBNA4, A*11) [404], RPPIFIRRL (EBNA3, B*07) [405], RAKFKQLL (BZLF1, B*08) [406], VEITPYKPTW (EBNA4, B*44) [407], and many more. However, there is a blatant gap concerning HLA-A*01-restricted epitopes. Not a single HLA-A*01 restricted epitope is mentioned in an epitope list from 2015 by Taylor *et al.* [160] who claims to list all EBV-derived, $CD8^+$ T cell epitopes identified to this date. Even the IEDB lists merely seven peptides that have only been tested for their binding properties to HLA-A*01 but not been proven as T cell epitopes. This work therefore intended to fill this gap by revealing novel HLA-A*01-restricted EBV epitopes.

Different approaches can be employed to identify epitope candidates. In this part of the work, candidate epitopes were identified by *in silico* prediction with SYFPEITHI and NetMHC. The size of the viral proteome allowed a prediction with the complete proteome without focusing on specific antigens. This unbiased approach resulted in hundreds of potentially HLA-A*01-binding peptides. Of these, 171 top scoring peptides were selected to be tested for their immunogenicity in PBMCs of healthy donors *via* IFNγ ELISpot assay. The first assays were performed with peptide pools containing nine peptides each in order to reduce the amount of necessary ELISpot assays. This allowed the swift elimination of 62 weakly or non-immunogenic peptides. The rest of the predicted peptides were tested individually. Of these, 29 (26.6%) stimulated specific memory T cells in at least one PBMC sample. All length variants that were predicted (9mers, 10mers, 11mers, 12mers, and 13mers) were represented in the set of epitopes. HLA-I molecules generally prefer 9mer peptides for binding. Therefore, it is not surprising that most of the identified epitopes had a length of nine amino acids. However, many longer peptides were observed and the length distribution was less

focused on 9mers than usual for HLA-I molecules [408]. This is in line with previous observations that HLA-A*01 presents longer ligands more frequently than most other HLA allotypes [408, 409].

The response rate of the 29 epitopes is loosely correlated with the mean response intensity in individual donor samples meaning that frequently recognized epitopes often elicited higher spot counts in ELISpot assays after stimulation compared to weakly immunogenic epitopes. This is apparently reflected by the size of the original peptide-specific memory T cell population in the blood since only the two most frequently recognized epitopes stimulated detectable numbers of memory T cells in *ex vivo* ELISpots.

Seven of the 29 epitopes were defined as dominant epitopes with an ELISpot response rate of > 50% of healthy, HLA-matched donor PBMCs. However, one of the dominant epitopes (CTESLVARYY) was a length variant of the top epitope CTESLVARY. The restriction by HLA-A*01 and the presence of reactive, multifunctional memory T cells was confirmed for all dominant epitopes *via* HLA-A*01:01 tetramer staining and ICS. The only exception is the peptide LTDRSFPAY, which could not trigger TNF production in ICS.

ELISpots with HLA-mismatched donors indicate that most of the dominant epitopes are exclusively recognized in the context of HLA-A*01. Only MSDWTGGALLVLY elicited responses in HLA-A*01-negative donor samples. Especially long peptides can harbor several epitopes that bind to different HLA-I types or even to class I and class II types. ICS with other epitopes occasionally shows activated $CD8^+$ T cells in one donor and $CD4^+$ T cells in another. Since the 'mismatch' ELISpot was performed with only 16 donor samples, it cannot be ruled out that rare HLA types may bind those epitopes. Furthermore, it cannot be excluded that the epitopes can also be presented by other members of the HLA-A*01 supertype, since both 'matched' and 'mismatched' ELISpots were performed with donor samples that do not exhibit supertype members such as HLA-A*26, -A*30, -A*32.

Interestingly, the 29 epitopes originate from 20 different proteins, and no focus on a particular antigen could be observed. However, there was a clear dominance of lytic proteins over latent proteins. The focus of $CD8^+$ T cell-mediated responses on lytic antigens was already demonstrated before [410, 411]. However, the usual hierarchy of immunodominance is described as IE > E > L with IE antigens being predominantly targeted by the T cell response and with rare responses to L antigens [402, 412]. Pudney *et al.* claimed that this hierarchy would directly reflect the immune evasion and the efficiency of antigen presentation in lytically infected cells [412]. This cannot be confirmed by this work since late proteins are by far the most frequent source of identified epitopes; also the most frequently recognized epitope CTESLVARY stems from the late antigen BILF1. Moreover, not a single epitope from the IE proteins BZLF1 (Zta) and BRLF1 (Rta) were identified although several peptides from those proteins were predicted binders and were tested

for their immunogenicity. Even when considering the seven dominant epitopes alone, the mentioned hierarchy cannot be confirmed. Four epitopes originated from late lytic proteins, two from latent proteins, and only one from early lytic proteins.

The $CD8^+$ T cell responses to latent EBV antigens were reported to be mainly focused on the EBNA3A, -3B, and 3C proteins followed by responses to LMP2, EBNA2. Responses against EBNA-LP, LMP1 were rarely detected and memory T cells against EBNA1 were not detected at all in early studies [183, 184]. Later studies, however, revealed $CD8^+$ memory responses against EBNA1 in individuals with particular HLA types such as HLA-B*35:01, -B*07, and -B*53 [413]. Moreover, strong, dominant responses to EBNA2, EBNA-LP, and LMP2 epitopes restricted to particular HLA types were then detected questioning the original hierarchy. In contrast, LMP1 still remained an outlier with occasional and weak responses (reviewed by [414]). Interestingly, the highly immunogenic epitopes MSDWTGGALLVLY and ESEERPPTPY originate from LMP1 and LMP2, respectively. Epitopes from LMP1 could be of special interest since LMP1 is the key oncoprotein of EBV-mediated tumorigenesis [415], and such epitopes could be targets for anti-cancer therapies.

Apart from that, it is noteworthy that no epitope was identified from the highly immunogenic antigen BZLF1 [416]. In total, it seems that there are no generally applicable rules concerning the immunodominance of particular antigens across different HLA allotypes. Rather, the respective HLA allotype seems to select its antigens and therefore determines the hierarchy of antigens as T cell targets.

This work presents an unbiased analysis of the complete HLA-A*01-restricted T cell response to EBV. All EBV B95-8 proteins contained in the Swiss-Prot database were included in this analysis, and all peptides exceeding a threshold prediction score were tested for immunogenicity. Nevertheless, it can never be excluded that epitopes have lower prediction scores and were thus not characterized in this work. Three (YLEKESIYY, respiratory syncytial virus; LFETDPVTFLY, YMESVFQMY, both herpes simplex virus 1) of twelve dominant, HLA-A*01-restricted viral epitopes analyzed in our working group for other studies exhibited prediction scores slightly below the cut-off threshold for immunogenicity testing and had response rates of 50%-75%. However, well characterized, dominant epitopes with response rates of > 75% had predictions scores well above the thresholds set here. Therefore, we are confident not to have missed any strong HLA-A*01-restricted epitope.

All epitopes except one are novel epitopes that have never before been described as T cell epitopes. ESEERPPTPY was previously discovered and characterized as a T cell epitope by Huisman *et al.* [417] and was also validated in a MD project of our working group [418].

Parallel testing of highly immunogenic epitopes demonstrated that up to seven epitopes restricted by the same HLA type can be recognized by one donor. Nevertheless, the most immunogenic epitope CTESLVARY was clearly the immunodominant epitope with the strongest responses of all epitopes in all tested donors. Curiously, the peptide pool containing CTESVARY could not stimulate memory T cells in all PBMC cultures, although the epitope had a 100% recognition rate in individual tests. However, the PBMC culture that was evaluated as negative showed a slight unspecific activation and the spot count was just below three times the negative control.

In summary, this part of the work provides an unbiased, comprehensive analysis of the HLA-A*01-restricted T cell response to EBV and revealed 28 novel EBV-derived epitopes, among them CTESVARY with an overwhelming recognition frequency.

4.2 Naturally presented HCMV-derived T cell epitopes

Various immune evasion strategies employed by HCMV strongly interfere with HLA-I presentation of viral peptides on the host cell surface. However, ~10% of the memory T cell compartment of seropositive individuals consists of HCMV-specific T cells [299], and this number can dramatically rise in the elderly [419].

With the approach described here, it was possible to bypass immune evasion by the US6 family genes and perform the direct isolation and identification of physiologically relevant HCMV-specific HLA ligands by MS. These data clearly confirm that memory T cell responses toward peptides derived from viral proteins of all expression stages and functional areas can be detected in immunocompetent HCMV carriers. The fact that memory T cells specific for a significant proportion of these ligands are present in HCMV-seropositive individuals clearly indicates priming of naive T cells against these antigens at any time during infection.

HLA-I ligands can either originate from mature proteins that are degraded at the end of their functional lifetime, also termed ‘retirees’, or from defective ribosomal products (DRiPs), which are rapidly degraded after their synthesis [420]. To which extent those sources contribute to the HLA-I ligandome is still debated [421]. Although late proteins (Tp5) should not be produced for the first time until about 48 h.p.i., peptides could be isolated from these proteins at this time point. This suggests that at least the majority of these peptides originated from DRiPs and not from proteins that were degraded after their normal lifetime.

By now, the initial perception that HCMV-specific T cell responses are directed only against a few immunodominant antigens has been challenged by several groups. Using predictive bioinformatics and functional T cell assays, Elkington *et al.* [296] identified numerous novel HCMV epitopes from a heterogeneous group of 14 preselected proteins (pp28 [UL99], pp50 [UL112-UL113], pp65 [UL83], pp150 [UL32], pp71 [UL82], gH [UL75], gB [UL55], IE1 [UL123], US2, US3, US6, US11, UL16, and UL18) as T cell targets. Sylwester *et al.* [299] analyzed overlapping 15mer peptides from 213 HCMV ORFs by cytokine flow cytometry. Of the tested ORFs, 70% were shown to be immunogenic for $CD4^+$ and/or $CD8^+$ T cells. Immunogenicity was influenced only modestly by ORF expression kinetics and function. Interestingly, besides pp65 and IE1, UL48 was the only tested ORF recognized by CD8+ T cells of >50% of tested donors. In contrast to that particular finding, from a total of 50 identified immunogenic HCMV-derived peptides, 13 epitopes, representing 13 different proteins, were classified as dominant in our study. However, Sylwester *et al.* only stimulated the cells for 6 h before staining and flow cytometry analysis. Considering our *ex vivo* ELISpot results, their approach certainly underestimates the presence of HCMV-specific T cells. We found immunogenic peptides from 36 HCMV proteins, confirming previous findings that HCMV-specific $CD8^+$ T cell immunity in healthy virus carriers is based on a broad repertoire of HCMV antigens. We were able to validate four previously known epitopes, but some well-established epitopes such as $YSEHPTFTSQY_{pp65/UL83}$ (A*01) [422], $RIKEHMLKK_{IE1/UL123}$ (A*03) [423], $QIKVRVDMV_{IE1/UL123}$ (B*08), and $ELRRKMMYM_{IE1/UL123}$ (B*08) [296] were not detected in our assays. While our approach has technical limitations, other reasons for the lack of detection of some dominant epitopes are imaginable. The HLA-I antigen presentation pathway could be insufficient for processing of specific peptides in the infected fibroblasts. To assess this, in future studies we will apply IFNγ to induce the HLA-I antigen presentation machinery before infection, as IFNγ induction strongly improves antigen presentation to $CD8^+$ T cells [424] and may as well induce HLA-II expression for elution and characterization of class II ligands [4]. In addition, ligandome analysis at different time points during infection could yield peptides of different quality. The lack of three established IE1 epitopes indicates that the 48 h.p.i. time point might be too late to efficiently obtain epitopes of the IE expression stage. Moreover, it should be taken into account that expression of one or combinations of several immunoevasins could result in different HLA-I ligandome qualities. In experiments carried out by Stefanie Spalt, who established this approach with another cell line and different HCMV mutants, it could be observed that HLA-B*44:02 ligand numbers were strongly induced in ΔUS2-6-infected cells compared to ΔUS2-6/ΔUS11-infected cells, i.e., in the presence of US11 expression [394]. The group of Anne Halenius has begun to address the molecular mechanism behind this phenomenon and it seems that immunoevasins target different HLA gene products in distinct manners [425]. Thus,

immunoevasins affect not only the efficiency, but also the quality of antigen presentation. Finally, it cannot be excluded that the ΔUS2-11 deletion mutant virus still expresses factors, such as pp71, that interfere with HLA-I peptide loading and presentation.

The broad $CD8^+$ T cell response against HCMV detected in healthy donors clearly shows that inhibition of HLA-I antigen presentation by immunoevasins is not sufficient to prevent the induction of $CD8^+$ T cells [298], emphasizing the role of priming of $CD8^+$ T cells through cross-presentation [312]. However, HCMV will have a major impact, not only quantitatively, but also qualitatively, on antigen processing and presentation in the infected cells. This could partly explain why a large portion of HCMV-derived HLA ligands failed to elicit a memory response in seropositive donors. Also, different expression/presentation patterns in different cell types could have an effect on memory responses [426, 427]. Such non-immunogenic ligands might not be processed and presented during an infection *in vivo* or are not recognized by naive T cells. Furthermore, donors might lack specific naive T cells, leaving a hole in the T cell repertoire [428-430]. Despite the large number of non-immunogenic HLA ligands identified, all these peptides are naturally presented on HLA molecules, providing a solid foundation for epitope screening. By using *in silico* analyses only, it would have been necessary to screen several thousands of peptides to identify our set of epitopes, as opposed to 181 in our approach.

The infection of another two cell lines with a different infection scheme allowed the identification of 696 novel peptides, most of which originate from late (Tp5) proteins. Infection of various cell cultures expressing distinct HLA allotypes with different HCMV deletion mutants will allow for deeper and broader insights into the quality of viral $CD8^+$ T cell targets. Moreover, methods such as ribosome profiling will enable the identification of novel ORFs that might be a source of additional viral T cell epitopes [231, 233]. The presence of a broad range of specific memory T cells in healthy seropositive individuals suggests that strategies using subdominant epitopes and targeting multiple antigens in vaccination and cellular therapies may be beneficial for sustainable virus control [431-433]. Therefore, the identification of a large number of immunogenic HCMV-derived cytotoxic T cell targets for the most frequent HLA restrictions is, in our opinion, indispensable for the development and improvement of such therapies.

5 Summary

Both human cytomegalovirus (HCMV) and Epstein-Barr virus (EBV) are widespread in the population. They can cause severe morbidity and mortality, especially in immunocompromised hosts. Apart from the standard treatment with antiviral drugs, T cell-based immune therapies such as adoptive T cell transfer have been successfully used in recent years. A prerequisite for this treatment is the comprehensive knowledge about virus-specific T cell epitopes.

The T cell epitopes of both viruses have already been the subject of numerous studies. Nevertheless, the epitope mapping in both cases shows certain gaps. In EBV there is a striking gap in HLA-A*01-restricted epitopes. While dominant epitopes are known and characterized for all other common HLAs, not a single useful HLA-A*01-restricted epitope has been described. In contrast, due to the size of HCMV, studies on its epitopes have mostly focused on specific antigens, which also prevented comprehensive mapping. The aim of this work was therefore the identification and characterization of novel HCMV-specific and HLA-A*01-restricted, EBV-specific T cell epitopes.

To this end, epitope prediction was performed to identify HLA-A*01-binding peptides throughout the entire EBV proteome. From this list of peptides, 171 peptides were evaluated for immunogenicity using IFNγ ELISpot assays. Subsequently, the HLA restriction of strongly immunogenic peptides was verified *via* flow cytometry. Of the tested peptides, 29 were immunogenic; seven of them were dominant epitopes. For all dominant epitopes the HLA-A*01 restriction was confirmed and reactive $CD8^+$ T cells in healthy donors were identified.

In the second project, candidate HCMV epitopes were isolated as HLA ligands from cell lines infected with HCMV mutants and then sequenced by mass spectrometry. Of the 181 ligands, 50 (30%) could be characterized as epitopes. For all 13 dominant epitopes the predicted HLA restriction could be confirmed. The infection of two further cell lines allowed the isolation of hundreds of new peptides, which can be subjected to immunogenicity testing. Since the HLA ligands originate from more than 100 different proteins, this method is ideally suited for an unbiased, comprehensive analysis of the epitopes throughout the entire proteome.

In summary, novel, strongly immunogenic epitopes were identified for both viruses, which could be employed for vaccination and antigen-specific immunotherapy in the future.

6 Zusammenfassung

Das Humane Cytomegalievirus (HCMV) und das Epstein-Barr-Virus sind weitverbreitet in der Bevölkerung. Beide können schwere Erkrankungen auslösen, die vor allem in immunsupprimierten Infizierten lebensgefährlich werden können. Neben Standardtherapien werden seit geraumer Zeit T-Zell-basierte Immuntherapien wie der adoptive T-Zell-Transfer erfolgreich zur Behandlung eingesetzt. Voraussetzung dafür ist die möglichst umfangreiche Kenntnis der Virus-spezifischen T-Zell-Epitope.

Die T-Zell-Epitope beider Viren waren bereits Gegenstand zahlreicher Studien. Dennoch weist die Epitopkartierung in beiden Fällen gewisse Lücken auf. Bei EBV gibt es eine eklatante Lücke bei HLA-A*01-restringierten Epitopen. Während für alle anderen häufigen HLA-Allotypen dominante Epitope bekannt und charakterisiert sind, ist kein einziges HLA-A*01-restringiertes Epitop beschrieben. Aufgrund der Größe von HCMV haben sich Studien bezüglich seiner Epitope dagegen meist auf bestimmte Antigene konzentriert, was ebenfalls eine umfassende Kartierung verhinderte. Ziel dieser Arbeit war es deshalb, neue HCMV-spezifische und HLA-A*01-restringierte, EBV-spezifische T-Zell-Epitope zu identifizieren und zu charakterisieren.

Im Falle von EBV wurde hierfür eine Epitopvorhersage durchgeführt, welche die potenziell HLA-A*01-bindenen Peptide im gesamten EBV-Proteom identifizieren sollte. Aus dieser Liste wurden 171 Peptide mittels IFNγ ELISpot Assays auf ihre Immunogenität hin untersucht und nachfolgend die HLA-Restriktion stark immunogener Peptide mittels Durchflusszytometrie verifiziert. Von den untersuchten Peptiden waren 29 immunogen; sieben davon waren dominante Epitope. Für alle dominanten Epitope konnte die HLA-A*01-Restriktion bestätigt und reaktive $CD8^+$ T-Zellen in gesunden Spendern identifiziert werden.

Im Gegensatz dazu wurden im zweiten Projekt potenzielle HCMV-Epitope als HLA-Liganden aus mit Virusmutanten infizierten Zelllinien isoliert und danach mittels Massenspektrometrie sequenziert. Von den 181 Liganden konnten 50 (30%) als Epitope charakterisiert werden. Für alle 13 dominanten Epitope konnte nachfolgend die vorhergesagte HLA-Restriktion bestätigt werden. Die Infektion von zwei weiteren Zelllinien erlaubte die Isolation hunderter neuer Peptide, die einer Immunogenitätstestung unterzogen werden können. Da die HLA-Liganden aus über 100 verschiedenen Proteinen stammen, eignet sich diese Methode hervorragend für eine umfangreiche Analyse der Epitope über das gesamte Proteom hinweg.

Für beide Viren konnten damit neue, stark immunogene Epitope identifiziert werden, die in Zukunft für Antigen-spezifische Immuntherapien Verwendung finden können.

Abbreviations

aAPC	Artificial antigen presenting cell
APC	Allophycocyanin
APC	Antigen presenting cell
BAC	Bacterial artificial chromosome
BSA	Bovine serum albumin
CD	Cluster of differentiation
CDR	Complementarity determining region
CNX	Calnexin
CRT	Calreticulin
CTL	Cytotoxic T cell
DC	Dendritic cells
DMSO	Dimethyl sulfoxide
DN	double-negative
DRiPs	Defective ribosomal products
DTT	Dithiothreitol
EBV	Epstein-Barr virus
EDTA	Ethylendiaminetetraacetic acid
ELISpot	Enzyme-linked immunospot assay
ER	Endoplasmic reticulum
ERAP	ER aminopeptidase
f.c.	Final concentration
FACS	Fluorescence activated cell sorting
FCS	Fetal calf serum
FITC	Fluorescein isothiocyanate
GM-CSF	Granulocyte macrophage colony stimulating factor
HCMV	Human cytomegalovirus
HLA	Human leukocyte antigen
HLA-I	HLA class I
HLA-II	HLA class II
h.p.i.	Hours post infection
HSA	Human serum albumin
ICS	Intracellular cytokine staining

IE	Immediate-early
IFN	Interferon
IL	Interleukin
IM	Infectious mononucleosis
ITAM	Immunoreceptor tyrosine-based activation motif
LC-MS/MS	Liquid chromatography-coupled tandem-mass spectrometry
LB-Amp/Cam	Lysogeny broth with ampicillin and chloramphenicol
MACS	Magnetic activated cell sorting
MHC	Major histocompatibility complex
MIEP	Major immediate-early promoter
MOI	Multiplicity of infection
MS	Mass spectrometry
NK cell	Natural killer cell
OD	Optical density
ORF	Open reading frame
PAMP	Pathogen-associated molecular pattern
PBS	Phosphate buffered saline
PE	R-Phycoerythrin
Pen/Strep	Penicillin/Streptomycin
PerCP	Peridinin chlorophyll protein
PLC	Peptide loading complex
PMSF	Phenylmethylsulfonyl fluoride
pp	Phosphoprotein
PSM	Peptide spectrum matches
RT	Room temperature
SFC	Spot forming cells
TAA	Tumor-associated antigen
TAP	Transporter associated with antigen processing
TBS	Tris-buffered saline
TCM	T cell medium
TCR	T cell receptor
TGF	Transforming growth factor
T_H cell	T helper cell
TNF	Tumor necrosis factor

T_{reg}	Regulatory T cell
Tris	Tris(hydroxymethyl)aminomethane
UL	Unique long
US	Unique short
VCA	Viral capsid antigen
WT	Wild type
β2m	β2-microglobulin
β-Me	β-Mercaptoethanol

7 References

1. The MHC sequencing consortium (1999) Complete sequence and gene map of a human major histocompatibility complex. *Nature* 401:921-923.
2. Murphy K, Travers P, Walport M, Janeway C (2012) *Janeway's Immunobiology* (Garland Science, New York) 8th Ed.
3. Robinson J, Halliwell JA, Hayhurst JD, Flicek P, Parham P, Marsh SG (2015) The IPD and IMGT/HLA database: allele variant databases. *Nucleic Acids Res* 43:D423-431.
4. Boehm U, Klamp T, Groot M, Howard JC (1997) Cellular responses to interferon-gamma. *Annu Rev Immunol* 15:749-795.
5. Seliger B, Kloor M, Ferrone S (2017) HLA class II antigen-processing pathway in tumors: Molecular defects and clinical relevance. *Oncoimmunology* 6:e1171447.
6. Goodfellow PN, Jones EA, Van Heyningen V, Solomon E, Bobrow M, Miggiano V, Bodmer WF (1975) The beta2-microglobulin gene is on chromosome 15 and not in the HL-A region. *Nature* 254:267-269.
7. Bjorkman PJ, Saper MA, Samraoui B, Bennett WS, Strominger JL, Wiley DC (1987) The foreign antigen binding site and T cell recognition regions of class I histocompatibility antigens. *Nature* 329:512-518.
8. Falk K, Rötzschke O, Stevanovic S, Jung G, Rammensee HG (1991) Allele-specific motifs revealed by sequencing of self-peptides eluted from MHC molecules. *Nature* 351:290-296.
9. Garrett TP, Saper MA, Bjorkman PJ, Strominger JL, Wiley DC (1989) Specificity pockets for the side chains of peptide antigens in HLA-Aw68. *Nature* 342:692-696.
10. Rammensee HG, Friede T, Stevanovic S (1995) MHC ligands and peptide motifs: first listing. *Immunogenetics* 41:178-228.
11. Sidney J, Grey HM, Kubo RT, Sette A (1996) Practical, biochemical and evolutionary implications of the discovery of HLA class I supermotifs. *Immunol Today* 17:261-266.
12. Sidney J, Peters B, Frahm N, Brander C, Sette A (2008) HLA class I supertypes: a revised and updated classification. *BMC Immunol* 9:1.
13. Threlkeld SC, Wentworth PA, Kalams SA, Wilkes BM, Ruhl DJ, Keogh E, Sidney J, Southwood S, Walker BD, Sette A (1997) Degenerate and promiscuous recognition by CTL of peptides presented by the MHC class I A3-like superfamily: implications for vaccine development. *J Immunol* 159:1648-1657.
14. Burrows SR, Elkington RA, Miles JJ, Green KJ, Walker S, Haryana SM, Moss DJ, Dunckley H, Burrows JM, Khanna R (2003) Promiscuous CTL recognition of viral epitopes on multiple human leukocyte antigens: biological validation of the proposed HLA A24 supertype. *J Immunol* 171:1407-1412.
15. Sabbaj S, Bansal A, Ritter GD, Perkins C, Edwards BH, Gough E, Tang J, Szinger JJ, Korber B, Wilson CM, Kaslow RA, Mulligan MJ, Goepfert PA (2003) Cross-reactive CD8+ T cell epitopes identified in US adolescent minorities. *J Acquir Immune Defic Syndr* 33:426-438.
16. Frahm N, Yusim K, Suscovich TJ, Adams S, Sidney J, Hraber P, Hewitt HS, Linde CH, Kavanagh DG, Woodberry T, Henry LM, Faircloth K, Listgarten J, Kadie C, Jojic N, Sango K, Brown NV, Pae E, Zaman MT, Bihl F, Khatri A, John M, Mallal S, Marincola FM, Walker BD, Sette A, Heckerman D, Korber BT, Brander C (2007) Extensive HLA class I allele promiscuity among viral CTL epitopes. *Eur J Immunol* 37:2419-2433.
17. Burrows SR, Rossjohn J, McCluskey J (2006) Have we cut ourselves too short in mapping CTL epitopes? *Trends Immunol* 27:11-16.
18. Guo HC, Jardetzky TS, Garrett TP, Lane WS, Strominger JL, Wiley DC (1992) Different length peptides bind to HLA-Aw68 similarly at their ends but bulge out in the middle. *Nature* 360:364-366.
19. Collins EJ, Garboczi DN, Wiley DC (1994) Three-dimensional structure of a peptide extending from one end of a class I MHC binding site. *Nature* 371:626-629.
20. McMurtrey C, Trolle T, Sansom T, Remesh SG, Kaever T, Bardet W, Jackson K, McLeod R, Sette A, Nielsen M, Zajonc DM, Blader IJ, Peters B, Hildebrand W (2016) Toxoplasma gondii peptide ligands open the gate of the HLA class I binding groove. *Elife* 5.
21. Chicz RM, Urban RG, Lane WS, Gorga JC, Stern LJ, Vignali DA, Strominger JL (1992) Predominant naturally processed peptides bound to HLA-DR1 are derived from MHC-related molecules and are heterogeneous in size. *Nature* 358:764-768.
22. Panina-Bordignon P, Tan A, Termijtelen A, Demotz S, Corradin G, Lanzavecchia A (1989) Universally immunogenic T cell epitopes: promiscuous binding to human MHC class II and promiscuous recognition by T cells. *Eur J Immunol* 19:2237-2242.

23. Hammer J, Valsasnini P, Tolba K, Bolin D, Higelin J, Takacs B, Sinigaglia F (1993) Promiscuous and allele-specific anchors in HLA-DR-binding peptides. *Cell* 74:197-203.
24. Rammensee H, Bachmann J, Emmerich NP, Bachor OA, Stevanovic S (1999) SYFPEITHI: database for MHC ligands and peptide motifs. *Immunogenetics* 50:213-219.
25. Nielsen M, Lundegaard C, Worning P, Lauemoller SL, Lamberth K, Buus S, Brunak S, Lund O (2003) Reliable prediction of T-cell epitopes using neural networks with novel sequence representations. *Protein Sci* 12:1007-1017.
26. Vita R, Mahajan S, Overton JA, Dhanda SK, Martini S, Cantrell JR, Wheeler DK, Sette A, Peters B (2019) The Immune Epitope Database (IEDB): 2018 update. *Nucleic Acids Res* 47:D339-d343.
27. Finley D (2009) Recognition and processing of ubiquitin-protein conjugates by the proteasome. *Annu Rev Biochem* 78:477-513.
28. Cresswell P (2019) A personal retrospective on the mechanisms of antigen processing. *Immunogenetics* 71:141-160.
29. Beninga J, Rock KL, Goldberg AL (1998) Interferon-gamma can stimulate post-proteasomal trimming of the N terminus of an antigenic peptide by inducing leucine aminopeptidase. *J Biol Chem* 273:18734-18742.
30. Rock KL, York IA, Goldberg AL (2004) Post-proteasomal antigen processing for major histocompatibility complex class I presentation. *Nat Immunol* 5:670-677.
31. Raule M, Cerruti F, Benaroudj N, Migotti R, Kikuchi J, Bachi A, Navon A, Dittmar G, Cascio P (2014) PA28alphabeta reduces size and increases hydrophilicity of 20S immunoproteasome peptide products. *Chem Biol* 21:470-480.
32. Van den Eynde BJ, Morel S (2001) Differential processing of class-I-restricted epitopes by the standard proteasome and the immunoproteasome. *Curr Opin Immunol* 13:147-153.
33. Dubiel W, Pratt G, Ferrell K, Rechsteiner M (1992) Purification of an 11 S regulator of the multicatalytic protease. *J Biol Chem* 267:22369-22377.
34. Gaczynska M, Rock KL, Goldberg AL (1993) Gamma-interferon and expression of MHC genes regulate peptide hydrolysis by proteasomes. *Nature* 365:264-267.
35. Groettrup M, Ruppert T, Kuehn L, Seeger M, Standera S, Koszinowski U, Kloetzel PM (1995) The interferon-gamma-inducible 11 S regulator (PA28) and the LMP2/LMP7 subunits govern the peptide production by the 20 S proteasome in vitro. *J Biol Chem* 270:23808-23815.
36. Toes RE, Nussbaum AK, Degermann S, Schirle M, Emmerich NP, Kraft M, Laplace C, Zwinderman A, Dick TP, Muller J, Schonfisch B, Schmid C, Fehling HJ, Stevanovic S, Rammensee HG, Schild H (2001) Discrete cleavage motifs of constitutive and immunoproteasomes revealed by quantitative analysis of cleavage products. *J Exp Med* 194:1-12.
37. Kisselev AF, Akopian TN, Woo KM, Goldberg AL (1999) The sizes of peptides generated from protein by mammalian 26 and 20 S proteasomes. Implications for understanding the degradative mechanism and antigen presentation. *J Biol Chem* 274:3363-3371.
38. Stoltze L, Schirle M, Schwarz G, Schröter C, Thompson MW, Hersh LB, Kalbacher H, Stevanovic S, Rammensee HG, Schild H (2000) Two new proteases in the MHC class I processing pathway. *Nat Immunol* 1:413-418.
39. Reits E, Neijssen J, Herberts C, Benckhuijsen W, Janssen L, Drijfhout JW, Neefjes J (2004) A major role for TPPII in trimming proteasomal degradation products for MHC class I antigen presentation. *Immunity* 20:495-506.
40. Saric T, Chang SC, Hattori A, York IA, Markant S, Rock KL, Tsujimoto M, Goldberg AL (2002) An IFN-gamma-induced aminopeptidase in the ER, ERAP1, trims precursors to MHC class I-presented peptides. *Nat Immunol* 3:1169-1176.
41. Serwold T, Gonzalez F, Kim J, Jacob R, Shastri N (2002) ERAAP customizes peptides for MHC class I molecules in the endoplasmic reticulum. *Nature* 419:480-483.
42. Reits E, Griekspoor A, Neijssen J, Groothuis T, Jalink K, van Veelen P, Janssen H, Calafat J, Drijfhout JW, Neefjes J (2003) Peptide diffusion, protection, and degradation in nuclear and cytoplasmic compartments before antigen presentation by MHC class I. *Immunity* 18:97-108.
43. York IA, Chang SC, Saric T, Keys JA, Favreau JM, Goldberg AL, Rock KL (2002) The ER aminopeptidase ERAP1 enhances or limits antigen presentation by trimming epitopes to 8-9 residues. *Nat Immunol* 3:1177-1184.
44. Tanioka T, Hattori A, Masuda S, Nomura Y, Nakayama H, Mizutani S, Tsujimoto M (2003) Human leukocyte-derived arginine aminopeptidase. The third member of the oxytocinase subfamily of aminopeptidases. *J Biol Chem* 278:32275-32283.
45. Saveanu L, Carroll O, Lindo V, Del Val M, Lopez D, Lepelletier Y, Greer F, Schomburg L, Fruci D, Niedermann G, van Endert PM (2005) Concerted peptide trimming by human ERAP1 and ERAP2 aminopeptidase complexes in the endoplasmic reticulum. *Nat Immunol* 6:689-697.
46. Wearsch PA, Cresswell P (2007) Selective loading of high-affinity peptides onto major histocompatibility complex class I molecules by the tapasin-ERp57 heterodimer. *Nat Immunol* 8:873-881.

47. Caramelo JJ, Castro OA, de Prat-Gay G, Parodi AJ (2004) The endoplasmic reticulum glucosyltransferase recognizes nearly native glycoprotein folding intermediates. *J Biol Chem* 279:46280-46285.
48. Blum JS, Wearsch PA, Cresswell P (2013) Pathways of antigen processing. *Annu Rev Immunol* 31:443-473.
49. Wearsch PA, Jakob CA, Vallin A, Dwek RA, Rudd PM, Cresswell P (2004) Major histocompatibility complex class I molecules expressed with monoglucosylated N-linked glycans bind calreticulin independently of their assembly status. *J Biol Chem* 279:25112-25121.
50. Bevan MJ (1976) Cross-priming for a secondary cytotoxic response to minor H antigens with H-2 congenic cells which do not cross-react in the cytotoxic assay. *J Exp Med* 143:1283-1288.
51. Bevan MJ (1976) Minor H antigens introduced on H-2 different stimulating cells cross-react at the cytotoxic T cell level during in vivo priming. *J Immunol* 117:2233-2238.
52. Embgenbroich M, Burgdorf S (2018) Current Concepts of Antigen Cross-Presentation. *Front Immunol* 9:1643.
53. Kovacsovics-Bankowski M, Rock KL (1995) A phagosome-to-cytosol pathway for exogenous antigens presented on MHC class I molecules. *Science* 267:243-246.
54. Roche PA, Marks MS, Cresswell P (1991) Formation of a nine-subunit complex by HLA class II glycoproteins and the invariant chain. *Nature* 354:392-394.
55. Machamer CE, Cresswell P (1982) Biosynthesis and glycosylation of the invariant chain associated with HLA-DR antigens. *J Immunol* 129:2564-2569.
56. Zhong G, Romagnoli P, Germain RN (1997) Related leucine-based cytoplasmic targeting signals in invariant chain and major histocompatibility complex class II molecules control endocytic presentation of distinct determinants in a single protein. *J Exp Med* 185:429-438.
57. Peters PJ, Neefjes JJ, Oorschot V, Ploegh HL, Geuze HJ (1991) Segregation of MHC class II molecules from MHC class I molecules in the Golgi complex for transport to lysosomal compartments. *Nature* 349:669-676.
58. Benaroch P, Yilla M, Raposo G, Ito K, Miwa K, Geuze HJ, Ploegh HL (1995) How MHC class II molecules reach the endocytic pathway. *Embo j* 14:37-49.
59. Roche PA, Teletski CL, Stang E, Bakke O, Long EO (1993) Cell surface HLA-DR-invariant chain complexes are targeted to endosomes by rapid internalization. *Proc Natl Acad Sci U S A* 90:8581-8585.
60. McCormick PJ, Martina JA, Bonifacino JS (2005) Involvement of clathrin and AP-2 in the trafficking of MHC class II molecules to antigen-processing compartments. *Proc Natl Acad Sci U S A* 102:7910-7915.
61. Ghosh P, Amaya M, Mellins E, Wiley DC (1995) The structure of an intermediate in class II MHC maturation: CLIP bound to HLA-DR3. *Nature* 378:457-462.
62. Wieczorek M, Abualrous ET, Sticht J, Alvaro-Benito M, Stolzenberg S, Noe F, Freund C (2017) Major Histocompatibility Complex (MHC) Class I and MHC Class II Proteins: Conformational Plasticity in Antigen Presentation. *Front Immunol* 8:292.
63. Denzin LK, Fallas JL, Prendes M, Yi W (2005) Right place, right time, right peptide: DO keeps DM focused. *Immunol Rev* 207:279-292.
64. Shi GP, Villadangos JA, Dranoff G, Small C, Gu L, Haley KJ, Riese R, Ploegh HL, Chapman HA (1999) Cathepsin S required for normal MHC class II peptide loading and germinal center development. *Immunity* 10:197-206.
65. Arunachalam B, Phan UT, Geuze HJ, Cresswell P (2000) Enzymatic reduction of disulfide bonds in lysosomes: characterization of a gamma-interferon-inducible lysosomal thiol reductase (GILT). *Proc Natl Acad Sci U S A* 97:745-750.
66. Paludan C, Schmid D, Landthaler M, Vockerodt M, Kube D, Tuschl T, Münz C (2005) Endogenous MHC class II processing of a viral nuclear antigen after autophagy. *Science* 307:593-596.
67. Hayday AC, Saito H, Gillies SD, Kranz DM, Tanigawa G, Eisen HN, Tonegawa S (1985) Structure, organization, and somatic rearrangement of T cell gamma genes. *Cell* 40:259-269.
68. Davis MM, Bjorkman PJ (1988) T-cell antigen receptor genes and T-cell recognition. *Nature* 334:395-402.
69. Komori T, Okada A, Stewart V, Alt FW (1993) Lack of N regions in antigen receptor variable region genes of TdT-deficient lymphocytes. *Science* 261:1171-1175.
70. Venturi V, Price DA, Douek DC, Davenport MP (2008) The molecular basis for public T-cell responses? *Nat Rev Immunol* 8:231-238.
71. Laydon DJ, Bangham CR, Asquith B (2015) Estimating T-cell repertoire diversity: limitations of classical estimators and a new approach. *Philos Trans R Soc Lond B Biol Sci* 370.
72. Weiss A, Stobo JD (1984) Requirement for the coexpression of T3 and the T cell antigen receptor on a malignant human T cell line. *J Exp Med* 160:1284-1299.
73. Kappes DJ, Tonegawa S (1991) Surface expression of alternative forms of the TCR/CD3 complex. *Proc Natl Acad Sci U S A* 88:10619-10623.

74. Birnbaum ME, Berry R, Hsiao YS, Chen Z, Shingu-Vazquez MA, Yu X, Waghray D, Fischer S, McCluskey J, Rossjohn J, Walz T, Garcia KC (2014) Molecular architecture of the alphabeta T cell receptor-CD3 complex. *Proc Natl Acad Sci U S A* 111:17576-17581.
75. Love PE, Hayes SM (2010) ITAM-mediated signaling by the T-cell antigen receptor. *Cold Spring Harb Perspect Biol* 2:a002485.
76. Russell JH, Ley TJ (2002) Lymphocyte-mediated cytotoxicity. *Annu Rev Immunol* 20:323-370.
77. Sun Q, Burton RL, Lucas KG (2002) Cytokine production and cytolytic mechanism of CD4(+) cytotoxic T lymphocytes in ex vivo expanded therapeutic Epstein-Barr virus-specific T-cell cultures. *Blood* 99:3302-3309.
78. Perez-Diez A, Joncker NT, Choi K, Chan WF, Anderson CC, Lantz O, Matzinger P (2007) CD4 cells can be more efficient at tumor rejection than CD8 cells. *Blood* 109:5346-5354.
79. Mosmann TR, Cherwinski H, Bond MW, Giedlin MA, Coffman RL (1986) Two types of murine helper T cell clone. I. Definition according to profiles of lymphokine activities and secreted proteins. *J Immunol* 136:2348-2357.
80. Stout RD, Bottomly K (1989) Antigen-specific activation of effector macrophages by IFN-gamma producing (TH1) T cell clones. Failure of IL-4-producing (TH2) T cell clones to activate effector function in macrophages. *J Immunol* 142:760-765.
81. Ridge JP, Di Rosa F, Matzinger P (1998) A conditioned dendritic cell can be a temporal bridge between a CD4+ T-helper and a T-killer cell. *Nature* 393:474-478.
82. Bennett SR, Carbone FR, Karamalis F, Flavell RA, Miller JF, Heath WR (1998) Help for cytotoxic-T-cell responses is mediated by CD40 signalling. *Nature* 393:478-480.
83. Croft M, Swain SL (1991) B cell response to fresh and effector T helper cells. Role of cognate T-B interaction and the cytokines IL-2, IL-4, and IL-6. *J Immunol* 146:4055-4064.
84. Zhu J, Paul WE (2008) CD4 T cells: fates, functions, and faults. *Blood* 112:1557-1569.
85. Harrington LE, Hatton RD, Mangan PR, Turner H, Murphy TL, Murphy KM, Weaver CT (2005) Interleukin 17-producing CD4+ effector T cells develop via a lineage distinct from the T helper type 1 and 2 lineages. *Nat Immunol* 6:1123-1132.
86. Sakaguchi S, Sakaguchi N, Asano M, Itoh M, Toda M (1995) Immunologic self-tolerance maintained by activated T cells expressing IL-2 receptor alpha-chains (CD25). Breakdown of a single mechanism of self-tolerance causes various autoimmune diseases. *J Immunol* 155:1151-1164.
87. Fontenot JD, Gavin MA, Rudensky AY (2003) Foxp3 programs the development and function of CD4+CD25+ regulatory T cells. *Nat Immunol* 4:330-336.
88. Hori S, Nomura T, Sakaguchi S (2003) Control of regulatory T cell development by the transcription factor Foxp3. *Science* 299:1057-1061.
89. Kondo M, Weissman IL, Akashi K (1997) Identification of clonogenic common lymphoid progenitors in mouse bone marrow. *Cell* 91:661-672.
90. Germain RN (2002) T-cell development and the CD4-CD8 lineage decision. *Nat Rev Immunol* 2:309-322.
91. Godfrey DI, Kennedy J, Suda T, Zlotnik A (1993) A developmental pathway involving four phenotypically and functionally distinct subsets of CD3-CD4-CD8- triple-negative adult mouse thymocytes defined by CD44 and CD25 expression. *J Immunol* 150:4244-4252.
92. Schatz DG, Oettinger MA, Baltimore D (1989) The V(D)J recombination activating gene, RAG-1. *Cell* 59:1035-1048.
93. Shinkai Y, Koyasu S, Nakayama K, Murphy KM, Loh DY, Reinherz EL, Alt FW (1993) Restoration of T cell development in RAG-2-deficient mice by functional TCR transgenes. *Science* 259:822-825.
94. Scollay RG, Butcher EC, Weissman IL (1980) Thymus cell migration. Quantitative aspects of cellular traffic from the thymus to the periphery in mice. *Eur J Immunol* 10:210-218.
95. Banchereau J, Steinman RM (1998) Dendritic cells and the control of immunity. *Nature* 392:245-252.
96. Warnock RA, Askari S, Butcher EC, von Andrian UH (1998) Molecular mechanisms of lymphocyte homing to peripheral lymph nodes. *J Exp Med* 187:205-216.
97. Jenkins MK, Schwartz RH (1987) Antigen presentation by chemically modified splenocytes induces antigen-specific T cell unresponsiveness in vitro and in vivo. *J Exp Med* 165:302-319.
98. Guerder S, Meyerhoff J, Flavell R (1994) The role of the T cell costimulator B7-1 in autoimmunity and the induction and maintenance of tolerance to peripheral antigen. *Immunity* 1:155-166.
99. Bakdash G, Sittig SP, van Dijk T, Figdor CG, de Vries IJ (2013) The nature of activatory and tolerogenic dendritic cell-derived signal II. *Front Immunol* 4:53.
100. Green JM, Noel PJ, Sperling AI, Walunas TL, Gray GS, Bluestone JA, Thompson CB (1994) Absence of B7-dependent responses in CD28-deficient mice. *Immunity* 1:501-508.
101. Linsley PS, Brady W, Grosmaire L, Aruffo A, Damle NK, Ledbetter JA (1991) Binding of the B cell activation antigen B7 to CD28 costimulates T cell proliferation and interleukin 2 mRNA accumulation. *J Exp Med* 173:721-730.

102. Curtsinger JM, Schmidt CS, Mondino A, Lins DC, Kedl RM, Jenkins MK, Mescher MF (1999) Inflammatory cytokines provide a third signal for activation of naive CD4+ and CD8+ T cells. *J Immunol* 162:3256-3262.
103. Curtsinger JM, Lins DC, Mescher MF (2003) Signal 3 determines tolerance versus full activation of naive CD8 T cells: dissociating proliferation and development of effector function. *J Exp Med* 197:1141-1151.
104. Viola A, Lanzavecchia A (1996) T cell activation determined by T cell receptor number and tunable thresholds. *Science* 273:104-106.
105. Labrecque N, Whitfield LS, Obst R, Waltzinger C, Benoist C, Mathis D (2001) How much TCR does a T cell need? *Immunity* 15:71-82.
106. Schodin BA, Tsomides TJ, Kranz DM (1996) Correlation between the number of T cell receptors required for T cell activation and TCR-ligand affinity. *Immunity* 5:137-146.
107. Harding CV, Unanue ER (1990) Quantitation of antigen-presenting cell MHC class II/peptide complexes necessary for T-cell stimulation. *Nature* 346:574-576.
108. Demotz S, Grey HM, Sette A (1990) The minimal number of class II MHC-antigen complexes needed for T cell activation. *Science* 249:1028-1030.
109. Sykulev Y, Joo M, Vturina I, Tsomides TJ, Eisen HN (1996) Evidence that a single peptide-MHC complex on a target cell can elicit a cytolytic T cell response. *Immunity* 4:565-571.
110. Valitutti S, Muller S, Cella M, Padovan E, Lanzavecchia A (1995) Serial triggering of many T-cell receptors by a few peptide-MHC complexes. *Nature* 375:148-151.
111. Valitutti S (2012) The Serial Engagement Model 17 Years After: From TCR Triggering to Immunotherapy. *Front Immunol* 3:272.
112. Feng Y, Reinherz EL, Lang MJ (2018) alphabeta T Cell Receptor Mechanosensing Forces out Serial Engagement. *Trends Immunol* 39:596-609.
113. Hammarlund E, Lewis MW, Hansen SG, Strelow LI, Nelson JA, Sexton GJ, Hanifin JM, Slifka MK (2003) Duration of antiviral immunity after smallpox vaccination. *Nat Med* 9:1131-1137.
114. Farber DL, Yudanin NA, Restifo NP (2014) Human memory T cells: generation, compartmentalization and homeostasis. *Nat Rev Immunol* 14:24-35.
115. Macallan DC, Borghans JA, Asquith B (2017) Human T Cell Memory: A Dynamic View. *Vaccines (Basel)* 5.
116. Smith SH, Brown MH, Rowe D, Callard RE, Beverley PC (1986) Functional subsets of human helper-inducer cells defined by a new monoclonal antibody, UCHL1. *Immunology* 58:63-70.
117. Sanders ME, Makgoba MW, Sharrow SO, Stephany D, Springer TA, Young HA, Shaw S (1988) Human memory T lymphocytes express increased levels of three cell adhesion molecules (LFA-3, CD2, and LFA-1) and three other molecules (UCHL1, CDw29, and Pgp-1) and have enhanced IFN-gamma production. *J Immunol* 140:1401-1407.
118. Sallusto F, Lenig D, Forster R, Lipp M, Lanzavecchia A (1999) Two subsets of memory T lymphocytes with distinct homing potentials and effector functions. *Nature* 401:708-712.
119. Gattinoni L, Lugli E, Ji Y, Pos Z, Paulos CM, Quigley MF, Almeida JR, Gostick E, Yu Z, Carpenito C, Wang E, Douek DC, Price DA, June CH, Marincola FM, Roederer M, Restifo NP (2011) A human memory T cell subset with stem cell-like properties. *Nat Med* 17:1290-1297.
120. Epstein MA, Achong BG, Barr YM (1964) VIRUS PARTICLES IN CULTURED LYMPHOBLASTS FROM BURKITT'S LYMPHOMA. *Lancet* 1:702-703.
121. Henle W, Diehl V, Kohn G, Zur Hausen H, Henle G (1967) Herpes-type virus and chromosome marker in normal leukocytes after growth with irradiated Burkitt cells. *Science* 157:1064-1065.
122. Pope JH, Horne MK, Scott W (1968) Transformation of foetal human leukocytes in vitro by filtrates of a human leukaemic cell line containing herpes-like virus. *Int J Cancer* 3:857-866.
123. Gerper P, Whang-Peng J, Monroe JH (1969) Transformation and chromosome changes induced by Epstein-Barr virus in normal human leukocyte cultures. *Proc Natl Acad Sci U S A* 63:740-747.
124. de-Thé G, Geser A, Day NE, Tukei PM, Williams EH, Beri DP, Smith PG, Dean AG, Bornkamm GW, Feorino P, Henle W (1978) Epidemiological evidence for causal relationship between Epstein-Barr virus and Burkitt's lymphoma from Ugandan prospective study. *Nature* 274:756-761.
125. Henle G, Henle W, Horwitz CA (1974) Antibodies to Epstein-Barr virus-associated nuclear antigen in infectious mononucleosis. *J Infect Dis* 130:231-239.
126. Luzuriaga K, Sullivan JL (2010) Infectious mononucleosis. *N Engl J Med* 362:1993-2000.
127. Rickinson AB, Young LS, Rowe M (1987) Influence of the Epstein-Barr virus nuclear antigen EBNA 2 on the growth phenotype of virus-transformed B cells. *J Virol* 61:1310-1317.
128. Tzellos S, Farrell PJ (2012) Epstein-barr virus sequence variation-biology and disease. *Pathogens* 1:156-174.
129. Zimber U, Adldinger HK, Lenoir GM, Vuillaume M, Knebel-Doeberitz MV, Laux G, Desgranges C, Wittmann P, Freese UK, Schneider U, et al. (1986) Geographical prevalence of two types of Epstein-Barr virus. *Virology* 154:56-66.

130. Young LS, Yao QY, Rooney CM, Sculley TB, Moss DJ, Rupani H, Laux G, Bornkamm GW, Rickinson AB (1987) New type B isolates of Epstein-Barr virus from Burkitt's lymphoma and from normal individuals in endemic areas. *J Gen Virol* 68 (Pt 11):2853-2862.
131. Smatti MK, Al-Sadeq DW, Ali NH, Pintus G, Abou-Saleh H, Nasrallah GK (2018) Epstein-Barr Virus Epidemiology, Serology, and Genetic Variability of LMP-1 Oncogene Among Healthy Population: An Update. *Front Oncol* 8:211.
132. Kieff E, Dambaugh T, Heller M, King W, Cheung A, van Santen V, Hummel M, Beisel C, Fennewald S, Hennessy K, Heineman T (1982) The biology and chemistry of Epstein-Barr virus. *J Infect Dis* 146:506-517.
133. Baer R, Bankier AT, Biggin MD, Deininger PL, Farrell PJ, Gibson TJ, Hatfull G, Hudson GS, Satchwell SC, Seguin C, et al. (1984) DNA sequence and expression of the B95-8 Epstein-Barr virus genome. *Nature* 310:207-211.
134. Bornkamm GW, Delius H, Zimber U, Hudewentz J, Epstein MA (1980) Comparison of Epstein-Barr virus strains of different origin by analysis of the viral DNAs. *J Virol* 35:603-618.
135. Skare J, Edson C, Farley J, Strominger JL (1982) The B95-8 isolate of Epstein-Barr virus arose from an isolate with a standard genome. *J Virol* 44:1088-1091.
136. Lindahl T, Adams A, Bjursell G, Bornkamm GW, Kaschka-Dierich C, Jehn U (1976) Covalently closed circular duplex DNA of Epstein-Barr virus in a human lymphoid cell line. *J Mol Biol* 102:511-530.
137. Arrand JR, Rymo L, Walsh JE, Bjorck E, Lindahl T, Griffin BE (1981) Molecular cloning of the complete Epstein-Barr virus genome as a set of overlapping restriction endonuclease fragments. *Nucleic Acids Res* 9:2999-3014.
138. Young LS, Yap LF, Murray PG (2016) Epstein-Barr virus: more than 50 years old and still providing surprises. *Nat Rev Cancer* 16:789-802.
139. Brooks LA, Lear AL, Young LS, Rickinson AB (1993) Transcripts from the Epstein-Barr virus BamHI A fragment are detectable in all three forms of virus latency. *J Virol* 67:3182-3190.
140. van Zyl DG, Mautner J, Delecluse HJ (2019) Progress in EBV Vaccines. *Front Oncol* 9:104.
141. Alfieri C, Tanner J, Carpentier L, Perpete C, Savoie A, Paradis K, Delage G, Joncas J (1996) Epstein-Barr virus transmission from a blood donor to an organ transplant recipient with recovery of the same virus strain from the recipient's blood and oropharynx. *Blood* 87:812-817.
142. Trottier H, Buteau C, Robitaille N, Duval M, Tucci M, Lacroix J, Alfieri C (2012) Transfusion-related Epstein-Barr virus infection among stem cell transplant recipients: a retrospective cohort study in children. *Transfusion* 52:2653-2663.
143. Sixbey JW, Nedrud JG, Raab-Traub N, Hanes RA, Pagano JS (1984) Epstein-Barr virus replication in oropharyngeal epithelial cells. *N Engl J Med* 310:1225-1230.
144. Jones JF, Shurin S, Abramowsky C, Tubbs RR, Sciotto CG, Wahl R, Sands J, Gottman D, Katz BZ, Sklar J (1988) T-cell lymphomas containing Epstein-Barr viral DNA in patients with chronic Epstein-Barr virus infections. *N Engl J Med* 318:733-741.
145. Harabuchi Y, Yamanaka N, Kataura A, Imai S, Kinoshita T, Mizuno F, Osato T (1990) Epstein-Barr virus in nasal T-cell lymphomas in patients with lethal midline granuloma. *Lancet* 335:128-130.
146. Tanner J, Weis J, Fearon D, Whang Y, Kieff E (1987) Epstein-Barr virus gp350/220 binding to the B lymphocyte C3d receptor mediates adsorption, capping, and endocytosis. *Cell* 50:203-213.
147. Ogembo JG, Kannan L, Ghiran I, Nicholson-Weller A, Finberg RW, Tsokos GC, Fingeroth JD (2013) Human complement receptor type 1/CD35 is an Epstein-Barr Virus receptor. *Cell Rep* 3:371-385.
148. Chesnokova LS, Hutt-Fletcher LM (2011) Fusion of Epstein-Barr virus with epithelial cells can be triggered by alphavbeta5 in addition to alphavbeta6 and alphavbeta8, and integrin binding triggers a conformational change in glycoproteins gHgL. *J Virol* 85:13214-13223.
149. Borza CM, Hutt-Fletcher LM (2002) Alternate replication in B cells and epithelial cells switches tropism of Epstein-Barr virus. *Nat Med* 8:594-599.
150. Shannon-Lowe C, Rowe M (2014) Epstein Barr virus entry; kissing and conjugation. *Curr Opin Virol* 4:78-84.
151. Odumade OA, Hogquist KA, Balfour HH, Jr. (2011) Progress and problems in understanding and managing primary Epstein-Barr virus infections. *Clin Microbiol Rev* 24:193-209.
152. Gires O, Zimber-Strobl U, Gonnella R, Ueffing M, Marschall G, Zeidler R, Pich D, Hammerschmidt W (1997) Latent membrane protein 1 of Epstein-Barr virus mimics a constitutively active receptor molecule. *Embo j* 16:6131-6140.
153. Caldwell RG, Wilson JB, Anderson SJ, Longnecker R (1998) Epstein-Barr virus LMP2A drives B cell development and survival in the absence of normal B cell receptor signals. *Immunity* 9:405-411.
154. Hochberg D, Middeldorp JM, Catalina M, Sullivan JL, Luzuriaga K, Thorley-Lawson DA (2004) Demonstration of the Burkitt's lymphoma Epstein-Barr virus phenotype in dividing latently infected memory cells in vivo. *Proc Natl Acad Sci U S A* 101:239-244.
155. Khan G, Miyashita EM, Yang B, Babcock GJ, Thorley-Lawson DA (1996) Is EBV persistence in vivo a model for B cell homeostasis? *Immunity* 5:173-179.

156. Laichalk LL, Thorley-Lawson DA (2005) Terminal differentiation into plasma cells initiates the replicative cycle of Epstein-Barr virus in vivo. *J Virol* 79:1296-1307.
157. Maurmann S, Fricke L, Wagner HJ, Schlenke P, Hennig H, Steinhoff J, Jabs WJ (2003) Molecular parameters for precise diagnosis of asymptomatic Epstein-Barr virus reactivation in healthy carriers. *J Clin Microbiol* 41:5419-5428.
158. Henle G, Henle W, Diehl V (1968) Relation of Burkitt's tumor-associated herpes-type virus to infectious mononucleosis. *Proc Natl Acad Sci U S A* 59:94-101.
159. Balfour HH, Jr., Odumade OA, Schmeling DO, Mullan BD, Ed JA, Knight JA, Vezina HE, Thomas W, Hogquist KA (2013) Behavioral, virologic, and immunologic factors associated with acquisition and severity of primary Epstein-Barr virus infection in university students. *J Infect Dis* 207:80-88.
160. Taylor GS, Long HM, Brooks JM, Rickinson AB, Hislop AD (2015) The immunology of Epstein-Barr virus-induced disease. *Annu Rev Immunol* 33:787-821.
161. Rea TD, Russo JE, Katon W, Ashley RL, Buchwald DS (2001) Prospective study of the natural history of infectious mononucleosis caused by Epstein-Barr virus. *J Am Board Fam Pract* 14:234-242.
162. Kimura H, Cohen JI (2017) Chronic Active Epstein-Barr Virus Disease. *Front Immunol* 8:1867.
163. Cesaro S, Murrone A, Mengoli C, Pillon M, Biasolo MA, Calore E, Tridello G, Varotto S, Alaggio R, Zanesco L, Palu G, Messina C (2005) The real-time polymerase chain reaction-guided modulation of immunosuppression enables the pre-emptive management of Epstein-Barr virus reactivation after allogeneic haematopoietic stem cell transplantation. *Br J Haematol* 128:224-233.
164. Dierickx D, Habermann TM (2018) Post-Transplantation Lymphoproliferative Disorders in Adults. *N Engl J Med* 378:549-562.
165. Van Besien K, Bachier-Rodriguez L, Satlin M, Brown MA, Gergis U, Guarneri D, Hsu J, Phillips AA, Mayer SA, Singh AD, Soave R, Rossi A, Small CB, Walsh TJ, Rennert H, Shore TB (2019) Prophylactic rituximab prevents EBV PTLD in haplo-cord transplant recipients at high risk. *Leuk Lymphoma* 60:1693-1696.
166. Oertel SH, Verschuuren E, Reinke P, Zeidler K, Papp-Vary M, Babel N, Trappe RU, Jonas S, Hummel M, Anagnostopoulos I, Dorken B, Riess HB (2005) Effect of anti-CD 20 antibody rituximab in patients with post-transplant lymphoproliferative disorder (PTLD). *Am J Transplant* 5:2901-2906.
167. Trappe R, Oertel S, Leblond V, Mollee P, Sender M, Reinke P, Neuhaus R, Lehmkuhl H, Horst HA, Salles G, Morschhauser F, Jaccard A, Lamy T, Leithauser M, Zimmermann H, Anagnostopoulos I, Raphael M, Riess H, Choquet S (2012) Sequential treatment with rituximab followed by CHOP chemotherapy in adult B-cell post-transplant lymphoproliferative disorder (PTLD): the prospective international multicentre phase 2 PTLD-1 trial. *Lancet Oncol* 13:196-206.
168. Zimmermann H, Trappe RU (2011) Therapeutic options in post-transplant lymphoproliferative disorders. *Ther Adv Hematol* 2:393-407.
169. Haque T, Wilkie GM, Jones MM, Higgins CD, Urquhart G, Wingate P, Burns D, McAulay K, Turner M, Bellamy C, Amlot PL, Kelly D, MacGilchrist A, Gandhi MK, Swerdlow AJ, Crawford DH (2007) Allogeneic cytotoxic T-cell therapy for EBV-positive posttransplantation lymphoproliferative disease: results of a phase 2 multicenter clinical trial. *Blood* 110:1123-1131.
170. McLaughlin LP, Bollard CM, Keller MD (2018) Adoptive T Cell Therapy for Epstein-Barr Virus Complications in Patients With Primary Immunodeficiency Disorders. *Front Immunol* 9:556.
171. Shannon-Lowe C, Rickinson A (2019) The Global Landscape of EBV-Associated Tumors. *Front Oncol* 9:713.
172. Cohen JI, Fauci AS, Varmus H, Nabel GJ (2011) Epstein-Barr virus: an important vaccine target for cancer prevention. *Sci Transl Med* 3:107fs107.
173. Harley JB, Chen X, Pujato M, Miller D, Maddox A, Forney C, Magnusen AF, Lynch A, Chetal K, Yukawa M, Barski A, Salomonis N, Kaufman KM, Kottyan LC, Weirauch MT (2018) Transcription factors operate across disease loci, with EBNA2 implicated in autoimmunity. *Nat Genet* 50:699-707.
174. Fugl A, Andersen CL (2019) Epstein-Barr virus and its association with disease - a review of relevance to general practice. *BMC Fam Pract* 20:62.
175. Yao QY, Tierney RJ, Croom-Carter D, Dukers D, Cooper GM, Ellis CJ, Rowe M, Rickinson AB (1996) Frequency of multiple Epstein-Barr virus infections in T-cell-immunocompromised individuals. *J Virol* 70:4884-4894.
176. Middeldorp JM (2015) Epstein-Barr Virus-Specific Humoral Immune Responses in Health and Disease. *Curr Top Microbiol Immunol* 391:289-323.
177. Sokal EM, Hoppenbrouwers K, Vandermeulen C, Moutschen M, Leonard P, Moreels A, Haumont M, Bollen A, Smets F, Denis M (2007) Recombinant gp350 vaccine for infectious mononucleosis: a phase 2, randomized, double-blind, placebo-controlled trial to evaluate the safety, immunogenicity, and efficacy of an Epstein-Barr virus vaccine in healthy young adults. *J Infect Dis* 196:1749-1753.

178. Martinez OM, Krams SM (2017) The Immune Response to Epstein Barr Virus and Implications for Posttransplant Lymphoproliferative Disorder. *Transplantation* 101:2009-2016.
179. Pappworth IY, Wang EC, Rowe M (2007) The switch from latent to productive infection in epstein-barr virus-infected B cells is associated with sensitization to NK cell killing. *J Virol* 81:474-482.
180. Chijioke O, Muller A, Feederle R, Barros MH, Krieg C, Emmel V, Marcenaro E, Leung CS, Antsiferova O, Landtwing V, Bossart W, Moretta A, Hassan R, Boyman O, Niedobitek G, Delecluse HJ, Capaul R, Munz C (2013) Human natural killer cells prevent infectious mononucleosis features by targeting lytic Epstein-Barr virus infection. *Cell Rep* 5:1489-1498.
181. Azzi T, Lunemann A, Murer A, Ueda S, Beziat V, Malmberg KJ, Staubli G, Gysin C, Berger C, Münz C, Chijioke O, Nadal D (2014) Role for early-differentiated natural killer cells in infectious mononucleosis. *Blood* 124:2533-2543.
182. Long HM, Meckiff BJ, Taylor GS (2019) The T-cell Response to Epstein-Barr Virus-New Tricks From an Old Dog. *Front Immunol* 10:2193.
183. Murray RJ, Kurilla MG, Brooks JM, Thomas WA, Rowe M, Kieff E, Rickinson AB (1992) Identification of target antigens for the human cytotoxic T cell response to Epstein-Barr virus (EBV): implications for the immune control of EBV-positive malignancies. *J Exp Med* 176:157-168.
184. Khanna R, Burrows SR, Kurilla MG, Jacob CA, Misko IS, Sculley TB, Kieff E, Moss DJ (1992) Localization of Epstein-Barr virus cytotoxic T cell epitopes using recombinant vaccinia: implications for vaccine development. *J Exp Med* 176:169-176.
185. Yin Y, Manoury B, Fahraeus R (2003) Self-inhibition of synthesis and antigen presentation by Epstein-Barr virus-encoded EBNA1. *Science* 301:1371-1374.
186. Levitskaya J, Coram M, Levitsky V, Imreh S, Steigerwald-Mullen PM, Klein G, Kurilla MG, Masucci MG (1995) Inhibition of antigen processing by the internal repeat region of the Epstein-Barr virus nuclear antigen-1. *Nature* 375:685-688.
187. Levitskaya J, Sharipo A, Leonchiks A, Ciechanover A, Masucci MG (1997) Inhibition of ubiquitin/proteasome-dependent protein degradation by the Gly-Ala repeat domain of the Epstein-Barr virus nuclear antigen 1. *Proc Natl Acad Sci U S A* 94:12616-12621.
188. Callan MF, Tan L, Annels N, Ogg GS, Wilson JD, O'Callaghan CA, Steven N, McMichael AJ, Rickinson AB (1998) Direct visualization of antigen-specific CD8+ T cells during the primary immune response to Epstein-Barr virus In vivo. *J Exp Med* 187:1395-1402.
189. Silins SL, Sherritt MA, Silleri JM, Cross SM, Elliott SL, Bharadwaj M, Le TT, Morrison LE, Khanna R, Moss DJ, Suhrbier A, Misko IS (2001) Asymptomatic primary Epstein-Barr virus infection occurs in the absence of blood T-cell repertoire perturbations despite high levels of systemic viral load. *Blood* 98:3739-3744.
190. Forrest C, Hislop AD, Rickinson AB, Zuo J (2018) Proteome-wide analysis of CD8+ T cell responses to EBV reveals differences between primary and persistent infection. *PLoS Pathog* 14:e1007110.
191. Hislop AD, Gudgeon NH, Callan MF, Fazou C, Hasegawa H, Salmon M, Rickinson AB (2001) EBV-specific CD8+ T cell memory: relationships between epitope specificity, cell phenotype, and immediate effector function. *J Immunol* 167:2019-2029.
192. Precopio ML, Sullivan JL, Willard C, Somasundaran M, Luzuriaga K (2003) Differential kinetics and specificity of EBV-specific CD4+ and CD8+ T cells during primary infection. *J Immunol* 170:2590-2598.
193. Long HM, Chagoury OL, Leese AM, Ryan GB, James E, Morton LT, Abbott RJ, Sabbah S, Kwok W, Rickinson AB (2013) MHC II tetramers visualize human CD4+ T cell responses to Epstein-Barr virus infection and demonstrate atypical kinetics of the nuclear antigen EBNA1 response. *J Exp Med* 210:933-949.
194. Long HM, Leese AM, Chagoury OL, Connerty SR, Quarcoopome J, Quinn LL, Shannon-Lowe C, Rickinson AB (2011) Cytotoxic CD4+ T cell responses to EBV contrast with CD8 responses in breadth of lytic cycle antigen choice and in lytic cycle recognition. *J Immunol* 187:92-101.
195. Cannon MJ, Schmid DS, Hyde TB (2010) Review of cytomegalovirus seroprevalence and demographic characteristics associated with infection. *Rev Med Virol* 20:202-213.
196. Schottstedt V, Blumel J, Burger R, Drosten C, Groner A, Gurtler L, Heiden M, Hildebrandt M, Jansen B, Montag-Lessing T, Offergeld R, Pauli G, Seitz R, Schlenkrich U, Strobel J, Willkommen H, von Konig CH (2010) Human Cytomegalovirus (HCMV) - Revised. *Transfus Med Hemother* 37:365-375.
197. Soderberg-Naucler C (2008) HCMV microinfections in inflammatory diseases and cancer. *J Clin Virol* 41:218-223.
198. Li S, Zhu J, Zhang W, Chen Y, Zhang K, Popescu LM, Ma X, Lau WB, Rong R, Yu X, Wang B, Li Y, Xiao C, Zhang M, Wang S, Yu L, Chen AF, Yang X, Cai J (2011) Signature microRNA expression profile of essential hypertension and its novel link to human cytomegalovirus infection. *Circulation* 124:175-184.
199. Zhou YF, Leon MB, Waclawiw MA, Popma JJ, Yu ZX, Finkel T, Epstein SE (1996) Association between prior cytomegalovirus infection and the risk of restenosis after coronary atherectomy. *N Engl J Med* 335:624-630.

200. Castillo JP, Yurochko AD, Kowalik TF (2000) Role of human cytomegalovirus immediate-early proteins in cell growth control. *J Virol* 74:8028-8037.
201. Siew VK, Duh CY, Wang SK (2009) Human cytomegalovirus UL76 induces chromosome aberrations. *J Biomed Sci* 16:107.
202. Slinger E, Maussang D, Schreiber A, Siderius M, Rahbar A, Fraile-Ramos A, Lira SA, Soderberg-Naucler C, Smit MJ (2010) HCMV-encoded chemokine receptor US28 mediates proliferative signaling through the IL-6-STAT3 axis. *Sci Signal* 3:ra58.
203. Kumar A, Tripathy MK, Pasquereau S, Al Moussawi F, Abbas W, Coquard L, Khan KA, Russo L, Algros MP, Valmary-Degano S, Adotevi O, Morot-Bizot S, Herbein G (2018) The Human Cytomegalovirus Strain DB Activates Oncogenic Pathways in Mammary Epithelial Cells. *EBioMedicine* 30:167-183.
204. Cobbs CS, Harkins L, Samanta M, Gillespie GY, Bharara S, King PH, Nabors LB, Cobbs CG, Britt WJ (2002) Human cytomegalovirus infection and expression in human malignant glioma. *Cancer Res* 62:3347-3350.
205. Harkins L, Volk AL, Samanta M, Mikolaenko I, Britt WJ, Bland KI, Cobbs CS (2002) Specific localisation of human cytomegalovirus nucleic acids and proteins in human colorectal cancer. *Lancet* 360:1557-1563.
206. Baryawno N, Rahbar A, Wolmer-Solberg N, Taher C, Odeberg J, Darabi A, Khan Z, Sveinbjornsson B, FuskevAg OM, Segerstrom L, Nordenskjold M, Siesjo P, Kogner P, Johnsen JI, Soderberg-Naucler C (2011) Detection of human cytomegalovirus in medulloblastomas reveals a potential therapeutic target. *J Clin Invest* 121:4043-4055.
207. Wolmer-Solberg N, Baryawno N, Rahbar A, Fuchs D, Odeberg J, Taher C, Wilhelmi V, Milosevic J, Mohammad AA, Martinsson T, Sveinbjornsson B, Johnsen JI, Kogner P, Soderberg-Naucler C (2013) Frequent detection of human cytomegalovirus in neuroblastoma: a novel therapeutic target? *Int J Cancer* 133:2351-2361.
208. Butcher SJ, Aitken J, Mitchell J, Gowen B, Dargan DJ (1998) Structure of the human cytomegalovirus B capsid by electron cryomicroscopy and image reconstruction. *J Struct Biol* 124:70-76.
209. Kalejta RF (2008) Tegument proteins of human cytomegalovirus. *Microbiol Mol Biol Rev* 72:249-265.
210. Varnum SM, Streblow DN, Monroe ME, Smith P, Auberry KJ, Pasa-Tolic L, Wang D, Camp DG, 2nd, Rodland K, Wiley S, Britt W, Shenk T, Smith RD, Nelson JA (2004) Identification of proteins in human cytomegalovirus (HCMV) particles: the HCMV proteome. *J Virol* 78:10960-10966.
211. Britt WJ (1984) Neutralizing antibodies detect a disulfide-linked glycoprotein complex within the envelope of human cytomegalovirus. *Virology* 135:369-378.
212. Cranage MP, Kouzarides T, Bankier AT, Satchwell S, Weston K, Tomlinson P, Barrell B, Hart H, Bell SE, Minson AC, et al. (1986) Identification of the human cytomegalovirus glycoprotein B gene and induction of neutralizing antibodies via its expression in recombinant vaccinia virus. *Embo j* 5:3057-3063.
213. Lehner R, Meyer H, Mach M (1989) Identification and characterization of a human cytomegalovirus gene coding for a membrane protein that is conserved among human herpesviruses. *J Virol* 63:3792-3800.
214. Kari B, Li W, Cooper J, Goertz R, Radeke B (1994) The human cytomegalovirus UL100 gene encodes the gC-II glycoproteins recognized by group 2 monoclonal antibodies. *J Gen Virol* 75 (Pt 11):3081-3086.
215. Cranage MP, Smith GL, Bell SE, Hart H, Brown C, Bankier AT, Tomlinson P, Barrell BG, Minson TC (1988) Identification and expression of a human cytomegalovirus glycoprotein with homology to the Epstein-Barr virus BXLF2 product, varicella-zoster virus gpIII, and herpes simplex virus type 1 glycoprotein H. *J Virol* 62:1416-1422.
216. Kaye JF, Gompels UA, Minson AC (1992) Glycoprotein H of human cytomegalovirus (HCMV) forms a stable complex with the HCMV UL115 gene product. *J Gen Virol* 73 (Pt 10):2693-2698.
217. Huber MT, Compton T (1997) Characterization of a novel third member of the human cytomegalovirus glycoprotein H-glycoprotein L complex. *J Virol* 71:5391-5398.
218. Mach M, Kropff B, Dal Monte P, Britt W (2000) Complex formation by human cytomegalovirus glycoproteins M (gpUL100) and N (gpUL73). *J Virol* 74:11881-11892.
219. Chang CP, Vesole DH, Nelson J, Oldstone MB, Stinski MF (1989) Identification and expression of a human cytomegalovirus early glycoprotein. *J Virol* 63:3330-3337.
220. Spaderna S, Blessing H, Bogner E, Britt W, Mach M (2002) Identification of glycoprotein gpTRL10 as a structural component of human cytomegalovirus. *J Virol* 76:1450-1460.
221. Margulies BJ, Browne H, Gibson W (1996) Identification of the human cytomegalovirus G protein-coupled receptor homologue encoded by UL33 in infected cells and enveloped virus particles. *Virology* 225:111-125.
222. O'Connor CM, Shenk T (2011) Human cytomegalovirus pUS27 G protein-coupled receptor homologue is required for efficient spread by the extracellular route but not for direct cell-to-cell spread. *J Virol* 85:3700-3707.
223. Ryckman BJ, Rainish BL, Chase MC, Borton JA, Nelson JA, Jarvis MA, Johnson DC (2008) Characterization of the human cytomegalovirus gH/gL/UL128-131 complex that mediates entry into epithelial and endothelial cells. *J Virol* 82:60-70.

224. Shikhagaie M, Merce-Maldonado E, Isern E, Muntasell A, Alba MM, Lopez-Botet M, Hengel H, Angulo A (2012) The human cytomegalovirus-specific UL1 gene encodes a late-phase glycoprotein incorporated in the virion envelope. *J Virol* 86:4091-4101.
225. O'Connor CM, Shenk T (2012) Human cytomegalovirus pUL78 G protein-coupled receptor homologue is required for timely cell entry in epithelial cells but not fibroblasts. *J Virol* 86:11425-11433.
226. Calo S, Cortese M, Ciferri C, Bruno L, Gerrein R, Benucci B, Monda G, Gentile M, Kessler T, Uematsu Y, Maione D, Lilja AE, Carfi A, Merola M (2016) The Human Cytomegalovirus UL116 Gene Encodes an Envelope Glycoprotein Forming a Complex with gH Independently from gL. *J Virol* 90:4926-4938.
227. Spaderna S, Kropff B, Kodel Y, Shen S, Coley S, Lu S, Britt W, Mach M (2005) Deletion of gpUL132, a structural component of human cytomegalovirus, results in impaired virus replication in fibroblasts. *J Virol* 79:11837-11847.
228. Dolan A, Cunningham C, Hector RD, Hassan-Walker AF, Lee L, Addison C, Dargan DJ, McGeoch DJ, Gatherer D, Emery VC, Griffiths PD, Sinzger C, McSharry BP, Wilkinson GWG, Davison AJ (2004) Genetic content of wild-type human cytomegalovirus. *J Gen Virol* 85:1301-1312.
229. Chee MS, Bankier AT, Beck S, Bohni R, Brown CM, Cerny R, Horsnell T, Hutchison CA, 3rd, Kouzarides T, Martignetti JA, et al. (1990) Analysis of the protein-coding content of the sequence of human cytomegalovirus strain AD169. *Curr Top Microbiol Immunol* 154:125-169.
230. Murphy E, Rigoutsos I, Shibuya T, Shenk TE (2003) Reevaluation of human cytomegalovirus coding potential. *Proc Natl Acad Sci U S A* 100:13585-13590.
231. Stern-Ginossar N, Weisburd B, Michalski A, Le VT, Hein MY, Huang SX, Ma M, Shen B, Qian SB, Hengel H, Mann M, Ingolia NT, Weissman JS (2012) Decoding human cytomegalovirus. *Science* 338:1088-1093.
232. Gatherer D, Seirafian S, Cunningham C, Holton M, Dargan DJ, Baluchova K, Hector RD, Galbraith J, Herzyk P, Wilkinson GW, Davison AJ (2011) High-resolution human cytomegalovirus transcriptome. *Proc Natl Acad Sci U S A* 108:19755-19760.
233. Erhard F, Halenius A, Zimmermann C, L'Hernault A, Kowalewski DJ, Weekes MP, Stevanovic S, Zimmer R, Dölken L (2018) Improved Ribo-seq enables identification of cryptic translation events. *Nat Methods* 15:363-366.
234. UniProt Consortium (2019) UniProt: a worldwide hub of protein knowledge. *Nucleic Acids Res* 47:D506-d515.
235. Nelson JA, Fleckenstein B, Jahn G, Galloway DA, McDougall JK (1984) Structure of the transforming region of human cytomegalovirus AD169. *J Virol* 49:109-115.
236. Cha TA, Tom E, Kemble GW, Duke GM, Mocarski ES, Spaete RR (1996) Human cytomegalovirus clinical isolates carry at least 19 genes not found in laboratory strains. *J Virol* 70:78-83.
237. Dargan DJ, Douglas E, Cunningham C, Jamieson F, Stanton RJ, Baluchova K, McSharry BP, Tomasec P, Emery VC, Percivalle E, Sarasini A, Gerna G, Wilkinson GW, Davison AJ (2010) Sequential mutations associated with adaptation of human cytomegalovirus to growth in cell culture. *J Gen Virol* 91:1535-1546.
238. Fryer JF, Heath AB, Minor PD (2016) A collaborative study to establish the 1st WHO International Standard for human cytomegalovirus for nucleic acid amplification technology. *Biologicals* 44:242-251.
239. Le VT, Trilling M, Hengel H (2011) The cytomegaloviral protein pUL138 acts as potentiator of tumor necrosis factor (TNF) receptor 1 surface density to enhance ULb'-encoded modulation of TNF-alpha signaling. *J Virol* 85:13260-13270.
240. Sinzger C, Digel M, Jahn G (2008) Cytomegalovirus cell tropism. *Curr Top Microbiol Immunol* 325:63-83.
241. Isaacson MK, Compton T (2009) Human cytomegalovirus glycoprotein B is required for virus entry and cell-to-cell spread but not for virion attachment, assembly, or egress. *J Virol* 83:3891-3903.
242. Bowman JJ, Lacayo JC, Burbelo P, Fischer ER, Cohen JI (2011) Rhesus and human cytomegalovirus glycoprotein L are required for infection and cell-to-cell spread of virus but cannot complement each other. *J Virol* 85:2089-2099.
243. Huber MT, Compton T (1998) The human cytomegalovirus UL74 gene encodes the third component of the glycoprotein H-glycoprotein L-containing envelope complex. *J Virol* 72:8191-8197.
244. Wang D, Shenk T (2005) Human cytomegalovirus virion protein complex required for epithelial and endothelial cell tropism. *Proc Natl Acad Sci U S A* 102:18153-18158.
245. Hahn G, Revello MG, Patrone M, Percivalle E, Campanini G, Sarasini A, Wagner M, Gallina A, Milanesi G, Koszinowski U, Baldanti F, Gerna G (2004) Human cytomegalovirus UL131-128 genes are indispensable for virus growth in endothelial cells and virus transfer to leukocytes. *J Virol* 78:10023-10033.
246. Ryckman BJ, Jarvis MA, Drummond DD, Nelson JA, Johnson DC (2006) Human cytomegalovirus entry into epithelial and endothelial cells depends on genes UL128 to UL150 and occurs by endocytosis and low-pH fusion. *J Virol* 80:710-722.
247. Kari B, Gehrz R (1993) Structure, composition and heparin binding properties of a human cytomegalovirus glycoprotein complex designated gC-II. *J Gen Virol* 74 (Pt 2):255-264.

248. Compton T, Nowlin DM, Cooper NR (1993) Initiation of human cytomegalovirus infection requires initial interaction with cell surface heparan sulfate. *Virology* 193:834-841.
249. Kabanova A, Marcandalli J, Zhou T, Bianchi S, Baxa U, Tsybovsky Y, Lilleri D, Silacci-Fregni C, Foglierini M, Fernandez-Rodriguez BM, Druz A, Zhang B, Geiger R, Pagani M, Sallusto F, Kwong PD, Corti D, Lanzavecchia A, Perez L (2016) Platelet-derived growth factor-alpha receptor is the cellular receptor for human cytomegalovirus gHgLgO trimer. *Nat Microbiol* 1:16082.
250. Wu Y, Prager A, Boos S, Resch M, Brizic I, Mach M, Wildner S, Scrivano L, Adler B (2017) Human cytomegalovirus glycoprotein complex gH/gL/gO uses PDGFR-alpha as a key for entry. *PLoS Pathog* 13:e1006281.
251. Martinez-Martin N, Marcandalli J, Huang CS, Arthur CP, Perotti M, Foglierini M, Ho H, Dosey AM, Shriver S, Payandeh J, Leitner A, Lanzavecchia A, Perez L, Ciferri C (2018) An Unbiased Screen for Human Cytomegalovirus Identifies Neuropilin-2 as a Central Viral Receptor. *Cell* 174:1158-1171.e1119.
252. Cooper RS, Heldwein EE (2015) Herpesvirus gB: A Finely Tuned Fusion Machine. *Viruses* 7:6552-6569.
253. Wang X, Huong SM, Chiu ML, Raab-Traub N, Huang ES (2003) Epidermal growth factor receptor is a cellular receptor for human cytomegalovirus. *Nature* 424:456-461.
254. Soroceanu L, Akhavan A, Cobbs CS (2008) Platelet-derived growth factor-alpha receptor activation is required for human cytomegalovirus infection. *Nature* 455:391-395.
255. Feire AL, Koss H, Compton T (2004) Cellular integrins function as entry receptors for human cytomegalovirus via a highly conserved disintegrin-like domain. *Proc Natl Acad Sci U S A* 101:15470-15475.
256. Feire AL, Roy RM, Manley K, Compton T (2010) The glycoprotein B disintegrin-like domain binds beta 1 integrin to mediate cytomegalovirus entry. *J Virol* 84:10026-10037.
257. Wille PT, Wisner TW, Ryckman B, Johnson DC (2013) Human cytomegalovirus (HCMV) glycoprotein gB promotes virus entry in trans acting as the viral fusion protein rather than as a receptor-binding protein. *mBio* 4:e00332-00313.
258. Nguyen CC, Kamil JP (2018) Pathogen at the Gates: Human Cytomegalovirus Entry and Cell Tropism. *Viruses* 10.
259. Ogawa-Goto K, Tanaka K, Gibson W, Moriishi E, Miura Y, Kurata T, Irie S, Sata T (2003) Microtubule network facilitates nuclear targeting of human cytomegalovirus capsid. *J Virol* 77:8541-8547.
260. Wathen MW, Stinski MF (1982) Temporal patterns of human cytomegalovirus transcription: mapping the viral RNAs synthesized at immediate early, early, and late times after infection. *J Virol* 41:462-477.
261. Arvin A, Campadelli-Fiume G, Mocarski E, Moore P, Roizman B, Whitley R, Yamanishi K (2007) *Human Herpesviruses: Biology, Therapy, and Immunoprophylaxis* (Cambridge University Press, Cambridge).
262. Malone CL, Vesole DH, Stinski MF (1990) Transactivation of a human cytomegalovirus early promoter by gene products from the immediate-early gene IE2 and augmentation by IE1: mutational analysis of the viral proteins. *J Virol* 64:1498-1506.
263. Depto AS, Stenberg RM (1989) Regulated expression of the human cytomegalovirus pp65 gene: octamer sequence in the promoter is required for activation by viral gene products. *J Virol* 63:1232-1238.
264. Weekes MP, Tomasec P, Huttlin EL, Fielding CA, Nusinow D, Stanton RJ, Wang EC, Aicheler R, Murrell I, Wilkinson GW, Lehner PJ, Gygi SP (2014) Quantitative temporal viromics: an approach to investigate host-pathogen interaction. *Cell* 157:1460-1472.
265. Fortunato EA, Spector DH (1998) p53 and RPA are sequestered in viral replication centers in the nuclei of cells infected with human cytomegalovirus. *J Virol* 72:2033-2039.
266. Wills MR, Poole E, Lau B, Krishna B, Sinclair JH (2015) The immunology of human cytomegalovirus latency: could latent infection be cleared by novel immunotherapeutic strategies? *Cell Mol Immunol* 12:128-138.
267. Taylor-Wiedeman J, Sissons JG, Borysiewicz LK, Sinclair JH (1991) Monocytes are a major site of persistence of human cytomegalovirus in peripheral blood mononuclear cells. *J Gen Virol* 72 (Pt 9):2059-2064.
268. Sindre H, Tjoonnfjord GE, Rollag H, Ranneberg-Nilsen T, Veiby OP, Beck S, Degre M, Hestdal K (1996) Human cytomegalovirus suppression of and latency in early hematopoietic progenitor cells. *Blood* 88:4526-4533.
269. Jenkins C, Abendroth A, Slobedman B (2004) A novel viral transcript with homology to human interleukin-10 is expressed during latent human cytomegalovirus infection. *J Virol* 78:1440-1447.
270. Bego M, Maciejewski J, Khaiboullina S, Pari G, St Jeor S (2005) Characterization of an antisense transcript spanning the UL81-82 locus of human cytomegalovirus. *J Virol* 79:11022-11034.
271. Goodrum F, Reeves M, Sinclair J, High K, Shenk T (2007) Human cytomegalovirus sequences expressed in latently infected individuals promote a latent infection in vitro. *Blood* 110:937-945.
272. Humby MS, O'Connor CM (2015) Human Cytomegalovirus US28 Is Important for Latent Infection of Hematopoietic Progenitor Cells. *J Virol* 90:2959-2970.
273. Cheng S, Caviness K, Buehler J, Smithey M, Nikolich-Zugich J, Goodrum F (2017) Transcriptome-wide characterization of human cytomegalovirus in natural infection and experimental latency. *Proc Natl Acad Sci U S A* 114:E10586-e10595.

274. Shnayder M, Nachshon A, Krishna B, Poole E, Boshkov A, Binyamin A, Maza I, Sinclair J, Schwartz M, Stern-Ginossar N (2018) Defining the Transcriptional Landscape during Cytomegalovirus Latency with Single-Cell RNA Sequencing. *mBio* 9.
275. Dupont L, Reeves MB (2016) Cytomegalovirus latency and reactivation: recent insights into an age old problem. *Rev Med Virol* 26:75-89.
276. Mettenleiter TC, Klupp BG, Granzow H (2009) Herpesvirus assembly: an update. *Virus Res* 143:222-234.
277. Compton T, Kurt-Jones EA, Boehme KW, Belko J, Latz E, Golenbock DT, Finberg RW (2003) Human cytomegalovirus activates inflammatory cytokine responses via CD14 and Toll-like receptor 2. *J Virol* 77:4588-4596.
278. Boehme KW, Guerrero M, Compton T (2006) Human cytomegalovirus envelope glycoproteins B and H are necessary for TLR2 activation in permissive cells. *J Immunol* 177:7094-7102.
279. Bukowski JF, Woda BA, Welsh RM (1984) Pathogenesis of murine cytomegalovirus infection in natural killer cell-depleted mice. *J Virol* 52:119-128.
280. Bukowski JF, Warner JF, Dennert G, Welsh RM (1985) Adoptive transfer studies demonstrating the antiviral effect of natural killer cells in vivo. *J Exp Med* 161:40-52.
281. Orange JS (2013) Natural killer cell deficiency. *J Allergy Clin Immunol* 132:515-525.
282. Quinnan GV, Jr., Kirmani N, Rook AH, Manischewitz JF, Jackson L, Moreschi G, Santos GW, Saral R, Burns WH (1982) Cytotoxic t cells in cytomegalovirus infection: HLA-restricted T-lymphocyte and non-T-lymphocyte cytotoxic responses correlate with recovery from cytomegalovirus infection in bone-marrow-transplant recipients. *N Engl J Med* 307:7-13.
283. Macagno A, Bernasconi NL, Vanzetta F, Dander E, Sarasini A, Revello MG, Gerna G, Sallusto F, Lanzavecchia A (2010) Isolation of human monoclonal antibodies that potently neutralize human cytomegalovirus infection by targeting different epitopes on the gH/gL/UL128-131A complex. *J Virol* 84:1005-1013.
284. Ciferri C, Chandramouli S, Leitner A, Donnarumma D, Cianfrocco MA, Gerrein R, Friedrich K, Aggarwal Y, Palladino G, Aebersold R, Norais N, Settembre EC, Carfi A (2015) Antigenic Characterization of the HCMV gH/gL/gO and Pentamer Cell Entry Complexes Reveals Binding Sites for Potently Neutralizing Human Antibodies. *PLoS Pathog* 11:e1005230.
285. Jackson SE, Mason GM, Wills MR (2011) Human cytomegalovirus immunity and immune evasion. *Virus Res* 157:151-160.
286. Reddehase MJ, Mutter W, Munch K, Bühring HJ, Koszinowski UH (1987) CD8-positive T lymphocytes specific for murine cytomegalovirus immediate-early antigens mediate protective immunity. *J Virol* 61:3102-3108.
287. Reddehase MJ, Jonjic S, Weiland F, Mutter W, Koszinowski UH (1988) Adoptive immunotherapy of murine cytomegalovirus adrenalitis in the immunocompromised host: CD4-helper-independent antiviral function of CD8-positive memory T lymphocytes derived from latently infected donors. *J Virol* 62:1061-1065.
288. Cwynarski K, Ainsworth J, Cobbold M, Wagner S, Mahendra P, Apperley J, Goldman J, Craddock C, Moss PA (2001) Direct visualization of cytomegalovirus-specific T-cell reconstitution after allogeneic stem cell transplantation. *Blood* 97:1232-1240.
289. Avetisyan G, Aschan J, Hagglund H, Ringden O, Ljungman P (2007) Evaluation of intervention strategy based on CMV-specific immune responses after allogeneic SCT. *Bone Marrow Transplant* 40:865-869.
290. Barron MA, Gao D, Springer KL, Patterson JA, Brunvand MW, McSweeney PA, Zeng C, Baron AE, Weinberg A (2009) Relationship of reconstituted adaptive and innate cytomegalovirus (CMV)-specific immune responses with CMV viremia in hematopoietic stem cell transplant recipients. *Clin Infect Dis* 49:1777-1783.
291. Riddell SR, Watanabe KS, Goodrich JM, Li CR, Agha ME, Greenberg PD (1992) Restoration of viral immunity in immunodeficient humans by the adoptive transfer of T cell clones. *Science* 257:238-241.
292. Walter EA, Greenberg PD, Gilbert MJ, Finch RJ, Watanabe KS, Thomas ED, Riddell SR (1995) Reconstitution of cellular immunity against cytomegalovirus in recipients of allogeneic bone marrow by transfer of T-cell clones from the donor. *N Engl J Med* 333:1038-1044.
293. Einsele H, Roosnek E, Rufer N, Sinzger C, Riegler S, Löffler J, Grigoleit U, Moris A, Rammensee HG, Kanz L, Kleihauer A, Frank F, Jahn G, Hebart H (2002) Infusion of cytomegalovirus (CMV)-specific T cells for the treatment of CMV infection not responding to antiviral chemotherapy. *Blood* 99:3916-3922.
294. McLaughlin-Taylor E, Pande H, Forman SJ, Tanamachi B, Li CR, Zaia JA, Greenberg PD, Riddell SR (1994) Identification of the major late human cytomegalovirus matrix protein pp65 as a target antigen for CD8+ virus-specific cytotoxic T lymphocytes. *J Med Virol* 43:103-110.
295. Kern F, Surel IP, Faulhaber N, Frommel C, Schneider-Mergener J, Schonemann C, Reinke P, Volk HD (1999) Target structures of the CD8(+)-T-cell response to human cytomegalovirus: the 72-kilodalton major immediate-early protein revisited. *J Virol* 73:8179-8184.

296. Elkington R, Walker S, Crough T, Menzies M, Tellam J, Bharadwaj M, Khanna R (2003) Ex vivo profiling of CD8+-T-cell responses to human cytomegalovirus reveals broad and multispecific reactivities in healthy virus carriers. *J Virol* 77:5226-5240.
297. Slezak SL, Bettinotti M, Selleri S, Adams S, Marincola FM, Stroncek DF (2007) CMV pp65 and IE-1 T cell epitopes recognized by healthy subjects. *J Transl Med* 5:17.
298. Manley TJ, Luy L, Jones T, Boeckh M, Mutimer H, Riddell SR (2004) Immune evasion proteins of human cytomegalovirus do not prevent a diverse CD8+ cytotoxic T-cell response in natural infection. *Blood* 104:1075-1082.
299. Sylwester AW, Mitchell BL, Edgar JB, Taormina C, Pelte C, Ruchti F, Sleath PR, Grabstein KH, Hosken NA, Kern F, Nelson JA, Picker LJ (2005) Broadly targeted human cytomegalovirus-specific CD4+ and CD8+ T cells dominate the memory compartments of exposed subjects. *J Exp Med* 202:673-685.
300. van de Berg PJ, van Stijn A, Ten Berge IJ, van Lier RA (2008) A fingerprint left by cytomegalovirus infection in the human T cell compartment. *J Clin Virol* 41:213-217.
301. Wills MR, Carmichael AJ, Weekes MP, Mynard K, Okecha G, Hicks R, Sissons JG (1999) Human virus-specific CD8+ CTL clones revert from CD45ROhigh to CD45RAhigh in vivo: CD45RAhighCD8+ T cells comprise both naive and memory cells. *J Immunol* 162:7080-7087.
302. Klenerman P (2018) The (gradual) rise of memory inflation. *Immunol Rev* 283:99-112.
303. Khan N, Shariff N, Cobbold M, Bruton R, Ainsworth JA, Sinclair AJ, Nayak L, Moss PA (2002) Cytomegalovirus seropositivity drives the CD8 T cell repertoire toward greater clonality in healthy elderly individuals. *J Immunol* 169:1984-1992.
304. Karrer U, Wagner M, Sierro S, Oxenius A, Hengel H, Dumrese T, Freigang S, Koszinowski UH, Phillips RE, Klenerman P (2004) Expansion of protective CD8+ T-cell responses driven by recombinant cytomegaloviruses. *J Virol* 78:2255-2264.
305. Hutchinson S, Sims S, O'Hara G, Silk J, Gileadi U, Cerundolo V, Klenerman P (2011) A dominant role for the immunoproteasome in CD8+ T cell responses to murine cytomegalovirus. *PLoS One* 6:e14646.
306. Bolinger B, Sims S, O'Hara G, de Lara C, Tchilian E, Firner S, Engeler D, Ludewig B, Klenerman P (2013) A new model for CD8+ T cell memory inflation based upon a recombinant adenoviral vector. *J Immunol* 190:4162-4174.
307. Jackson SE, Sedikides GX, Mason GM, Okecha G, Wills MR (2017) Human Cytomegalovirus (HCMV)-Specific CD4(+) T Cells Are Polyfunctional and Can Respond to HCMV-Infected Dendritic Cells In Vitro. *J Virol* 91.
308. Gamadia LE, Remmerswaal EB, Weel JF, Bemelman F, van Lier RA, Ten Berge IJ (2003) Primary immune responses to human CMV: a critical role for IFN-gamma-producing CD4+ T cells in protection against CMV disease. *Blood* 101:2686-2692.
309. Pourgheysari B, Khan N, Best D, Bruton R, Nayak L, Moss PA (2007) The cytomegalovirus-specific CD4+ T-cell response expands with age and markedly alters the CD4+ T-cell repertoire. *J Virol* 81:7759-7765.
310. Arens R, Wang P, Sidney J, Loewendorf A, Sette A, Schoenberger SP, Peters B, Benedict CA (2008) Cutting edge: murine cytomegalovirus induces a polyfunctional CD4 T cell response. *J Immunol* 180:6472-6476.
311. van Leeuwen EM, Remmerswaal EB, Vossen MT, Rowshani AT, Wertheim-van Dillen PM, van Lier RA, ten Berge IJ (2004) Emergence of a CD4+CD28- granzyme B+, cytomegalovirus-specific T cell subset after recovery of primary cytomegalovirus infection. *J Immunol* 173:1834-1841.
312. Busche A, Jirmo AC, Welten SP, Zischke J, Noack J, Constabel H, Gatzke AK, Keyser KA, Arens R, Behrens GM, Messerle M (2013) Priming of CD8+ T cells against cytomegalovirus-encoded antigens is dominated by cross-presentation. *J Immunol* 190:2767-2777.
313. Terrazzini N, Bajwa M, Vita S, Cheek E, Thomas D, Seddiki N, Smith H, Kern F (2014) A novel cytomegalovirus-induced regulatory-type T-cell subset increases in size during older life and links virus-specific immunity to vascular pathology. *J Infect Dis* 209:1382-1392.
314. Dechanet J, Merville P, Berge F, Bone-Mane G, Taupin JL, Michel P, Joly P, Bonneville M, Potaux L, Moreau JF (1999) Major expansion of gammadelta T lymphocytes following cytomegalovirus infection in kidney allograft recipients. *J Infect Dis* 179:1-8.
315. Khairallah C, Netzer S, Villacreces A, Juzan M, Rousseau B, Dulanto S, Giese A, Costet P, Praloran V, Moreau JF, Dubus P, Vermijlen D, Dechanet-Merville J, Capone M (2015) gammadelta T cells confer protection against murine cytomegalovirus (MCMV). *PLoS Pathog* 11:e1004702.
316. Dunn W, Chou C, Li H, Hai R, Patterson D, Stolc V, Zhu H, Liu F (2003) Functional profiling of a human cytomegalovirus genome. *Proc Natl Acad Sci U S A* 100:14223-14228.
317. Berry R, Watson GM, Jonjic S, Degli-Esposti MA, Rossjohn J (2020) Modulation of innate and adaptive immunity by cytomegaloviruses. *Nat Rev Immunol* 20:113-127.
318. Wiertz EJ, Jones TR, Sun L, Bogyo M, Geuze HJ, Ploegh HL (1996) The human cytomegalovirus US11 gene product dislocates MHC class I heavy chains from the endoplasmic reticulum to the cytosol. *Cell* 84:769-779.

319. Wiertz EJ, Tortorella D, Bogyo M, Yu J, Mothes W, Jones TR, Rapoport TA, Ploegh HL (1996) Sec61-mediated transfer of a membrane protein from the endoplasmic reticulum to the proteasome for destruction. *Nature* 384:432-438.
320. Jones TR, Sun L (1997) Human cytomegalovirus US2 destabilizes major histocompatibility complex class I heavy chains. *J Virol* 71:2970-2979.
321. Jones TR, Wiertz EJ, Sun L, Fish KN, Nelson JA, Ploegh HL (1996) Human cytomegalovirus US3 impairs transport and maturation of major histocompatibility complex class I heavy chains. *Proc Natl Acad Sci U S A* 93:11327-11333.
322. Park B, Kim Y, Shin J, Lee S, Cho K, Fruh K, Lee S, Ahn K (2004) Human cytomegalovirus inhibits tapasin-dependent peptide loading and optimization of the MHC class I peptide cargo for immune evasion. *Immunity* 20:71-85.
323. Ahn K, Gruhler A, Galocha B, Jones TR, Wiertz EJ, Ploegh HL, Peterson PA, Yang Y, Fruh K (1997) The ER-luminal domain of the HCMV glycoprotein US6 inhibits peptide translocation by TAP. *Immunity* 6:613-621.
324. Lehner PJ, Karttunen JT, Wilkinson GW, Cresswell P (1997) The human cytomegalovirus US6 glycoprotein inhibits transporter associated with antigen processing-dependent peptide translocation. *Proc Natl Acad Sci U S A* 94:6904-6909.
325. Hewitt EW, Gupta SS, Lehner PJ (2001) The human cytomegalovirus gene product US6 inhibits ATP binding by TAP. *Embo j* 20:387-396.
326. Furman MH, Dey N, Tortorella D, Ploegh HL (2002) The human cytomegalovirus US10 gene product delays trafficking of major histocompatibility complex class I molecules. *J Virol* 76:11753-11756.
327. Park B, Spooner E, Houser BL, Strominger JL, Ploegh HL (2010) The HCMV membrane glycoprotein US10 selectively targets HLA-G for degradation. *J Exp Med* 207:2033-2041.
328. Karre K, Ljunggren HG, Piontek G, Kiessling R (1986) Selective rejection of H-2-deficient lymphoma variants suggests alternative immune defence strategy. *Nature* 319:675-678.
329. Storkus WJ, Alexander J, Payne JA, Dawson JR, Cresswell P (1989) Reversal of natural killing susceptibility in target cells expressing transfected class I HLA genes. *Proc Natl Acad Sci U S A* 86:2361-2364.
330. Beck S, Barrell BG (1988) Human cytomegalovirus encodes a glycoprotein homologous to MHC class-I antigens. *Nature* 331:269-272.
331. Chapman TL, Heikeman AP, Bjorkman PJ (1999) The inhibitory receptor LIR-1 uses a common binding interaction to recognize class I MHC molecules and the viral homolog UL18. *Immunity* 11:603-613.
332. Braud V, Jones EY, McMichael A (1997) The human major histocompatibility complex class Ib molecule HLA-E binds signal sequence-derived peptides with primary anchor residues at positions 2 and 9. *Eur J Immunol* 27:1164-1169.
333. Braud VM, Allan DS, O'Callaghan CA, Soderstrom K, D'Andrea A, Ogg GS, Lazetic S, Young NT, Bell JI, Phillips JH, Lanier LL, McMichael AJ (1998) HLA-E binds to natural killer cell receptors CD94/NKG2A, B and C. *Nature* 391:795-799.
334. Tomasec P, Braud VM, Rickards C, Powell MB, McSharry BP, Gadola S, Cerundolo V, Borysiewicz LK, McMichael AJ, Wilkinson GW (2000) Surface expression of HLA-E, an inhibitor of natural killer cells, enhanced by human cytomegalovirus gpUL40. *Science* 287:1031.
335. Ulbrecht M, Martinozzi S, Grzeschik M, Hengel H, Ellwart JW, Pla M, Weiss EH (2000) Cutting edge: the human cytomegalovirus UL40 gene product contains a ligand for HLA-E and prevents NK cell-mediated lysis. *J Immunol* 164:5019-5022.
336. Furukawa T, Hornberger E, Sakuma S, Plotkin SA (1975) Demonstration of immunoglobulin G receptors induced by human cytomegalovirus. *J Clin Microbiol* 2:332-336.
337. Kotenko SV, Saccani S, Izotova LS, Mirochnitchenko OV, Pestka S (2000) Human cytomegalovirus harbors its own unique IL-10 homolog (cmvIL-10). *Proc Natl Acad Sci U S A* 97:1695-1700.
338. Chang WL, Baumgarth N, Yu D, Barry PA (2004) Human cytomegalovirus-encoded interleukin-10 homolog inhibits maturation of dendritic cells and alters their functionality. *J Virol* 78:8720-8731.
339. Avdic S, McSharry BP, Steain M, Poole E, Sinclair J, Abendroth A, Slobedman B (2016) Human Cytomegalovirus-Encoded Human Interleukin-10 (IL-10) Homolog Amplifies Its Immunomodulatory Potential by Upregulating Human IL-10 in Monocytes. *J Virol* 90:3819-3827.
340. Spencer JV, Lockridge KM, Barry PA, Lin G, Tsang M, Penfold ME, Schall TJ (2002) Potent immunosuppressive activities of cytomegalovirus-encoded interleukin-10. *J Virol* 76:1285-1292.
341. Jenkins C, Garcia W, Godwin MJ, Spencer JV, Stern JL, Abendroth A, Slobedman B (2008) Immunomodulatory properties of a viral homolog of human interleukin-10 expressed by human cytomegalovirus during the latent phase of infection. *J Virol* 82:3736-3750.

342. Tomazin R, Boname J, Hegde NR, Lewinsohn DM, Altschuler Y, Jones TR, Cresswell P, Nelson JA, Riddell SR, Johnson DC (1999) Cytomegalovirus US2 destroys two components of the MHC class II pathway, preventing recognition by CD4+ T cells. *Nat Med* 5:1039-1043.
343. Hegde NR, Tomazin RA, Wisner TW, Dunn C, Boname JM, Lewinsohn DM, Johnson DC (2002) Inhibition of HLA-DR assembly, transport, and loading by human cytomegalovirus glycoprotein US3: a novel mechanism for evading major histocompatibility complex class II antigen presentation. *J Virol* 76:10929-10941.
344. Britt WJ, Prichard MN (2018) New therapies for human cytomegalovirus infections. *Antiviral Res* 159:153-174.
345. Jung D, Dorr A (1999) Single-dose pharmacokinetics of valganciclovir in HIV- and CMV-seropositive subjects. *J Clin Pharmacol* 39:800-804.
346. Lischka P, Zimmermann H (2008) Antiviral strategies to combat cytomegalovirus infections in transplant recipients. *Curr Opin Pharmacol* 8:541-548.
347. Lurain NS, Chou S (2010) Antiviral drug resistance of human cytomegalovirus. *Clin Microbiol Rev* 23:689-712.
348. Goldner T, Hewlett G, Ettischer N, Ruebsamen-Schaeff H, Zimmermann H, Lischka P (2011) The novel anticytomegalovirus compound AIC246 (Letermovir) inhibits human cytomegalovirus replication through a specific antiviral mechanism that involves the viral terminase. *J Virol* 85:10884-10893.
349. Chen SJ, Wang SC, Chen YC (2019) Antiviral Agents as Therapeutic Strategies Against Cytomegalovirus Infections. *Viruses* 12.
350. Acosta E, Bowlin T, Brooks J, Chiang L, Hussein I, Kimberlin D, Kauvar LM, Leavitt R, Prichard M, Whitley R (2020) Advances in the Development of Therapeutics for Cytomegalovirus Infections. *J Infect Dis* 221:S32-s44.
351. Nigro G, La Torre R, Anceschi MM, Mazzocco M, Cosmi EV (1999) Hyperimmunoglobulin therapy for a twin fetus with cytomegalovirus infection and growth restriction. *Am J Obstet Gynecol* 180:1222-1226.
352. Ishida JH, Patel A, Mehta AK, Gatault P, McBride JM, Burgess T, Derby MA, Snydman DR, Emu B, Feierbach B, Fouts AE, Maia M, Deng R, Rosenberger CM, Gennaro LA, Striano NS, Liao XC, Tavel JA (2017) Phase 2 Randomized, Double-Blind, Placebo-Controlled Trial of RG7667, a Combination Monoclonal Antibody, for Prevention of Cytomegalovirus Infection in High-Risk Kidney Transplant Recipients. *Antimicrob Agents Chemother* 61.
353. Goldstein G, Rutenberg TF, Mendelovich SL, Hutt D, Oikawa MT, Toren A, Bielorai B (2017) The role of immunoglobulin prophylaxis for prevention of cytomegalovirus infection in pediatric hematopoietic stem cell transplantation recipients. *Pediatr Blood Cancer* 64.
354. Kagan KO, Enders M, Schampera MS, Baeumel E, Hoopmann M, Geipel A, Berg C, Goelz R, De Catte L, Wallwiener D, Brucker S, Adler SP, Jahn G, Hamprecht K (2019) Prevention of maternal-fetal transmission of cytomegalovirus after primary maternal infection in the first trimester by biweekly hyperimmunoglobulin administration. *Ultrasound Obstet Gynecol* 53:383-389.
355. Starr SE, Allison AC (1977) Role of T lymphocytes in recovery from murine cytomegalovirus infection. *Infect Immun* 17:458-462.
356. Ho M (1980) Role of specific cytotoxic lymphocytes in cellular immunity against murine cytomegalovirus. *Infect Immun* 27:767-776.
357. Reddehase MJ, Weiland F, Munch K, Jonjic S, Luske A, Koszinowski UH (1985) Interstitial murine cytomegalovirus pneumonia after irradiation: characterization of cells that limit viral replication during established infection of the lungs. *J Virol* 55:264-273.
358. Park KD, Marti L, Kurtzberg J, Szabolcs P (2006) In vitro priming and expansion of cytomegalovirus-specific Th1 and Tc1 T cells from naive cord blood lymphocytes. *Blood* 108:1770-1773.
359. Feuchtinger T, Opherk K, Bethge WA, Topp MS, Schuster FR, Weissinger EM, Mohty M, Or R, Maschan M, Schumm M, Hamprecht K, Handgretinger R, Lang P, Einsele H (2010) Adoptive transfer of pp65-specific T cells for the treatment of chemorefractory cytomegalovirus disease or reactivation after haploidentical and matched unrelated stem cell transplantation. *Blood* 116:4360-4367.
360. Koehne G, Hasan A, Doubrovina E, Prockop S, Tyler E, Wasilewski G, O'Reilly RJ (2015) Immunotherapy with Donor T Cells Sensitized with Overlapping Pentadecapeptides for Treatment of Persistent Cytomegalovirus Infection or Viremia. *Biol Blood Marrow Transplant* 21:1663-1678.
361. Micklethwaite K, Hansen A, Foster A, Snape E, Antonenas V, Sartor M, Shaw P, Bradstock K, Gottlieb D (2007) Ex vivo expansion and prophylactic infusion of CMV-pp65 peptide-specific cytotoxic T-lymphocytes following allogeneic hematopoietic stem cell transplantation. *Biol Blood Marrow Transplant* 13:707-714.
362. Micklethwaite KP, Clancy L, Sandher U, Hansen AM, Blyth E, Antonenas V, Sartor MM, Bradstock KF, Gottlieb DJ (2008) Prophylactic infusion of cytomegalovirus-specific cytotoxic T lymphocytes stimulated with Ad5f35pp65 gene-modified dendritic cells after allogeneic hemopoietic stem cell transplantation. *Blood* 112:3974-3981.
363. Cobbold M, Khan N, Pourgheysari B, Tauro S, McDonald D, Osman H, Assenmacher M, Billingham L, Steward C, Crawley C, Olavarria E, Goldman J, Chakraverty R, Mahendra P, Craddock C, Moss PA (2005) Adoptive transfer of

cytomegalovirus-specific CTL to stem cell transplant patients after selection by HLA-peptide tetramers. *J Exp Med* 202:379-386.

364. Peggs KS, Thomson K, Samuel E, Dyer G, Armoogum J, Chakraverty R, Pang K, Mackinnon S, Lowdell MW (2011) Directly selected cytomegalovirus-reactive donor T cells confer rapid and safe systemic reconstitution of virus-specific immunity following stem cell transplantation. *Clin Infect Dis* 52:49-57.
365. Eiz-Vesper B, Maecker-Kolhoff B, Blasczyk R (2012) Adoptive T-cell immunotherapy from third-party donors: characterization of donors and set up of a T-cell donor registry. *Front Immunol* 3:410.
366. Leen AM, Bollard CM, Mendizabal AM, Shpall EJ, Szabolcs P, Antin JH, Kapoor N, Pai SY, Rowley SD, Kebriaei P, Dey BR, Grilley BJ, Gee AP, Brenner MK, Rooney CM, Heslop HE (2013) Multicenter study of banked third-party virus-specific T cells to treat severe viral infections after hematopoietic stem cell transplantation. *Blood* 121:5113-5123.
367. Tzannou I, Papadopoulou A, Naik S, Leung K, Martinez CA, Ramos CA, Carrum G, Sasa G, Lulla P, Watanabe A, Kuvalekar M, Gee AP, Wu MF, Liu H, Grilley BJ, Krance RA, Gottschalk S, Brenner MK, Rooney CM, Heslop HE, Leen AM, Omer B (2017) Off-the-Shelf Virus-Specific T Cells to Treat BK Virus, Human Herpesvirus 6, Cytomegalovirus, Epstein-Barr Virus, and Adenovirus Infections After Allogeneic Hematopoietic Stem-Cell Transplantation. *J Clin Oncol* 35:3547-3557.
368. Plotkin SA, Boppana SB (2019) Vaccination against the human cytomegalovirus. *Vaccine* 37:7437-7442.
369. Elek SD, Stern H (1974) Development of a vaccine against mental retardation caused by cytomegalovirus infection in utero. *Lancet* 1:1-5.
370. Plotkin SA, Furukawa T, Zygraich N, Huygelen C (1975) Candidate cytomegalovirus strain for human vaccination. *Infect Immun* 12:521-527.
371. Glazer JP, Friedman HM, Grossman RA, Starr SE, Barker CF, Perloff LJ, Huang ES, Plotkin SA (1979) Live cytomegalovirus vaccination of renal transplant candidates. A preliminary trial. *Ann Intern Med* 91:676-683.
372. Fleisher GR, Starr SE, Friedman HM, Plotkin SA (1982) Vaccination of pediatric nurses with live attenuated cytomegalovirus. *Am J Dis Child* 136:294-296.
373. Plotkin SA, Higgins R, Kurtz JB, Morris PJ, Campbell DA, Jr., Shope TC, Spector SA, Dankner WM (1994) Multicenter trial of Towne strain attenuated virus vaccine in seronegative renal transplant recipients. *Transplantation* 58:1176-1178.
374. Adler SP, Starr SE, Plotkin SA, Hempfling SH, Buis J, Manning ML, Best AM (1995) Immunity induced by primary human cytomegalovirus infection protects against secondary infection among women of childbearing age. *J Infect Dis* 171:26-32.
375. Plotkin SA, Starr SE, Friedman HM, Gonczol E, Weibel RE (1989) Protective effects of Towne cytomegalovirus vaccine against low-passage cytomegalovirus administered as a challenge. *J Infect Dis* 159:860-865.
376. Pass RF, Zhang C, Evans A, Simpson T, Andrews W, Huang ML, Corey L, Hill J, Davis E, Flanigan C, Cloud G (2009) Vaccine prevention of maternal cytomegalovirus infection. *N Engl J Med* 360:1191-1199.
377. Bernstein DI, Munoz FM, Callahan ST, Rupp R, Wootton SH, Edwards KM, Turley CB, Stanberry LR, Patel SM, McNeal MM, Pichon S, Amegashie C, Bellamy AR (2016) Safety and efficacy of a cytomegalovirus glycoprotein B (gB) vaccine in adolescent girls: A randomized clinical trial. *Vaccine* 34:313-319.
378. Diamond DJ, York J, Sun JY, Wright CL, Forman SJ (1997) Development of a candidate HLA A*0201 restricted peptide-based vaccine against human cytomegalovirus infection. *Blood* 90:1751-1767.
379. La Rosa C, Longmate J, Lacey SF, Kaltcheva T, Sharan R, Marsano D, Kwon P, Drake J, Williams B, Denison S, Broyer S, Couture L, Nakamura R, Dadwal S, Kelsey MI, Krieg AM, Diamond DJ, Zaia JA (2012) Clinical evaluation of safety and immunogenicity of PADRE-cytomegalovirus (CMV) and tetanus-CMV fusion peptide vaccines with or without PF03512676 adjuvant. *J Infect Dis* 205:1294-1304.
380. Nakamura R, La Rosa C, Longmate J, Drake J, Slape C, Zhou Q, Lampa MG, O'Donnell M, Cai JL, Farol L, Salhotra A, Snyder DS, Aldoss I, Forman SJ, Miller JS, Zaia JA, Diamond DJ (2016) Viraemia, immunogenicity, and survival outcomes of cytomegalovirus chimeric epitope vaccine supplemented with PF03512676 (CMVPepVax) in allogeneic haemopoietic stem-cell transplantation: randomised phase 1b trial. *Lancet Haematol* 3:e87-98.
381. Schmitt M, Schmitt A, Wiesneth M, Huckelhoven A, Wu Z, Kuball J, Wang L, Schauwecker P, Hofmann S, Gotz M, Michels B, Maccari B, Wuchter P, Eckstein V, Mertens T, Schnitzler P, Dohner H, Ho AD, Bunjes DW, Dreger P, Schrezenmeier H, Greiner J (2017) Peptide vaccination in the presence of adjuvants in patients after hematopoietic stem cell transplantation with CD4+ T cell reconstitution elicits consistent CD8+ T cell responses. *Theranostics* 7:1705-1718.
382. Wagner M, Gutermann A, Podlech J, Reddehase MJ, Koszinowski UH (2002) Major histocompatibility complex class I allele-specific cooperative and competitive interactions between immune evasion proteins of cytomegalovirus. *J Exp Med* 196:805-816.

383. Atalay R, Zimmermann A, Wagner M, Borst E, Benz C, Messerle M, Hengel H (2002) Identification and expression of human cytomegalovirus transcription units coding for two distinct Fcgamma receptor homologs. *J Virol* 76:8596-8608.
384. Bradford MM (1976) A rapid and sensitive method for the quantitation of microgram quantities of protein utilizing the principle of protein-dye binding. *Anal Biochem* 72:248-254.
385. Corr M, Slanetz AE, Boyd LF, Jelonek MT, Khilko S, al-Ramadi BK, Kim YS, Maher SE, Bothwell AL, Margulies DH (1994) T cell receptor-MHC class I peptide interactions: affinity, kinetics, and specificity. *Science* 265:946-949.
386. Liu WC, Slusarchyk DS, Astle G, Trejo WH, Brown WE, Meyers E (1978) Ionomycin, a new polyether antibiotic. *J Antibiot (Tokyo)* 31:815-819.
387. Castagna M, Takai Y, Kaibuchi K, Sano K, Kikkawa U, Nishizuka Y (1982) Direct activation of calcium-activated, phospholipid-dependent protein kinase by tumor-promoting phorbol esters. *J Biol Chem* 257:7847-7851.
388. Kowalewski DJ, Stevanovic S (2013) Biochemical large-scale identification of MHC class I ligands. *Methods Mol Biol* 960:145-157.
389. Nelde A, Kowalewski DJ, Stevanovic S (2019) Purification and Identification of Naturally Presented MHC Class I and II Ligands. *Methods Mol Biol* 1988:123-136.
390. Eng JK, McCormack AL, Yates JR (1994) An approach to correlate tandem mass spectral data of peptides with amino acid sequences in a protein database. *J Am Soc Mass Spectrom* 5:976-989.
391. Kall L, Canterbury JD, Weston J, Noble WS, MacCoss MJ (2007) Semi-supervised learning for peptide identification from shotgun proteomics datasets. *Nat Methods* 4:923-925.
392. Nielsen M, Andreatta M (2016) NetMHCpan-3.0; improved prediction of binding to MHC class I molecules integrating information from multiple receptor and peptide length datasets. *Genome Med* 8:33.
393. Schubert B, Walzer M, Brachvogel HP, Szolek A, Mohr C, Kohlbacher O (2016) FRED 2: an immunoinformatics framework for Python. *Bioinformatics* 32:2044-2046.
394. Lübke M, Spalt S, Kowalewski DJ, Zimmermann C, Bauersfeld L, Nelde A, Bichmann L, Marcu A, Peper JK, Kohlbacher O, Walz JS, Le-Trilling VTK, Hengel H, Rammensee HG, Stevanovic S, Halenius A (2020) Identification of HCMV-derived T cell epitopes in seropositive individuals through viral deletion models. *J Exp Med* 217.
395. Kim S, Lee S, Shin J, Kim Y, Evnouchidou I, Kim D, Kim YK, Kim YE, Ahn JH, Riddell SR, Stratikos E, Kim VN, Ahn K (2011) Human cytomegalovirus microRNA miR-US4-1 inhibits CD8(+) T cell responses by targeting the aminopeptidase ERAP1. *Nat Immunol* 12:984-991.
396. Braendstrup P, Mortensen BK, Justesen S, Osterby T, Rasmussen M, Hansen AM, Christiansen CB, Hansen MB, Nielsen M, Vindelov L, Buus S, Stryhn A (2014) Identification and HLA-tetramer-validation of human CD4+ and CD8+ T cell responses against HCMV proteins IE1 and IE2. *PLoS One* 9:e94892.
397. Andreatta M, Nielsen M (2016) Gapped sequence alignment using artificial neural networks: application to the MHC class I system. *Bioinformatics* 32:511-517.
398. Jurtz V, Paul S, Andreatta M, Marcatili P, Peters B, Nielsen M (2017) NetMHCpan-4.0: Improved Peptide-MHC Class I Interaction Predictions Integrating Eluted Ligand and Peptide Binding Affinity Data. *J Immunol* 199:3360-3368.
399. Snary D, Barnstable CJ, Bodmer WF, Crumpton MJ (1977) Molecular structure of human histocompatibility antigens: the HLA-C series. *Eur J Immunol* 7:580-585.
400. McCutcheon JA, Gumperz J, Smith KD, Lutz CT, Parham P (1995) Low HLA-C expression at cell surfaces correlates with increased turnover of heavy chain mRNA. *J Exp Med* 181:2085-2095.
401. Schultze-Florey RE, Tischer S, Kuhlmann L, Hundsdoerfer P, Koch A, Anagnostopoulos I, Ravens S, Goudeva L, Schultze-Florey C, Koenecke C, Blasczyk R, Koehl U, Heuft HG, Prinz I, Eiz-Vesper B, Maecker-Kolhoff B (2018) Dissecting Epstein-Barr Virus-Specific T-Cell Responses After Allogeneic EBV-Specific T-Cell Transfer for Central Nervous System Posttransplant Lymphoproliferative Disease. *Front Immunol* 9:1475.
402. Steven NM, Annels NE, Kumar A, Leese AM, Kurilla MG, Rickinson AB (1997) Immediate early and early lytic cycle proteins are frequent targets of the Epstein-Barr virus-induced cytotoxic T cell response. *J Exp Med* 185:1605-1617.
403. Hill AB, Lee SP, Haurum JS, Murray N, Yao QY, Rowe M, Signoret N, Rickinson AB, McMichael AJ (1995) Class I major histocompatibility complex-restricted cytotoxic T lymphocytes specific for Epstein-Barr virus (EBV)-transformed B lymphoblastoid cell lines against which they were raised. *J Exp Med* 181:2221-2228.
404. Gavioli R, Kurilla MG, de Campos-Lima PO, Wallace LE, Dolcetti R, Murray RJ, Rickinson AB, Masucci MG (1993) Multiple HLA A11-restricted cytotoxic T-lymphocyte epitopes of different immunogenicities in the Epstein-Barr virus-encoded nuclear antigen 4. *J Virol* 67:1572-1578.
405. Hill A, Worth A, Elliott T, Rowland-Jones S, Brooks J, Rickinson A, McMichael A (1995) Characterization of two Epstein-Barr virus epitopes restricted by HLA-B7. *Eur J Immunol* 25:18-24.

406. Bogedain C, Wolf H, Modrow S, Stuber G, Jilg W (1995) Specific cytotoxic T lymphocytes recognize the immediate-early transactivator Zta of Epstein-Barr virus. *J Virol* 69:4872-4879.
407. Woodberry T, Suscovich TJ, Henry LM, Davis JK, Frahm N, Walker BD, Scadden DT, Wang F, Brander C (2005) Differential targeting and shifts in the immunodominance of Epstein-Barr virus--specific CD8 and CD4 T cell responses during acute and persistent infection. *J Infect Dis* 192:1513-1524.
408. Trolle T, McMurtrey CP, Sidney J, Bardet W, Osborn SC, Kaever T, Sette A, Hildebrand WH, Nielsen M, Peters B (2016) The Length Distribution of Class I-Restricted T Cell Epitopes Is Determined by Both Peptide Supply and MHC Allele-Specific Binding Preference. *J Immunol* 196:1480-1487.
409. Gfeller D, Guillaume P, Michaux J, Pak HS, Daniel RT, Racle J, Coukos G, Bassani-Sternberg M (2018) The Length Distribution and Multiple Specificity of Naturally Presented HLA-I Ligands. *J Immunol* 201:3705-3716.
410. Hislop AD, Annels NE, Gudgeon NH, Leese AM, Rickinson AB (2002) Epitope-specific evolution of human CD8(+) T cell responses from primary to persistent phases of Epstein-Barr virus infection. *J Exp Med* 195:893-905.
411. Abbott RJ, Quinn LL, Leese AM, Scholes HM, Pachnio A, Rickinson AB (2013) CD8+ T cell responses to lytic EBV infection: late antigen specificities as subdominant components of the total response. *J Immunol* 191:5398-5409.
412. Pudney VA, Leese AM, Rickinson AB, Hislop AD (2005) CD8+ immunodominance among Epstein-Barr virus lytic cycle antigens directly reflects the efficiency of antigen presentation in lytically infected cells. *J Exp Med* 201:349-360.
413. Blake N, Haigh T, Shaka'a G, Croom-Carter D, Rickinson A (2000) The importance of exogenous antigen in priming the human CD8+ T cell response: lessons from the EBV nuclear antigen EBNA1. *J Immunol* 165:7078-7087.
414. Hislop AD, Taylor GS, Sauce D, Rickinson AB (2007) Cellular responses to viral infection in humans: lessons from Epstein-Barr virus. *Annu Rev Immunol* 25:587-617.
415. Kaye KM, Izumi KM, Kieff E (1993) Epstein-Barr virus latent membrane protein 1 is essential for B-lymphocyte growth transformation. *Proc Natl Acad Sci U S A* 90:9150-9154.
416. Rist MJ, Neller MA, Burrows JM, Burrows SR (2015) T cell epitope clustering in the highly immunogenic BZLF1 antigen of Epstein-Barr virus. *J Virol* 89:703-712.
417. Huisman W, van der Maarel LE, Hageman L, de Jong RCM, Amsen D, Falkenburg JHF, Jedema I (2018) Isolation and Validation of the First Functional HLA-a*01:01 Restricted EBV-LMP2 Specific T Cells for Treatment of EBV Associated Type II/III Lymphomas. *Blood* 132:1578-1578.
418. Gabriel E (2019) Charakterisierung HLA-A*01- sowie HLA-A*26-restringierter EBV-Epitope - Implikationen für den Supertyp. Dissertation (Eberhard Karls University, Tübingen).
419. Vescovini R, Biasini C, Fagnoni FF, Telera AR, Zanlari L, Pedrazzoni M, Bucci L, Monti D, Medici MC, Chezzi C, Franceschi C, Sansoni P (2007) Massive load of functional effector CD4+ and CD8+ T cells against cytomegalovirus in very old subjects. *J Immunol* 179:4283-4291.
420. Yewdell JW, Anton LC, Bennink JR (1996) Defective ribosomal products (DRiPs): a major source of antigenic peptides for MHC class I molecules? *J Immunol* 157:1823-1826.
421. Rock KL, Farfan-Arribas DJ, Colbert JD, Goldberg AL (2014) Re-examining class-I presentation and the DRiP hypothesis. *Trends Immunol* 35:144-152.
422. Longmate J, York J, La Rosa C, Krishnan R, Zhang M, Senitzer D, Diamond DJ (2001) Population coverage by HLA class-I restricted cytotoxic T-lymphocyte epitopes. *Immunogenetics* 52:165-173.
423. Ameres S, Mautner J, Schlott F, Neuenhahn M, Busch DH, Plachter B, Moosmann A (2013) Presentation of an immunodominant immediate-early CD8+ T cell epitope resists human cytomegalovirus immunoevasion. *PLoS Pathog* 9:e1003383.
424. Hengel H, Lucin P, Jonjic S, Ruppert T, Koszinowski UH (1994) Restoration of cytomegalovirus antigen presentation by gamma interferon combats viral escape. *J Virol* 68:289-297.
425. Zimmermann C, Kowalewski D, Bauersfeld L, Hildenbrand A, Gerke C, Schwarzmüller M, Le-Trilling VTK, Stevanovic S, Hengel H, Momburg F, Halenius A (2019) HLA-B locus products resist degradation by the human cytomegalovirus immunoevasin US11. *PLoS Pathog* 15:e1008040.
426. Hengel H, Reusch U, Geginat G, Holtappels R, Ruppert T, Hellebrand E, Koszinowski UH (2000) Macrophages escape inhibition of major histocompatibility complex class I-dependent antigen presentation by cytomegalovirus. *J Virol* 74:7861-7868.
427. Frascaroli G, Lecher C, Varani S, Setz C, van der Merwe J, Brune W, Mertens T (2018) Human Macrophages Escape Inhibition of Major Histocompatibility Complex-Dependent Antigen Presentation by Cytomegalovirus and Drive Proliferation and Activation of Memory CD4(+) and CD8(+) T Cells. *Front Immunol* 9:1129.
428. Rolland M, Nickle DC, Deng W, Frahm N, Brander C, Learn GH, Heckerman D, Jojic N, Jojic V, Walker BD, Mullins JI (2007) Recognition of HIV-1 peptides by host CTL is related to HIV-1 similarity to human proteins. *PLoS One* 2:e823.

429. Wolfl M, Rutebemberwa A, Mosbruger T, Mao Q, Li HM, Netski D, Ray SC, Pardoll D, Sidney J, Sette A, Allen T, Kuntzen T, Kavanagh DG, Kuball J, Greenberg PD, Cox AL (2008) Hepatitis C virus immune escape via exploitation of a hole in the T cell repertoire. *J Immunol* 181:6435-6446.
430. Calis JJ, de Boer RJ, Kesmir C (2012) Degenerate T-cell recognition of peptides on MHC molecules creates large holes in the T-cell repertoire. *PLoS Comput Biol* 8:e1002412.
431. Holst PJ, Jensen BA, Ragonnaud E, Thomsen AR, Christensen JP (2015) Targeting of non-dominant antigens as a vaccine strategy to broaden T-cell responses during chronic viral infection. *PLoS One* 10:e0117242.
432. Steffensen MA, Pedersen LH, Jahn ML, Nielsen KN, Christensen JP, Thomsen AR (2016) Vaccine Targeting of Subdominant CD8+ T Cell Epitopes Increases the Breadth of the T Cell Response upon Viral Challenge, but May Impair Immediate Virus Control. *J Immunol* 196:2666-2676.
433. Panagioti E, Klenerman P, Lee LN, van der Burg SH, Arens R (2018) Features of Effective T Cell-Inducing Vaccines against Chronic Viral Infections. *Front Immunol* 9:276.

8 Appendix

Supplemental Table 1: HLA-A*01:01 epitope prediction from the EBV proteome for 9mers.

UniProt ID	Antigen	Position	Sequence	SYFPEITHI score	NetMHC 3.4 score	Immunogenicity testing	Internal No.
P03225	BDLF2	402-410	LTDRSFPAY	85.0	7	yes	151025
P03188	GB	131-139	ETDQMDTIY	80.0	7	yes	140542
P03208	BILF1	258-266	CTESLVARY	80.0	8	yes	151186
P03186	LTP	2723-2731	ASEQGPIVY	77.5	23	yes	151068
P03196	GN	43-51	LTEAQDQFY	77.5	8	yes	151074
P03233	UL25	548-556	ASDDYDRLY	77.5	10	yes	150081
P03182	EAR	42-50	PEDTVVLRY	75.0	1755	yes	164211
P03190	RIR1	149-157	ESDMEVFDY	75.0	8	yes	151054
P03213	PORTL	220-228	RSDEYVAYY	75.0	7	yes	151087
P03233	UL25	375-383	ALEALMLVY	75.0	32	yes	150073
P13288	KR2	295-303	RLDLQSLGY	75.0	18	yes	151016
P30117	BKRF4	47-55	VSDTDESDY	75.0	12	yes	151092
P03186	LTP	1062-1070	EWDYRELLY	72.5	3647	yes	154015
P03190	RIR1	604-612	CSDAFYPFY	72.5	6	yes	151055
P12978	EBNA2	112-120	PLDRDPLGY	72.5	25	yes	151023
P25939	TRM1	746-754	PPDGLYLTY	72.5	6421	yes	151242
P25939	TRM1	771-779	FKDLYALLY	72.5	32	yes	154197
P30117	BKRF4	86-94	PSDSDESDY	72.5	17	yes	151090
P03179	MTP	382-390	ALDTVRYDY	70.0	77	yes	110142
P03184	UL32	115-123	FEDYALLCY	70.0	622	yes	151088
P03184	UL32	243-251	PGDVGRGLY	70.0	3311	yes	151094
P03193	PRIM	261-269	SADLVRYVY	70.0	87	yes	150104 154209
P03198	DPOL	96-104	VYDILETVY	70.0	6003	yes	140513
P03206	BZLF1	25-33	AFDQATRVY	70.0	11562	yes	80090
P03206	BZLF1	172-180	DSELEIKRY	70.0	3423	yes	8138
P03226	MCP	985-993	RPEQLFAEY	70.0	15890	yes	150085
P25939	TRM1	376-384	VAELSELLY	70.0	25	yes	154192
Q8AZJ5	LF1	421-429	NLDAGRIFY	70.0	21	yes	154206
P03177	KITH	465-473	VNDAYHAVY	67.5	1135	yes	151029
P03179	MTP	175-183	LFDNALRKY	67.5	12537	yes	110146
P03184	UL32	167-175	AIDIQLHFY	67.5	17	yes	154055
P03186	LTP	714-722	TLDTARSQY	67.5	384	yes	154016
P03186	LTP	2024-2032	PCDPLNPAY	67.5	394	yes	151072
P03188	GB	148-156	TKDGLTRVY	67.5	14816	yes	140543
P03188	GB	656-664	DLEGIFREY	67.5	9058	yes	151014
P03190	RIR1	654-662	LPEALRQRY	67.5	14986	yes	151056
P03198	DPOL	388-396	ILDRARHIY	67.5	114	yes	141412
P03198	DPOL	879-887	VIDILNQAY	67.5	23	yes	141415
P03226	MCP	706-714	VGDESVGQY	67.5	1940	yes	154053
P0CK56	UL92	171-179	VVDVVLSLY	67.5	18	yes	151181
P13288	KR2	103-111	LYDSVTELY	67.5	266	yes	151018
Q2MG95		79-87	PDEYWYLLY	67.5	1730	yes	154279
Q9QCF2		28-36	STRACVLLY	67.5	542	yes	154210
P03179	MTP	426-434	ALELFSALY	65.0	69	yes	110279
P03179	MTP	650-658	PLDLPLADY	65.0	528	yes	110281
P03186	LTP	2337-2345	LRDFVKQAY	65.0	8949	no	
P03186	LTP	3140-3148	DLERLKFLY	65.0	1084	no	
P03187	VP19	151-159	LTRMANLLY	65.0	44	no	
P03190	RIR1	197-205	EWDVTQALY	65.0	4871	no	

Supplemental Table 1 continued (1/1)

UniProt ID	Antigen	Position	Sequence	SYFPEITHI score	NetMHC 3.4 score	Immunoge-nicity testing	Internal No.
P03191	EAD	192-200	NPDLYVTTY	65.0	9316	yes	110283
P03193	PRIM	276-284	FNEGTFKRY	65.0	11418	no	
P03203	EBNA4	328-336	TNEEIDLAY	65.0	1282	yes	110285
P03207	BRRF1	165-173	IADVCRSGY	65.0	741	no	
P03213	PORTL	30-38	LFEILQGKY	65.0	9797	no	
P03213	PORTL	388-396	GLEKERELY	65.0	1926	no	
P03213	PORTL	564-572	YIEDLGRKY	65.0	1538	no	
P03217	AN	238-246	EFDPIYPSY	65.0	10204	no	
P03227	DNBI	519-527	PDDEPRYTY	65.0	11636	yes	111205
P03227	DNBI	588-596	YKDLVKSCY	65.0	8712	yes	111206
P03231	GH	328-336	LKDIIGICY	65.0	7743	no	
P03231	GH	650-658	DFDNLHVHY	65.0	7092	no	
P13288	KR2	55-63	IDDMTETLY	65.0	1306	no	
P13288	KR2	327-335	GFDRSDPLY	65.0	4748	no	
P30118; Q8AZJ7	YBL2	422-430	EADATWWLY	65.0	10	no	
P03179	MTP	105-113	ALEASGNNY	62.5	2091	no	
P03186	LTP	155-163	LAEVLHGSY	62.5	305	no	
P03186	LTP	1605-1613	DLEAPYAEY	62.5	7296	no	
P03188	GB	134-142	QMDTIYQCY	62.5	53	no	
P03190	RIR1	322-330	YGEEFEREY	62.5	7433	no	
P03198	DPOL	282-290	REDSSWPSY	62.5	11168	no	
P03200	GP350	143-151	HAEMQNPVY	62.5	159	yes	110375
P03204	EBNA6	975-983	PKDAKQTDY	62.5	13850	no	
P03208	BILF1	24-32	TEDACTKSY	62.5	14830	no	
P03211	EBNA1	409-417	VGEADYFEY	62.5	9416	no	
P03212	GL	41-49	ALENISDIY	62.5	665	no	
P03214; Q777D7	HELI	496-504	GHEQPEYVY	62.5	19300	no	
P03215	GM	86-94	IADCVAFIY	62.5	55	no	
P03222	UL17	84-92	CDEGLPELY	62.5	2656	no	
P03226	MCP	51-59	KFEVLLGVY	62.5	14929	no	
P03226	MCP	380-388	AVESLQKMY	62.5	3703	no	
P03226	MCP	503-511	VDEFYDNKY	62.5	11034	no	
P03231	GH	125-133	PLEKQLFYY	62.5	206	no	
P0CAP6	RIR2	191-199	HTRAASLLY	62.5	178	no	
P13285	LMP2	104-112	RDDSSQHIY	62.5	2301	no	
P13288	KR2	130-138	GQDKALVDY	62.5	5337	no	
Q04360	ICP27	381-389	VVETLSSSY	62.5	285	yes	81085

Supplemental Table 2: HLA-A*01:01 epitope prediction from the EBV proteome for 10mers.

UniProt ID	Antigen	Position	Sequence	SYFPEITHI score	NetMHC 3.4 score	Immunoge-nicity testing	Internal No.
P03214; Q777D7	HELI	654-663	TTENYTLLGY	87.2	9	yes	150099, 161099
P25939	TRM1	755-764	DSDRPLILLY	84.6	58	yes	154202
P03186	LTP	2540-2549	PTDVLNPSFY	82.1	15	yes	151071
P03208	BILF1	23-32	ATEDACTKSY	79.5	161	yes	154194
P03184	UL32	472-481	VCDSLITLVY	76.9	83	yes	154056
P03186	LTP	314-323	TSDSFPAARY	76.9	14	yes	151067
P03227	DNBI	153-162	ITEAFKERLY	76.9	65	yes	110154

Supplemental Table 2 continued (1/1)

UniProt ID	Antigen	Position	Sequence	SYFPEITHI score	NetMHC 3.4 score	Immunoge-nicity testing	Internal No.
P0C725	LF2	304-313	ITELEYNNTY	76.9	91	yes	151077
Q2MG95		78-87	VPDEYWYLLY	76.9	534	yes	150221
P03186	LTP	2034-2043	SADTQEPLNY	74.4	162	yes	151073
P03190	RIR1	149-158	ESDMEVFDYY	74.4	13	yes	151057
P03198	DPOL	262-271	HRDSYAELEY	74.4	1300	yes	141416
P03198	DPOL	957-966	KTEMAEDPAY	74.4	195	yes	141422
P03208	BILF1	258-267	CTESLVARYY	74.4	18	yes	154195
P03179	MTP	1073-1082	VRDNTFLDKY	71.8	2244	yes	110180
P03182	EAR	41-50	SPEDTVVLRY	71.8	10525	yes	151022
P03184	UL32	114-123	FFEDYALLCY	71.8	104	yes	150188
P03188	GB	635-644	NIDFASLELY	71.8	40	yes	150044
P03189	V120	318-327	LLEPSGALFY	71.8	40	yes	151190
P03191	EAD	202-211	SGEACLTLDY	71.8	4275	yes	90301
P03198	DPOL	445-454	CRDKLSLSDY	71.8	3568	yes	141427
P03205	GP42	176-185	SLDGGTFKVY	71.8	474	yes	140510
P03225	BDLF2	228-237	GRDFGVPLSY	71.8	10212	yes	151028
P30118	YBL2	490-499	AADLGLTWAY	71.8	328	yes	154207
P03180	IL10H	151-160	MSEFDIFINY	69.2	43	yes	140512
P03184	UL32	115-124	FEDYALLCYY	69.2	607	yes	150213
P03213	PORTL	118-127	VRDLLTTNIY	69.2	5440	yes	150103
P03215	GM	71-80	YLEPPEMFVY	69.2	95	yes	150035
P03219	TRM3	357-366	SADQATSFLY	69.2	111	yes	154205
P03220	UL95	10-19	PDDPMLARRY	69.2	10639	yes	151185
P03222	UL17	83-92	YCDEGLPELY	69.2	51	yes	154054
P03226	MCP	804-813	HADVLEKIFY	69.2	280	yes	151081
P03226	MCP	1216-1225	NQEVAEGLIY	69.2	4530	yes	150072
P03227	DNBI	292-301	SHETPASLNY	69.2	12336	yes	150091
P03231	GH	523-532	DRDAWHLPAY	69.2	6147	yes	150025
P0C725	LF2	264-273	LDDVIIAFRY	69.2	2974	yes	151078
P0CK51	TEG2	48-57	CGETNEGLEY	69.2	917	yes	150094
P13285	LMP2	484-493	ESEERPPTPY	69.2	55	yes	70020, 110293
P03179	MTP	531-540	ACDMAGCQHY	66.7	459	yes	111230
P03186	LTP	714-723	TLDTARSQYY	66.7	38	no	
P03186	LTP	2551-2560	HEDPPLPVGY	66.7	11460	no	
P03189	V120	911-920	RVEHALELGY	66.7	958	no	
P03190	RIR1	52-61	YLEVFSDKFY	66.7	87	yes	154007
P03191	EAD	105-114	AVEQASLQFY	66.7	132	yes	110316
P03198	DPOL	342-351	CEDIEGVEVY	66.7	8496	no	
P03213	PORTL	249-258	TFDSPVQRLY	66.7	787	no	
P03213	PORTL	502-511	VVDNQGQRLY	66.7	111	no	
P03224	BDLF3	171-180	PDERQPSLSY	66.7	15041	no	
P03226	MCP	502-511	IVDEFYDNKY	66.7	148	no	
P03227	DNBI	518-527	RPDDEPRYTY	66.7	13837	yes	110278
P03227	DNBI	767-776	FPDTKLSSLY	66.7	1897	yes	110282
P03231	GH	204-213	LPDLRGPFSY	66.7	11991	no	
P0CAP6	RIR2	256-265	LGDIGQAPLY	66.7	1114	no	
P0CK51	TEG2	17-26	DVDGGIINLY	66.7	325	no	
P0CK58	BALF1	63-72	PDDKVAESSY	66.7	13206	no	
P12978	EBNA2	451-460	PADLDESWDY	66.7	461	no	
P13288	KR2	54-63	NIDDMTETLY	66.7	42	no	
P13288	KR2	95-104	HADNATVKLY	66.7	224	no	
P13288	KR2	312-321	LADSTHKIPY	66.7	226	no	
Q04360	ICP27	416-425	HDEVEFLGHY	66.7	4562	yes	110317

Supplemental Table 3: HLA-A*01:01 epitope prediction from the EBV proteome for 11mers.

UniProt ID	Antigen	Position	Sequence	SYFPEITHI score	NetMHC 3.4 score	Immunogenicity testing	Internal No.
P03186	LTP	1603-1613	NTDLEAPYAEY	87.2	9	yes	161074
P03198	DPOL	903-913	STELSRKLSAY	84.6	39	yes	141434
P03195	DUT	198-208	FSDQTVFLNKY	82.1	6	yes	151030
P03207	BRRF1	143-153	GSDYTAVSLQY	82.1	11	yes	150097
P03179	MTP	1237-1247	GTDAWRFAMNY	79.5	8	yes	151053
P03188	GB	584-594	MTEVCQATSQY	79.5	16	yes	151015
P0CK53	UL16	313-323	FSDLYSRAMLY	79.5	5	yes	150086
P25939	TRM1	443-453	ATERLFCGGVY	76.9	16	yes	154203
P25939	TRM1	527-537	LSDALKRKEQY	76.9	36	yes	154204
P30118; Q8AZJ7	YBL2	186-196	HSESPGQLDVY	76.9	46	yes	150276
P03190	RIR1	195-205	SSEWDVTQALY	74.4	26	yes	151062
P03196	GN	43-53	LTEAQDQFYSY	74.4	10	no (length variant)	
P03226	MCP	525-535	PTEDFLHPSNY	74.4	21	yes	150083
P03231	GH	62-72	TEDLASMLNRY	74.4	3550	yes	151020
P03231	GH	469-479	GTESGLFSPCY	74.4	39	yes	150023
P12978	EBNA2	464-474	TTESPSSDEDY	74.4	33	yes	151024
P13285	LMP2	410-420	LTEWGSGNRTY	74.4	40	yes	110190
Q8AZJ7; Q04343		674-684; 152-162	ATEHGLSPTAY	74.4	15	yes	151192
P03184	UL32	139-149	GMDFLHILIKY	71.8	32	yes	151182
P03186	LTP	1060-1070	SIEWDYRELLY	71.8	329	yes	150063
P03186	LTP	3138-3148	IADLERLKFLY	71.8	33	yes	151075
P03214; Q777D7	HELI	314-324	GLELSPDILAY	71.8	215	yes	150100
P03217	AN	236-246	KSEFDPIYPSY	71.8	213	yes	150027
P03224	BDLF3	170-180	VPDERQPSLSY	71.8	5013	yes	154193
P03188	GB	654-664	VFDLEGIFREY	69.2	5421	yes	151017
P03192	BMRF2	238-248	HAEVFFGLSRY	69.2	146	yes	141405
P03200	GP350	804-814	GGDSTTPRPRY	69.2	3857	yes	110185
P03204	EBNA6	41-51	ASERLVPEESY	69.2	111	yes	110189
P03204	EBNA6	382-392	ELESSDDELPY	69.2	99	yes	110184
P03206	BZLF1	8-18	SEDVKFTPDPY	69.2	5048	yes	151026
P03214; Q777D7	HELI	648-658; 648-658	LLDYASTTENY	69.2	66	yes	150101
P03214; Q777D7	HELI	653-663; 653-663	STTENYTLLGY	69.2	45	yes	150102
P03217	AN	78-88	SKDGPSLKSIY	69.2	13423	yes	150028
P03226	MCP	789-799	DHDFRLHLGPY	69.2	7887	yes	150082
P03227	DNBI	691-701	DLDAALQGRVY	69.2	1424	yes	150092
P03228	BARF1	204-214	KNDKEEAHGVY	69.2	9374	yes	141409
P0C725	LF2	263-273	LLDDVIIAFRY	69.2	14	yes	150087
P13288	KR2	72-82	RCDHLPITCEY	69.2	250	yes	150026
P30119	BTRF1	250-260	NPDLLPLQHLY	69.2	1055	yes	150098
Q04360	ICP27	415-425	RHDEVEFLGHY	69.2	7226	yes	71069
P03186	LTP	3098-3108	STAAPEQDLRY	66.7	61	no	
P03188	GB	247-257	RADSFHVRTNY	66.7	436	no	
P03190	RIR1	312-322	PKDAGDLERLY	66.7	8638	no	
P03190	RIR1	715-725	SYELGLKTIMY	66.7	10831	yes	151064
P03206	BZLF1	170-180	ECDSELEIKRY	66.7	3253	yes	110313
P03214; Q777D7	HELI	442-452	EQDEERVKVTY	66.7	3882	no	

Supplemental Table 3 continued (1/1)

UniProt ID	Antigen	Position	Sequence	SYFPEITHI score	NetMHC 3.4 score	Immunogenicity testing	Internal No.
P03217	AN	7-17	LEDPMEEMTSY	66.7	4458	no	
P03220	UL95	9-19	MPDDPMLARRY	66.7	5661	no	
P03226	MCP	539-549	RLELHPLYDIY	66.7	498	no	
P03226	MCP	804-814	HADVLEKIFYY	66.7	60	no	
P03231	GH	26-36	HLDIEGHASHY	66.7	36	no	
P03231	GH	648-658	YFDFDNLHVHY	66.7	413	no	
P0C725	LF2	282-292	RWDGESTDIRY	66.7	9714	no	
P12978	EBNA2	273-283	SPEPRSPTVFY	66.7	15688	no	
P03177	KITH	156-166	GADSTSRSFMY	64.1	82	yes	151052

Supplemental Table 4: HLA-A*01:01 epitope prediction from the EBV proteome for 12mers.

UniProt ID	Antigen	Position	Sequence	SYFPEITHI score	NetMHC 3.4 score	Immunogenicity testing	Internal No.
P03184	UL32	185-196	SSDMIRNANLGY	90.2	7	yes	161065
P03203	EBNA4	809-820	TSDKIVQAPIFY	80.5	7	yes	164259
P03214; Q777D7	HELI	640-651	SDEPLLHGLLDY	80.5	7503	no	
P03231	GH	555-566	SSDREVRGSALY	80.5	14	yes	161086
P25939	TRM1	373-384	PPEVAELSELLY	80.5	11878	yes	195129
P25939	TRM1	753-764	TYDSDRPLILLY	80.5	1184	no	
Q8AZJ5	LF1	418-429	RSDNLDAGRIFY	80.5	8	yes	161097
P03187	VP19	329-340	ATDGWRRSAFNY	78.1	14	yes	161066
P03217	AN	94-105	ATDEQRTVLCSY	78.1	7	yes	161080
P03231	GH	61-72	VTEDLASMLNRY	78.1	9	yes	194241
P03186	LTP	2214-2225	LGDLLSDSVLTY	75.6	185	no	
P03187	VP19	259-270	PADARLYVALTY	75.6	40	yes	194242
P03188	GB	131-142	ETDQMDTIYQCY	75.6	8	yes	not producible
P03188	GB	584-595	MTEVCQATSQYY	75.6	9	yes	195131
P03193	PRIM	458-469	LPDTCLTRALSY	75.6	3427	no	
P03230	LMP1	373-384	DDDPHGPVQLSY	75.6	3541	no	
P03233	UL25	551-562	DYDRLYFLTLGY	75.6	2186	no	
P30118; Q8AZJ7	YBL2	468-479	TSDTRRALGGLY	75.6	7	yes	161101
Q04360	ICP27	359-370	TRDYNFVKQLFY	75.6	1504	no	
P03185	UL34	236-247	FSEAETEDEASY	73.2	11	yes	161067
P03186	LTP	766-777	VPEADALSMIDY	73.2	13814	no	
P0CK53	UL16	24-35	LSDASTPQMKVY	73.2	16	yes	195133

Supplemental Table 5: HLA-A*01:01 epitope prediction from the EBV proteome for 13mers.

UniProt ID	Antigen	Position	Sequence	SYFPEITHI score	NetMHC 3.4 score	Immunoge-nicity testing	Internal No.
P03214; Q777D7	HELI	639-651	TSDEPLLHGLLDY	85.4	8	yes	161082, 161100
P13288	KR2	295-307	RLDLQSLGYSLLY	82.9	10	yes	161091
P0CK56	UL92	167-179	SSEKVVDVVLSLY	80.5	25	yes	161089
P25939	TRM1	622-634	SSEHLHALTHSLY	80.5	11	yes	195132
P03207	BRRF1	278-290	VTDAITLPDCAEY	78.1	7	yes	195134
P14347	BFRF2	44-56	LLDLGLACLDLSY	78.1	16	yes	161095
P03179	MTP	101-113	GTESALEASGNNY	75.6	63	yes	164210
P03184	UL32	185-197	SSDMIRNANLGYY	75.6	6	yes	195135
P03186	LTP	241-253	ETEDPRIFMLEHY	75.6	38	yes	195136
P03186	LTP	1058-1070	YTSIEWDYRELLY	75.6	7	yes	194250
P03186	LTP	2020-2032	ETESPCDPLNPAY	75.6	44	yes	194251
P03189	V120	521-533	SSELLRSLLWVRY	75.6	19	yes	161072
P03189	V120	908-920	LNERVEHALELGY	75.6	4999	yes	161075
P03200	GP350	312-324	SQDMPTNTTDITY	75.6	396	yes	164257
P03200	GP350	319-331	TTDITYVGDNATY	75.6	9	yes	164258
P03204	EBNA6	380-392	DVELESSDDELPY	75.6	376	yes	161078
P03214; Q777D7	HELI	440-452	GTEQDEERVKVTY	75.6	125	no	
P03219	TRM3	598-610	TNEKSKAFERLIY	75.6	10517	no	
P03220	UL95	157-169	PEDPLPWMWALFY	75.6	429	no	
P03226	MCP	829-841	GVDFQHVAQTLAY	75.6	16	yes	161084
P03226	MCP	1089-1101	HHEMASIDTGLSY	75.6	7399	no	
P03227	DNBI	206-218	NSDLSRCMHEALY	75.6	7	yes	194252
P03230	LMP1	44-56	MSDWTGGALLVLY	75.6	6	yes	161085
P03230	LMP1	372-384	DDDDPHGPVQLSY	75.6	4664	no	
P0CK56	UL92	15-27	GTDEPNPRHLCSY	75.6	11	yes	161093
P03184	UL32	239-251	SQDVPGDVGRGLY	70.7	1305	no	
P03192	BMRF2	36-48	SLEIFSPWQTHVY	70.7	186	no	
P03195	DUT	99-111	PSELKIHLAAFRY	70.7	27	no	
P03198	DPOL	931-943	NEELPQIHDRIQY	70.7	17640	no	
P03214; Q777D7	HELI	142-154	ALEELQRRDLAKY	70.7	1689	no	
P03226	MCP	702-714	GSDVVGDESVGQY	70.7	18	no	
P25939	TRM1	574-586	YWELARMRNHFLY	70.7	4135	no	
P25939	TRM1	683-695	PSDWIETSFNSFY	70.7	7	no	
P25939	TRM1	752-764	LTYDSDRPLILLY	70.7	69	no	
Q04360	ICP27	308-320	LEETIFWLQEITY	70.7	8341	no	
P03179	MTP	1070-1082	FREVRDNTFLDKY	68.3	11289	no	
P03210	BRRF2	262-274	YLEAFRNSDNHFY	68.3	17	no	
P03214; Q777D7	HELI	162-174	AAEFRRTKPRGLY	68.3	2188	no	
P03179	MTP	105-117	ALEASGNNYVYAY	68.3	268	yes	110318

Supplemental Table 6: HCMV-derived HLA ligands extracted from HF-99/7 cells. Abbreviations: n.a., not annotated; ND, not determined.

Source	Position	SYFPEITHI score [% of maximum score]	NetMHC score [nM]	NetMHC rank [%]	Sequence	Predicted HLA type	Temporal protein class according to Weekes *et al.**
UL31	309-317	66.67	5775	0.60	AAPFGRVSV	C*01:02	5
UL104	506-514	66.67	2666	0.15	AAPFRPLAV	C*01:02	5
UL56	365-373	76.67	2666	0.60	AAPNRIIDL	C*01:02	3
UL105	716-723	n.a.	1815	0.70	ADPFFLKY	A*01:01	3
UL47	400-408	70.97	41	0.17	ALIQPASQK	A*03:01	5
US20	249-259	75.00	788	1.70	ALLSDADWLQK	A*03:01	2
UL56	707-715	70.97	16	0.03	ALYNETFGK	A*03:01	3
UL69	268-276	65.79	1676	0.25	APYPADLKV	B*51:01	3
UL35	453-462	41.94	179	0.70	ASRQTGLTPK	A*03:01	5
UL86	1345-1354	56.41	155	0.12	ATSETHFGNY	A*01:01	5
UL98	337-345	34.88/ 57.89	792/ 15146	1.10/ 3.50	DAALFRATL	B*08:01 / B*51:01	3
UL84	406-413	71.05	28372	13.00	DAPLPYFV	B*51:01	5
UL25	66-73	83.87	33812	18.00	DAPSSFEL	C*01:02	5
TRL4	156-163	61.29	38137	27.00	DAPVAILM	C*01:02	ND
UL56	503-511	44.19/ 60.53	235/ 30278	0.40/ 3.50	DARSRIHNV	B*08:01 / B*51:01	3
UL102	423-430	63.16	26133	10.00	DATFTVHV	B*51:01	3
UL2	16-24	73.68	2906	0.40	DAYPSFGTL	B*51:01	ND
UL98	73-81	46.51	79	0.12	DFMTRVAAL	B*08:01	3
UL16	112-119	57.89	38413	32.00	DGLKMRTV	B*51:01	2
UL115	79-86	57.89	33866	21.00	DGPLSQLI	B*51:01	5
UL56	286-294	58.14/ 76.67	563/ 13663	0.80/ 2.50	DIPERIYSL	B*08:01 / C*01:02	3
UL105	360-369	82.05	90	0.07	DLDFGDLLKY	A*01:01	3
UL45	592-600	50.00	18307	4.50	DMPVQRLTV	C*01:02	5
US24	485-492	63.16	14490	3.50	DPFPLKSL	B*51:01	1
UL47	968-976	65.79	10670	2.00	DPPAGSTSV	B*51:01	5
US22	57-65	65.79	11633	2.50	DPPALRTYV	B*51:01	3
UL77	296-304	76.32	5129	0.80	DPPDSVATV	B*51:01	5
UL70	306-314	46.51	24	0.03	DVMQKYFSL	B*08:01	3
UL34	243-251	68.42	1797	0.25	EAYRMLFQI	B*51:01	3
UL84	500-507	62.50	154	0.25	FISSKHTL	B*08:01	5
UL14	66-74	50.00	385	0.04	FPAHDWPEV	B*51:01	2
UL95	336-343	63.16	2781	0.40	FPALLPKL	B*51:01	3
UL75	540-549	n.a.	542	0.06	FPDATVPATV	B*51:01	5
UL105	111-118	68.42	186	0.02	FPFRALLV	B*51:01	3
UL38	156-164	63.16	283	0.03	FPVEVRSHV	B*51:01	2
UL73	130-138	52.50/ 56.25	115/ 6151	0.09/ 2.50	FTATTTKGY	A*01:01 / C*07:01	5
UL56	284-292	77.50	17	0.01	FTDIPERIY	A*01:01	3
UL130	196-204	72.50	14	0.01	FTEANNQTY	A*01:01	5
UL148	189-199	41.03	1104	0.50	FVAGHGETDFY	A*01:01	5
UL36	82-91	61.54	132	0.10	FVEGPGFMRY	A*01:01	2
UL77	228-236	70.97	39	0.15	GLYTQPRWK	A*03:01	5
US34	92-101	76.92	21	0.01	GSDALPAGLY	A*01:01	ND
UL11	142-150	70.97	99	0.40	GTLPTTTTK	A*03:01	ND
UL25	580-588	77.42	21	0.07	GVSSVTLLK	A*03:01	5
UL83	519-528	67.74	81	0.40	GVWQPAAQPK	A*03:01	5

Supplemental Table 6 continued (1/3)

Source	Position	SYFPEITHI score [% of maximum score]	NetMHC score [nM]	NetMHC rank [%]	Sequence	Predicted HLA type	Temporal protein class according to Weekes *et al.**
UL77	596-604	20.93/ 50.00	478/ 14622	0.7/ 3.5	HGLGRLLSV	B*08:01 / B*51:01	5
UL40	170-178	74.42	15	0.01	HLKLRPATF	B*08:01	3
UL117	325-334	70.97	94	0.40	HTPQAVATFK	A*03:01	2
UL29	352-362/ 674-684	58.97	464	0.25	HTSPAYDVSEY	A*01:01	1
US28	158-166	63.16	571	0.07	IAIPHFMVV	B*51:01	4
UL34	210-217	50.00	518	0.70	IGHLRHYL	B*08:01	3
UL9	143-152	45.16	88	0.40	ILLYPPTSTY	A*03:01	ND
UL51	125-132	87.50	149	0.25	ILREKTQL	B*08:01	5
US23	65-73	57.89	106	0.01	IPHNWFLQV	B*51:01	1
UL71	330-338	57.89	443	0.05	IPPPQIPFV	B*51:01	3
IRS1	92-99	67.50	1130	1.40	IPVERQAL	B*08:01	3
UL112/ UL113	124-134	69.23	419	0.25	ISENGNLQVTY	A*01:01	5
UL75	601-609	50.00/ 20.00	1920/ 2829	0.17/ 0.30	ISYPVSTTV	B*51:01 / C*01:02	5
US28	122-130	75.00	28	0.02	ITEIALDRY	A*01:01	4
UL123	184-192	80.65	59	0.25	KLGGALQAK	A*03:01	1
US33A	13-21	80.65	24	0.08	KLGYRPHAK	A*03:01	ND
UL78	335-343	87.50	226	0.08	KRAMYSVEL	C*07:01	2
UL148	180-188	86.67	1326	0.04	LAPDLVSSL	C*01:02	5
UL56	154-162	70.00	4561	0.40	LAPEAGLEV	C*01:02	3
UL105	361-369	50.00	12020	4.50	LDFGDLLKY	A*01:01	3
UL97	672-682	48.72	157	0.12	LLATSDGLYLY	A*01:01	3
IRS1/ TRS1	464-474	66.67	263	0.17	LLDELGAVFGY	A*01:01	3/4
UL56	87-95	67.50	27	0.02	LLDRALMAY	A*01:01	3
UL70	304-311	n.a.	1352	0.60	LLDVMQKY	A*01:01	3
UL122	382-389	57.89	3284	0.50	LPFTIPSM	B*51:01	ND
UL34	180-188	62.79	53	0.08	LPHERHREL	B*08:01	3
UL83	116-123	68.42	1710	0.25	LPLKMLNI	B*51:01	5
UL102	62-70	65.79	1995	0.30	LPPAEVRAV	B*51:01	3
UL77	308-315	60.53	6960	1.10	LPQLLPRL	B*51:01	5
UL56	605-613	57.89	367	0.04	LPVESLPLL	B*51:01	3
UL48	1322-1331	n.a.	304	0.03	LPYLSAERTV	B*51:01	5
UL26	61-69	55.81/ 63.16	44/ 110	0.06/ 0.01	LPYPRGYTL	B*08:01 / B*51:01	5
US22	75-83	68.75	86	0.03	LRNPANWFL	C*07:01	3
UL36	256-264	67.50	23	0.02	LVDTFGVVY	A*01:01	2
TRL4	163-170	52.63	10069	1.80	MARTAISV	B*51:01	ND
UL54	801-811	75.00	148	0.60	MLLDKEQMALK	A*03:01	2
UL20	164-172	55.81	10	0.01	MLLPRQYTL	B*08:01	ND
UL148	1-8	57.5	39	0.05	MLRLLFTL	B*08:01	5
UL117	323-330	60.53	3697	0.60	MPHTPQAV	B*51:01	2
UL36	464-472	60.53	603	0.07	MPPLTPPHV	B*51:01	2
UL122	449-457	55.26	310	0.03	MPVTHPPEV	B*51:01	ND
UL54	815-823	57.89	3086	0.50	NAFYGFTGV	B*51:01	2
UL27	393-400	63.16	20334	6.00	NAVLALRI	B*51:01	1
US23	553-561	63.16	9914	1.80	NAYRTEAEV	B*51:01	1
UL145	20-27	25.00	1640	2.00	NFKHHNAV	B*08:01	ND
UL44	216-223	40.00	476	0.70	NMRINVQL	B*08:01	5
UL38	207-214	47.50	1332	1.70	NSYVRAIL	B*08:01	2

Supplemental Table 6 continued (2/3)

Source	Position	SYFPEITHI score [% of maximum score]	NetMHC score [nM]	NetMHC rank [%]	Sequence	Predicted HLA type	Temporal protein class according to Weekes *et al.**
UL55	657-665	52.50/ 68.75	624/ 3520	0.40/ 1.30	NTDFRVLEL	A*01:01 / C*07:01	5
UL55	657-666	87.18	9	0.01	NTDFRVLELY	A*01:01	5
UL44	26-34	55.81	207	0.30	QLRSVIRAL	B*08:01	5
US24	303-311	25.00	3188	1.10	QMDDPNHYV	A*01:01	1
US32	115-123	38.71	100	0.40	RAYHHRINR	A*03:01	ND
UL148	259-266	47.50	592	0.80	RGYVRYTL	B*08:01	5
UL80	698-706	87.10	11	0.01	RIFVAALNK	A*03:01	3
UL57	1044-1052	77.42	302	1.00	RLADVLIKR	A*03:01	5
UL54	564-572	77.42	96	0.40	RLAKIPLRR	A*03:01	2
US26	200-209	70.27	10769	1.70	RLHDNSISEL	C*01:02	3
UL150	524-532	74.19	169	0.60	RLLLPLSGY	A*03:01	5
UL51	96-105	77.42	20	0.06	RLNFVNAGQK	A*03:01	5
UL135	43-51	77.42	349	1.10	RLPGAASDK	A*03:01	1
UL27	541-549	83.33	281	0.01	RLPQFSSAL	C*01:02	1
UL44	6-15	78.38	5128	0.50	RLSEPPTLAL	C*01:02	5
UL52	557-566	48.39	53	0.25	RQAGVTGIYK	A*03:01	5
TRL9	104-113	58.06	290	0.90	RQGPGFLLEK	A*03:01	ND
UL70	368-376	48.84/ 53.12	421/ 2006	0.60/ 0.70	RQLERINTL	C*07:01	3
UL36	51-60	58.06	40	0.15	RSALGPFVGK	A*03:01	2
UL36	49-60	n.a.	209	0.70	RSRSALGPFVGK	A*03:01	2
UL70	697-706	48.39	11	0.01	RSVRLPYMYK	A*03:01	3
UL69	569-578	87.18	15	0.01	RTDPATLTAY	A*01:01	3
UL79	237-245	77.42	30	0.10	RTFAGTLSR	A*03:01	5
UL56	302-310	70.97	1439	2.50	RTSEVIVKR	A*03:01	3
UL75	337-345	52.50/ 75.00	288/ 8210	0.20/ 3.50	RTVEMAFAY	A*01:01 / C*07:01	5
UL84	3-11	70.97	2562	3.50	RVDPNLRNR	A*03:01	5
UL6	225-233	87.10	34	0.12	RVGNGTLSK	A*03:01	ND
UL57	790-798	70.97	108	0.50	RVKNRPIYR	A*03:01	5
US24	136-145	80.65	15	0.03	RVYAYDTREK	A*03:01	1
UL36	52-60	38.71	122	0.50	SALGPFVGK	A*03:01	2
UL89	237-245	64.52	109	0.50	SIGYVAHQK	A*03:01	5
UL70	313-321	67.50	28	0.03	SLDNFLHDY	A*01:01	3
UL148	282-290	67.50	116	0.09	SLDRFIVQY	A*01:01	5
UL45	502-510	61.29	59	0.25	SLFGRPVSR	A*03:01	5
U147A	2-10	67.44	30	0.04	SLFYRAVAL	B*08:01	ND
UL105	713-722	74.19	8	0.01	SLYADPFFLK	A*03:01	3
UL21A	4-12	57.89	875	0.12	SPVPQLTTV	B*51:01	ND
UL55	576-584	78.12	1770	0.60	SRPVVIFNF	C*07:01	5
UL32	764-772	53.33	20643	5.50	SSPMTTTST	C*01:02	5
UL70	490-498	57.50/ 62.50	24/ 5527	0.02/ 2.50	STSPETQFY	A*01:01 / C*07:01	3
UL70	490-499	58.97	26	0.02	STSPETQFYY	A*01:01	3
UL32	771-780	70.97	69	0.30	STSQKPVLGK	A*03:01	5
UL128	127-135	70.00	3965	0.30	SVPYRWINL	C*01:02	ND
UL78	351-361	68.75	1577	3.00	SVRDVAEAVKK	A*03:01	2
UL70	698-706	67.74	15	0.03	SVRLPYMYK	A*03:01	3
UL122	113-121	77.42	59	0.25	SVSSAPLNK	A*03:01	ND
UL105	537-545	80.00	4896	0.50	TAPDSRETL	C*01:02	3
US14	150-158	90.00	2379	0.12	TAPIGISSL	C*01:02	3
UL44	246-253	n.a.	406	0.25	TEHDTLLY	A*01:01	5

Supplemental Table 6 continued (3/3)

Source	Position	SYFPEITHI score [% of maximum score]	NetMHC score [nM]	NetMHC rank [%]	Sequence	Predicted HLA type	Temporal protein class according to Weekes *et al.**
UL104	589-597	67.50	65	0.06	TLDPVPEAY	A*01:01	5
UL11	199-206	65.00	604	0.80	TPKTHVEL	B*08:01	ND
UL84	239-247	62.79	20	0.02	TPLLKRLPL	B*08:01	5
UL112/ UL113	304-313	76.92	38	0.03	TSEAVAFLNY	A*01:01	5
UL86	1346-1354	72.50	123	0.09	TSETHFGNY	A*01:01	5
UL83	502-510	50.00/ 58.06	1518/ 4716	0.60/ 5.00	TVQGQNLKY	A*01:01 / A*03:01	5
UL34	383-391	52.63	2694	0.40	VAATPSPSV	B*51:01	3
UL33	254-261	60.53	16653	4.00	VALQTPYV	B*51:01	5
UL43	163-171	57.89	6064	1.00	VGYFGHLNI	B*51:01	5
UL13	331-339	73.33	651	0.01	VIPPAPTVL	C*01:02	1
UL89	177-185	64.52	44	0.17	VLANRVLQY	A*03:01	5
UL98	471-479	67.74	41	0.17	VLSQYYIKK	A*03:01	3
UL36	199-207	62.79	109	0.17	VMKFKETSF	B*08:01	2
UL33	162-170	65.79	225	0.02	VPAAVYTTV	B*51:01	5
UL57	962-970	60.53	143	0.01	VPAPMAATV	B*51:01	5
UL115	184-192	65.79	578	0.07	VPPSLFNVV	B*51:01	5
UL21A	108-115	63.16	7223	1.20	VPRPHPMI	B*51:01	ND
UL92	146-154	60.53	482	0.06	VPVISQLFI	B*51:01	5
UL105	616-624	63.33	5552	0.60	VSPYTTEEM	C*01:02	3
US28	182-190	39.47	5340	0.80	VSYPIILNV	B*51:01	4
UL105	916-924	52.50	94	0.07	VTDPEHLMM	A*01:01	3
UL48	1607-1617	82.05	31	0.03	VTDYGNVAFKY	A*01:01	5
UL44	245-252	66.67	30287	29.00	VTEHDTLL	C*07:01	5
UL44	245-253	85.00	6	0.01	VTEHDTLLY	A*01:01	5
UL44	245-254	48.72	138	0.10	VTEHDTLLYV	A*01:01	5
US24	481-490	77.42	17	0.04	VTYSDPFPLK	A*03:01	1
UL56	581-590	66.67	43	0.04	VVDVGDQFTY	A*01:01	3
UL31	233-241	77.42	86	0.40	VVLQPLITK	A*03:01	5
UL78	375-384	67.74	203	0.70	VVVTTTTSEK	A*03:01	2
UL105	715-723	82.50	6	0.01	YADPFFLKY	A*01:01	3
UL114	199-207	55.81	28	0.03	YLIDRRRHL	B*08:01	2
UL13	465-473	46.51	32	0.04	YLVRRPMTI	B*08:01	1
UL3	69-77	68.42	510	0.06	YPPSWSRTI	B*51:01	ND
UL16	162-170	51.16/ 47.37	1454/ 2912	1.80/ 0.40	YPRPPGSGL	B*08:01 / B*51:01	2
UL78	222-232	76.92	22	0.02	YSDRRDHVWSY	A*01:01	2
UL83	363-371	32.50	4145	1.40	YSEHPTFTS	A*01:01	5
UL25	370-379	64.10	13	0.01	YTSRGALYLY	A*01:01	5
UL70	404-412	57.50	89	0.07	YTTGTLTRY	A*01:01	3
UL104	269-277	47.50/ 64.52	172/ 1709	0.12/ 3.00	YVAAEPLAY	A*01:01 / A*03:01	5
UL105	723-731	48.84/ 46.67	464/ 822	0.70/ 0.01	YVKPPSLAL	B*08:01 / C*01:02	3

9 Danksagung

Zu allererst möchte ich meinen beiden Betreuern Prof. Dr. Stefan Stevanović und Prof. Dr. Hans-Georg Rammensee danken. Vielen Dank für euer Vertrauen, die großartige Betreuung, die konstruktive Kritik und die viele Unterstützung in allen Belangen.

Den Kampf mit der Bürokratie haben einem Lynne Yakes, Jürgen Frank, Carmen Höner und Gerhard Hörr erheblich erleichtert oder gänzlich abgenommen. Vielen Dank dafür.

Viele hundert Peptide wurden durch mich oder meine Studenten getestet. Ermöglicht haben das Patricia, Nici, Marion, Camille, Mirijam, Uli, die Hiwis und alle die sonst noch mit der Peptidsynthese geholfen haben. Dankeschön!

Auch der gesamten AG Gouttefangeas möchte ich danken. Sie war und ist eine nicht versiegende Quelle an Wissen über T-Zellen, Durchflusszytometrie und Protokolloptimierungen.

Bedanken möchte ich mich darüber hinaus bei meinen früheren Kollegen Janet, Lea, Heiko, Linus, Daniel, Nico und Armin, die mich nicht erst zum Doktor sondern schon zu meiner Hiwi-Zeit herzlich aufgenommen haben und immer ein offenes Ohr für einen Neuling hatten. Besonderen Dank gilt dabei Stefanie Spalt, die mir mit der Etablierung des Infektionsmodels mit HCMV-Mutanten nicht nur den Weg zu meinem Projekt geebnet hat, sondern mir auch immer mit Rat und Tat zur Seite stand.

Auch meinen aktuellen Kollegen der AG Stevanović und AG Walz möchte ich für die tolle Arbeitsatmosphäre, die gemeinsamen Kongresse, die fröhlichen Abende und die erbauenden Gespräche danken. Insbesondere Kollegen wie Moni, Ana, Annika, Tatjana und Timo, welche inzwischen zu Freunden geworden sind, haben die Doktorarbeit zu einer wundervollen Zeit gemacht. Ich werde diese Zeit mit euch vermissen.

Ich möchte außerdem allen meinen Freunden außerhalb des Instituts danken, die mich durch diese Zeit und mein Leben begleitet haben und begleiten – insbesondere meinem „Team Awesome“ gebührt ein riesiges Dankeschön.

Zuletzt gilt ein besonderer Dank meiner Familie: Danke für eure Unterstützung in jeglicher Hinsicht, euren Glauben an mich und eure Liebe. Vielen lieben Dank an Jörg, der mir in allen Lebenslagen zur Seite steht und mein Leben noch reicher macht, als es ohnehin schon ist.